This is to certify that the
thesis entitled

LASER DESORPTION/IONIZATION MASS SPECTROMETRIC (LD/MS) ANALYSIS OF SAMPLES OF FORENSIC INTEREST: CHEMICAL CHARACTERIZATION OF COLORANTS AND OTHER COMPOUNDS

presented by

Leah G. Balko

has been accepted towards fulfillment
of the requirements for the

M.S. degree in Chemistry

John Allen

Major Professor's Signature

12.12.02

Date

LASER DESORPTION/IONIZATION MASS SPECTROMETRIC (LD/MS) ANALYSIS OF SAMPLES OF FORENSIC INTEREST: CHEMICAL CHARACTERIZATION OF COLORANTS AND OTHER COMPOUNDS

By

Leah G. Balko

A THESIS

Submitted to
Michigan State University
In partial fulfillment of the requirements
for the degree of

MASTER OF SCIENCE

Department of Chemistry

2002

ABSTRACT

LASER DESORPTION/IONIZATION MASS SPECTROMETRIC (LD/MS) ANALYSIS OF SAMPLES OF FORENSIC INTEREST: CHEMICAL CHARACTERIZATION OF COLORANTS AND OTHER COMPOUNDS

By

Leah G. Balko

Mass spectrometry is a powerful analytical technique used for chemical characterization and can be particularly helpful in confirmatory forensic analysis. Recent research has shown laser desorption/ mass spectrometry (LD/MS) effective in the analysis of dyes found in inks on paper. In this thesis, mass spectra obtained from direct UV-laser irradiation of a variety of samples are presented. These samples include currency, postage stamps, fabric, watercolor pigments on paper, black and white photographs, glass, and compounds used in currency protection devices. While other techniques have been used to analyze these samples, LD/MS produces unique data. Both positive-ion and negative-ion mass spectra contain useful and relevant molecular level information about compounds present in the samples. The interpretation of LD/MS mass spectra and the relevance of the results are discussed. LD/MS of organic dyes typically produces intact molecular ions (as well as protonated, sodiated, and deprotonated ions). LD/MS of inorganics produces a variety of cluster ions representing the surface composition of the sample, suggesting the potential for elemental analysis using LD/MS. This thesis demonstrates the value and versatility of LD/MS in chemical characterization.

ACKNOWLEDGEMENTS

Thank you Dr. John Allison for your succinct teaching of mass spectrometry, your guidance with research, and your enormous patience.

Thank you labmates (Anne, Donna, Eric (token male), Jamie, and Qian) for all the laughter and stimulating conversations (both academic and non). You've made our lab an interesting and fun place to be.

Thank you housemates (Bekah, Jane, Janelle, Julie, Karen and Virginia) for your encouragement and prayers when I was stressed and for incessantly goofing around when I wasn't.

Thank you especially Abby (precious friend) and Dave (fiancé), for demonstrating 1 Thessalonians 5:11, by continually encouraging me and building me up in faith.

Thank you mom and dad for stepping back and letting me explore the world on my own.

TABLE OF CONTENTS

LIST OF TABLES

LIST OF FIGURES

CHAPTER 1: Introduction

Historical context

The practice of mass spectrometry

The general strategy/requirement for analysis of compounds by mass spectrometry is to create gas phase ions (in a location called the "ion source") and to move them to another region where the ions are analyzed, the mass analyser.

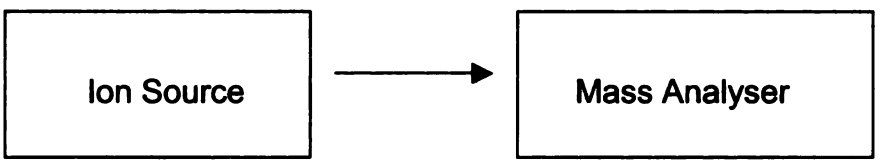

In the mass analyser, ions of different mass-to-charge (m/z) ratios behave differently. They may move in different directions or at different velocities. The disparate behavior of ions with differing m/z values allows the ions to be detected at different locations and/or times. The relative abundance of ions of certain m/z values can be plotted, and this forms the mass spectrum.

For volatile or gaseous molecules, such as those eluting off a gas chromatograph, the techniques of electron impact ionization (EI) or chemical ionization (CI) are used to ionize the gas phase neutrals to form gas phase ions. In EI, a beam of high energy (70 keV) electrons is passed through the gas phase samples. In chemical ionization, reagent ions such as CH_5^+ or NH_4^+ react with the gaseous analyte to produce ions through proton transfer.

Desorption/ionization techniques of ion formation

This first step (gas phase ion formation) of mass spectrometric analysis is more challenging for non-volatile compounds. As with volatile compounds, these compounds also must be ionized, but additional considerations must be made as to how to desorb these molecules/ions. These non-volatile or thermally-labile compounds can be analyzed by techniques of "desorption/ionization mass spectrometry." This umbrella term includes techniques such as field desorption (FD), fast atom bombardment (FAB), secondary-ion (mass spectrometry) (SIMS), matrix-assisted laser desorption ionization (MALDI), and direct laser desorption (LD).

In FD, the analyte on the surface of a probe is heated and experiences a high electric field (10^7-10^8 V/cm) producing intact ionized analyte molecules and some fragment ions[1]. In a FAB experiment, the analyte is dissolved in a liquid matrix, applied to a metal target, and bombarded with fast (keV) Xe atoms[1]. The parallel technique of SIMS uses a primary beam of high energy (keV) ions (e.g., Cs^+, Xe^+, Ar^+) in place of the Xe atoms of FAB to impart energy to the target (and analyte)[1]. Generally, for desorption/ionization of non-volatiles, the goal is to quickly deposit a large amount of energy into the target. The amount of energy must be sufficient to not only desorb the analyte, but to ionize it as well. If the energy is slowly added to the analyte, then analyte molecules might decompose before accumulating enough energy to desorb/ionize; therefore, energy must be

quickly added to the analyte so that the rate of desorption of ions will far exceed the rate of decomposition of the molecules.

In addition to the techniques described above, lasers are another effective pathway for depositing a high density of energy in a small area, and the use of lasers in desorption/ionization mass spectrometry (LD/MS) has been explored for over 30 years.

Pioneering work in LD/MS

Work in 1970 by Vastola and coworkers is considered by some[2] to be the earliest report of LD/MS. In this work[3], mass spectra of sodium hexylsulfonate salts were reported; these spectra contained peaks representing the sodiated analyte $(M+Na)^+$ with little fragmentation. Other early work in this area included elemental analysis[4] and vaporization of carbon compounds[5]; these represented an interesting, though unimpressive field. Noteworthy mass spectra reported in 1978[6] suggested the application of LD/MS to the analysis of high molecular mass, non-volatile compounds. Posthumus and co-workers presented spectra of oligosaccarides, glycosides, and peptides that were produced through CO_2 laser (10.6 μm) irradiation of a metal target coated with a thin layer of the analyte.

As one might expect, researchers encountered various difficulties and curious observations. Some compounds wouldn't desorb/ionize, some molecules produced single peak spectra[7], while other compounds displayed extreme fragmentation, some samples thermally decomposed, some compounds

produced well resolved spectra, while other compounds produced poorly resolved spectra. To better understand LD/MS, additional experiments were conducted to elucidate the mechanism of desorption/ ionization[8].

Instrument variables

Researchers have studied the effect of laser wavelength, laser pulse width, instrument design, surface the analyte is applied to (e.g., various metal surfaces), and sample preparation. As described in a comprehensive review article by Conzemius and Capellen[9] in 1980 virtually every laser type has been investigated for use in LD/MS. Some studies have reported no difference in fragmentation when changing the wavelength of the irradiating laser while other studies report dramatic fragmentation pattern changes[10]. Spectra have been obtained using IR lasers[11] and UV lasers[12-14] such as: Nd:Yag lasers (frequency-quadrupled 266 nm and frequency-tripled 355 nm), nitrogen lasers (337 nm), and excimer lasers (193 nm and 248 nm). Similarly, spectra were successfully obtained using a variety of pulse widths (from the earliest pulse widths of a few microseconds[15] down to the subnanosecond level[16,17]). Even continuous wave (CW) CO_2 lasers (with a quadrupole mass analyzer) were used to study low molecular weight, thermally labile compounds such as sucrose and citric acid[18].

To improve ionization yield (the ratio of desorbed ions to desorbed molecules), researchers have also explored the use of two lasers in the same experiment. One laser desorbs molecules from a surface, and a second (sometimes

orthogonal) laser ionizes the desorbed molecules. The theory of postionization[19] hypothesizes that one can optimize each of the laser conditions independently to improve ionization efficiency and resolution. Some researchers were able to increase ion signal 50-fold with the use of postionization[20].

While some CW lasers have been used in LD/MS experiments, the pulsed UV laser has emerged as the "laser of choice for LD/MS" because these lasers can produce more energy than CW lasers (thus preventing thermal decomposition) and because of their compatibility with time-of-flight mass analysers (discussed below).

Pulsed lasers and mass analyzers

Many earlier researchers used sector mass analyzers, because they were the most developed and available mass analyzers at the time. Since then, time-of-flight (TOF) mass analyzers have emerged as the most suitable mass analyzer for laser desorption mass spectrometry. The TOF mass analyzer works naturally with pulsed laser ionization. These geometrically simple mass analyzers have a theoretically unlimited mass range.[21,22] The length of time between each laser pulse can be adjusted, allowing an entire mass spectrum to be generated with each laser pulse. Research and development in the area of Fourier transform-mass spectrometry (FT-MS)[23] promises high resolution and mass accuracy, however, because of advances in the mass spectrometric analysis of biomolecules (discussed below), the dominant instruments commercially

available for mass spectrometric analysis of ions formed using lasers incorporate a pulsed UV laser and TOF mass analyser.

MALDI analysis of biomolecules

LD/MS has been explored as a technique to study a wide range of molecules, from inorganic metal complexes to small (less than 400 Daltons) organic molecules. Poor resolution[24] of organic ions relative to resolution of inorganic ions is attributed to post-source metastable decay, and delayed emission of ions from the surface from which they're desorbed. However, because of the exploding interest in the analysis of biomolecules, the development of a LD/MS technique for the analysis of high-molecular weight compounds seemed almost inevitable.

Researchers noted that many molecular and fragment ions were produced via alkali ion attachment[25]. Scientists extended early observations that the presence of one compound (such as platinum metal powder) facilitates the desorption/ionization of another compound and the concept of matrix-assisted laser desorption developed[26,27] . One pioneering scientist, Koichi Tanaka, was honored with the 2002 Nobel prize in chemistry for his work in the soft ionization of biomolecules. One of the earliest reports of an organic matrix was by Karas and Hillenkamp in 1988.[27] Nicotinic acid aided the desorption and ionization of proteins with masses above 10,000 daltons. Since then, a variety of matrices

have been studied and the current practical limits of detection have been pushed near 400,000 Daltons.

In MALDI, it is thought that the matrix serves two primary purposes: (1) to separate analyte molecules in a "solid solution" and (2) to absorb the energy of the irradiating laser and transfer the energy to the analyte. The wide range of analytes for which MALDI produces useful spectra, the sensitivity (1 pmole of analyte yields a satisfactory spectrum) of the technique, and theoretically infinite mass range of the pulsed UV-MALDI-TOF MS technique have led to the mass production of UV-MALDI instruments. More recently much of the work in the area of MALDI has been on understanding of the mechanism of, further developing of, and pressing the limits of the technique.

Desorption/ionization on silicon mass spectrometry (DIOS-MS)

While most of the current applications in laser mass spectrometry centers on studying and exploiting MALDI mass spectrometry, researchers are still interested in matrix-free alternatives. For certain analytes, the presence of matrix cluster ions in the low mass range and difficulties in matrix crystal formation present problems during analysis. Desorption/ionization on silicon mass spectrometry (DIOS-MS) is being studied as a possible alternative application of LD/MS.[29,30] In this technique, analyte solution is aliquotted onto a porous silicon surface; this surface is a scaffold for laser irradiation. Surface morphology of the

porous silicon strongly affects desorption/ ionization.[31] This technique has only been used for a limited number of analytes.

Summary of context

As described above, LD/MS is an analytical technique considered/explored for decades and most of the current work in LD/MS centers on the MALDI technique. However, there is still interest in non-MALDI techniques. Non-MALDI experiments will allow scientists to study a larger number of analytes and can even help scientists better understand the MALDI ionization process.

Instrument Description

LD/MS instrument overview

A PerSeptive Biosystems Voyager delayed extraction laser desorption time-of-flight mass spectrometer (PerSeptive Biosystems, Inc. Framingham, MA) outfitted with a pulsed nitrogen laser (3 ns, 337 nm, ThermoLaser Science, Franklin, MA) was used for each of the experiments. This instrument was designed for the analysis of large biomolecules using the matrix-assisted laser desorption ionization (MALDI) technique developed by Karas, Hillenkamp[33], and Tanaka[34] As shown in Figure 1.1, the laser radiation is directed (using a prism) into a low pressure (10^{-6} torr) chamber containing the sample to analyzed.

Traditionally, in the MALDI technique, approximately 1uL of a dilute analyte solution is spotted onto a planar "sample plate" measuring approximately 7 cm^2.

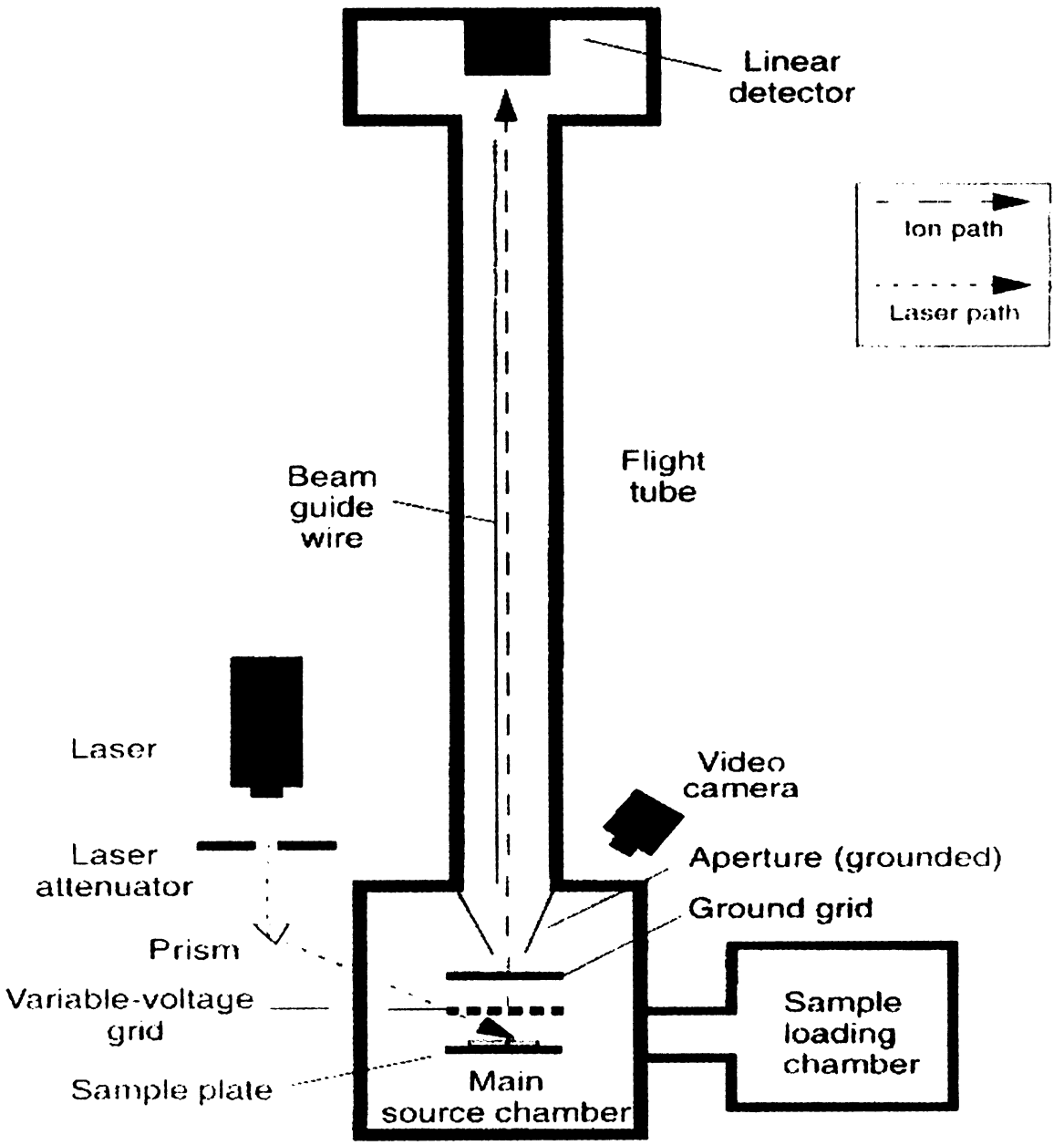

Figure 1.1: Diagram of the Voyager-DE Mass Spectrometer

This sample plate typically has 100 or 400 "wells" in which the analyte solution is deposited. Full range of X- and Y- motion of the sample plate allows a scientist using traditional MALDI to move between and around sample wells; this range of motion conveniently allows the non-MALDI user of the instrument to position the laser over different areas of a planar sample (e.g., a stamp, a thread, a coin) to collect mass spectra from various regions of the same (or different) sample.

After each laser pulse, ions are accelerated through the time-of-flight tube to a linear detector. Here, the ion current is converted from flight time into m/z ratios. The number of ions reaching the detector at a given time is described as the "ion count," the "ion abundance," or the "signal intensity." Multiple spectra can be averaged using the *Voyager Biospectrometry Data Explorer* software to improve the signal-to-noise ratio.

Additional LD/MS instrument parameters

For the positive ion LD spectra in this thesis, the accelerating voltage was +20 keV, the delay time ranged from 50 ns to 150 ns, the guide wire ranged from 0.05% to 0.2% of the accelerating voltage (but with the opposite sign), and the grid voltage was 94.5% of the accelerating voltage (unless noted otherwise).

For the negative ion LD spectra in this volume, the accelerating voltage was –15 keV, the delay time ranged from 50 ns to 100 ns, the guide wire ranged from

0.05% to 0.2% of the accelerating voltage (but with the opposite sign), and the grid voltage was 94.5% of the accelerating voltage. (unless noted otherwise).

Improving LD/MS spectral resolution

Longer delay times improve resolution for ions of larger molecules, as it compensates for the slower desorption of larger molecules, while shorter delay times yield better resolution in the lower mass region of the mass spectrum. The arbitrary "laser power" (attenuated through a neutral density filter) also can be varied. In general higher laser powers are required for analysis of heavier molecules. The guide wire running the length of the flight tube helps focus ions towards the detector; the higher the guide wire voltage, the more ions will be directed towards the detector. For some analytes, a higher grid voltage improves resolution, because for a given laser intensity, more ions are being accelerated to the detector. For other analytes, the larger number of ions being drawn to the detector (and hence the larger kinetic energy spread) yields poorer the resolution. The guide wire can range from 0% to 0.3% of the accelerating voltage (but with the opposite sign). Continually moving the location of laser spot on a sample can also influence the quality of the spectra. For some analytes (such as watercolor paints), a second laser ablation at a location on a sample produces far fewer ions than the first laser ablation of that same location. This observation is consistent with other laser desorption studies.[36] For this reason, the spectra presented in this work are an average of at least 50 individual spectra taken while continually moving the laser's location on the sample.

Calibration

In TOF-MS, to convert between the ion flight times (as collected in the mass analyzer) to the useful m/z information, a mass spectrum containing peaks representing ions of known mass must first be collected. The traditional calibration standards for MALDI are mixtures of peptides. Because most of the species studied in this work have mass-to-charge ratios below m/z 1000, to ensure the best mass determination accuracy, a calibration technique based on lower mass ions would be more accurate and useful. Laser irradiation of cesium iodide produces a set of positive ions of the formula $Cs_{n+1}I_n^+$, such as Cs^+, Cs_2I^+, $Cs_3I_2^+$. For neat analysis (i.e., ink and paint analyzed directly on the 100-well gold sample plate), 2 uL of a saturated solution of cesium iodide (99.9%; Aldrich, Milwaukee, WI) was pipetted directly onto the sample plate. For analysis of other samples, the cesium iodide solution was pipetted directly onto the surface of the sample itself (e.g., fabric, postage stamp). Most of the photographs even contained an "internal calibration standard;" the unmistakable peaks produced by the polymeric silver ions) observed in mass spectra of photographs were used to accurately assign masses to other peaks in the spectra.

Peripheral instrumentation

A JEOL HX 110 double-focusing magnetic sector mass spectrometer was used to analyze the positive ions formed following bombardment of photograph samples with 10keV Xe atoms.

A Hewlett Packard gas chromatography/mass spectrometer system (C1800B) was used to separate components of a dilution of the smoke pellet and analyze these components by electron impact ionization mass spectrometry.

Research Overview

Forensic Analysis

In some areas of forensic analysis (such as drug analysis) the instrumentation and techniques are well established and practiced. These techniques are extremely useful in forensic investigation because they probe the chemical composition of an object (e.g., infrared spectroscopy of fibers). In other areas, current forensic techniques are limited and leave conclusions open-ended. Authenticity of a painting, for example, is often determined using microscopy and subjective techniques such as considering the style of the artist's brush strokes or the artist's use of color. There are a number of other circumstances when a forensic analyst is asked to compare two samples of known and questioned origins. The more information you can determine about the chemical composition (of a fiber or glass sample, for example), the more substantive your conclusions about the relationship between the samples.

Forensic mass spectrometry

Chemical characterization of the sample of interest is the goal of many analytical forensic techniques. In mass spectrometry, the data we collect are the mass-to-

charge ratio (m/z) of ions produced from the sample. These ions represent different chemical species in the sample, and reflect the molecular mass of compounds in the sample. In some applications of mass spectrometry, fragmentation of the analyte is desirable because the fragmentation pattern can provide structural information about the analyte. In other applications of mass spectrometry, simpler ("molecular ion peak only") spectra are more useful and fragmentation undesirable. Mass spectrometry (especially through the use of gas chromatography- mass spectrometry (GC/MS)) is a powerful tool in the chemical characterization of compounds. However, some applications of forensic mass spectrometry are limited. For example, while GC/MS is established for the detection of some inks in currency security dye packs, this technique doesn't detect cationic dyes (which are also in use).

Research objectives

In this thesis research, we studied the use of laser desorption-mass spectrometry (LD/MS) for the chemical characterization of a range of forensically relevant samples. Other research in our lab[37] has recently demonstrated LD/MS as a tool for analyzing dyes in writing inks and we were curious to extend the technique to the analysis of other samples. In this research we have:

(1) evaluated the use of LD/MS in the dating of black and white photographs

(2) studied the detection and characterization of a variety of pigments found on paper substrates (i.e., watercolor pigments, stamp inks, currency printing inks)

(3) assessed the analysis of fabric dyes

(4) discussed the detection of dyes used in currency security devices

(5) evaluated the use of LD/MS in the elemental analysis of glass samples

A large number of LD mass spectra are presented in this thesis. Some of the spectra contain many peaks close to one another. These peaks could represent ions containing different elemental isotopes or they could represent two distinct ions with similar m/z values. To establish consistency in labeling, I will primarily be labeling the monoisotopic peak. For some ions, two peaks will be labeled to show the resolution between peaks.

References

(1) Watson, J. T. Introduction to Mass Spectrometry, Lippencott-Raven Publishing, Philadelphia, 1997

(2) R. J. Cotter, *Analytica Chimica Acta*, **195** (1987) 45-59.

(3) F. J. Vastola, R. O. Mumma and A. J. Pirone, *Organic Mass Spectrometry*, **3** (1970) 101.

(4) N.C. Fenner, N.R. Daly, *Material Science*, **3** (1968) 259.

(5) R. J. Cotter, *Analytica Chimica Acta*, **195** (1987) 45-59.

(6) M. A. Posthumus, P. G. Kistemaker, H. L. C. Meuzelaar , *Analytical Chemistry*, **50** (1978) 985-991.

(7) B. Spengler, M. Karas, U. Bahr, F. Hillenkamp, *Journal of Physical Chemistry*, **91** (1987) 6502-6506.

(8) R. J. Cotter, A. L. Yergey, *Analytical Chemistry*, **53** (1981) 1306-1307.

(9) R. J. Conzemius, J. M. Capellen, *International Journal of Mass Spectrometry and Ion Physics*, **34** (1980) 197- 271.

(10) M. Karas, D. Bachmann, F. Hillenkamp, *Analytical Chemistry*, **57** (1985) 2935-2939.

(11) R. Stoll, F. W. Rollgen, *Organic Mass Spectrometry*, **14** (1979) 642-645.

(12) B. Spengler, M. Karas, U. Bahr, F. Hillenkamp, *Journal of Physical Chemistry*, **91** (1987) 6502-6506.

(13) M. Karas, D. Bachmann, F. Hillenkamp, *Analytical Chemistry*, **57** (1985) 2935-2939.

(14) K. Dreisewerd, M. Schurenberg, M. Karas, F. Hillenkamp, *International Journal of Mass Spectrometry and Ion Processes*, **154** (1996) 171-178.

(15) M. A. Posthumus, P. G. Kistemaker, H. L. C. Meuzelaar , *Analytical Chemistry*, **50** (1978) 985-991.

(16) K. Dreisewerd, M. Schurenberg, M. Karas, F. Hillenkamp, *International Journal of Mass Spectrometry and Ion Processes*, **154** (1996) 171-178.

(17) L. Q. Huang, R. J. Conzemius, G. A. Junk, R. S. Houk, *Analytical Chemsitry*, **60** (1988) 1490-1494.

(18) R. Stoll, F. W. Rollgen, *Organic Mass Spectrometry*, **14** (1979) 642-645.

(19) R. Zenobi, Q. Zhan, P. Voumard, *Mikrochemica Acta*, **124** (1996) 273-281.

(20) B. Spengler, U. Bahr, M. Karas, F. Hillenkamp, *Analytical Instrumentation*, **17** (1988) 173-193.

(21) J. F. Holland, C. G. Enke, J. Allison, J. T. Stults, J. D. Pinkston, B. Newcome, J. T. Watson, *Analytical Chemistry*, **55** (1983) 997A-1012A.

(22) M. Guilhaus, V. Mlynski, D. Selby, *Rapid Communications in Mass Spectrometry*, **11** (1997) 951-962.

(23) I. J. Amster, *Journal of Mass Spectrometry*, **31** (1996) 1325-1337.

(24) L. Q. Huang, R. J. Conzemius, G. A. Junk, R. S. Houk, *Analytical Chemsitry*, **60** (1988) 1490-1494.

(25) M. A. Posthumus, P. G. Kistemaker, H. L. C. Meuzelaar , *Analytical Chemistry*, **50** (1978) 985-991.

(26) K. Tanaka, H. Waki, Y. Ido, S. Akita, Y. Yoshida, and T. Yoshida, *Rapid Communications in Mass Spectrometry*, **2** (1988) 151.

(27) J. A. McCloskey, Methods in Enzymology, vol. 193, Academic Press, San Diego. pp 29-31.

(28) M. Karas, F. Hillenkamp, *Analytical Chemistry*, **60** (1988) 2301-2303.

(29) Z. Shen et. al. *Analytical Chemistry*, **73** (2001) 612-619.

(30) J.J. Thomas, Z. Shen, R. Blackledge, G. Suizdak, *Analytica Chemica Acta*, **442** (2001) 183-190.

(32) R. A. Kruse, X. Li, P. W. Bohn, J. V. Sweedler, *Analytical Chemistry*, **73** (2001) 3639-3645.

(34) M. Karas, F. Hillenkamp, *Analytical Chemistry*, **60** (1988) 2301-2303.

(35) K. Tanaka, H. Waki, Y. Ido, S. Akita, Y. Yoshida, and T. Yoshida, *Rapid Communications in Mass Spectrometry*, **2** (1988) 151.

(36) A. M. Leach, G.M. Hieftje, *Analytical Chemistry*, **73** (2001) 2959-2967.

(37) D. M. Grim, J. Siegel, J. Allison, *Journal of Forensic Science*, **46** (2001) 1411-1420.

Chapter 2: Black and white photographs

Introduction

Recent discovery of forged photographs has called for the development of forensic techniques capable of analyzing and dating photographs. A forged photograph may be made from original negatives after the photographer's death. Artistic study of the print can't distinguish the forged prints from the originals, because the forged and genuine images are the same. Other characteristics could also be misleading. The forgeries could be printed on older materials. The genuine prints/ forgeries may not have distinguishing features such as the artist's signature. The key difference between the originals and the forgeries would be the age of the print. And genuine prints could be quite old since photography using silver halide chemistry was first recorded in 1802[1].

The Detroit Institute of Art (DIA) recently acquired forged photographs allegedly "signed" and printed by Lewis Hine[2]. Some of the prints were identified as forgeries because the printing paper contained a fluorescing brightening agent. These additives were introduced in the 1950's and would not have been present in a paper available to Hine prior to his death in 1940.

We were asked by scientists at the museum to determine whether genuine black and white photographs could be distinguished from forged ones using LD/MS.

We were interested in learning whether the surface composition, as detected by LD/MS, changes predictably with time. A number of photographs ranging in date from pre-1900 to the present, were collected. Some of the photographs were dated at the time of printing, but most were not. There was no standard storage of these photographs over the years, and they are most definitely un-controlled samples. In addition, the DIA generously provided samples of photographs developed using different developing solutions. For analysis, a portion of each photograph was securely taped onto the sample plate described earlier.

The dominant peaks in spectra of most of the photographs represent silver ions and small clusters of silver ions formed in the instrument. A clean, representative positive-ion mass spectrum of a photograph developed In 2001 is shown in Figure 2.1a.

The peaks at m/z 23 and m/z 39 represent sodium ions (Na^+) and potassium ions (K^+), respectively. The peaks at m/z 107 and m/z 109 represent the two isotopes of silver ions; they correspond well with the isotope distribution of small silver clusters, shown in Figure 2.1b, 2.1c, 2.1d. The clusters of peaks around m/z 216 and around m/z 323 represent silver dimer (Ag_2^+) and silver trimer (Ag_3^+) ions, respectively.

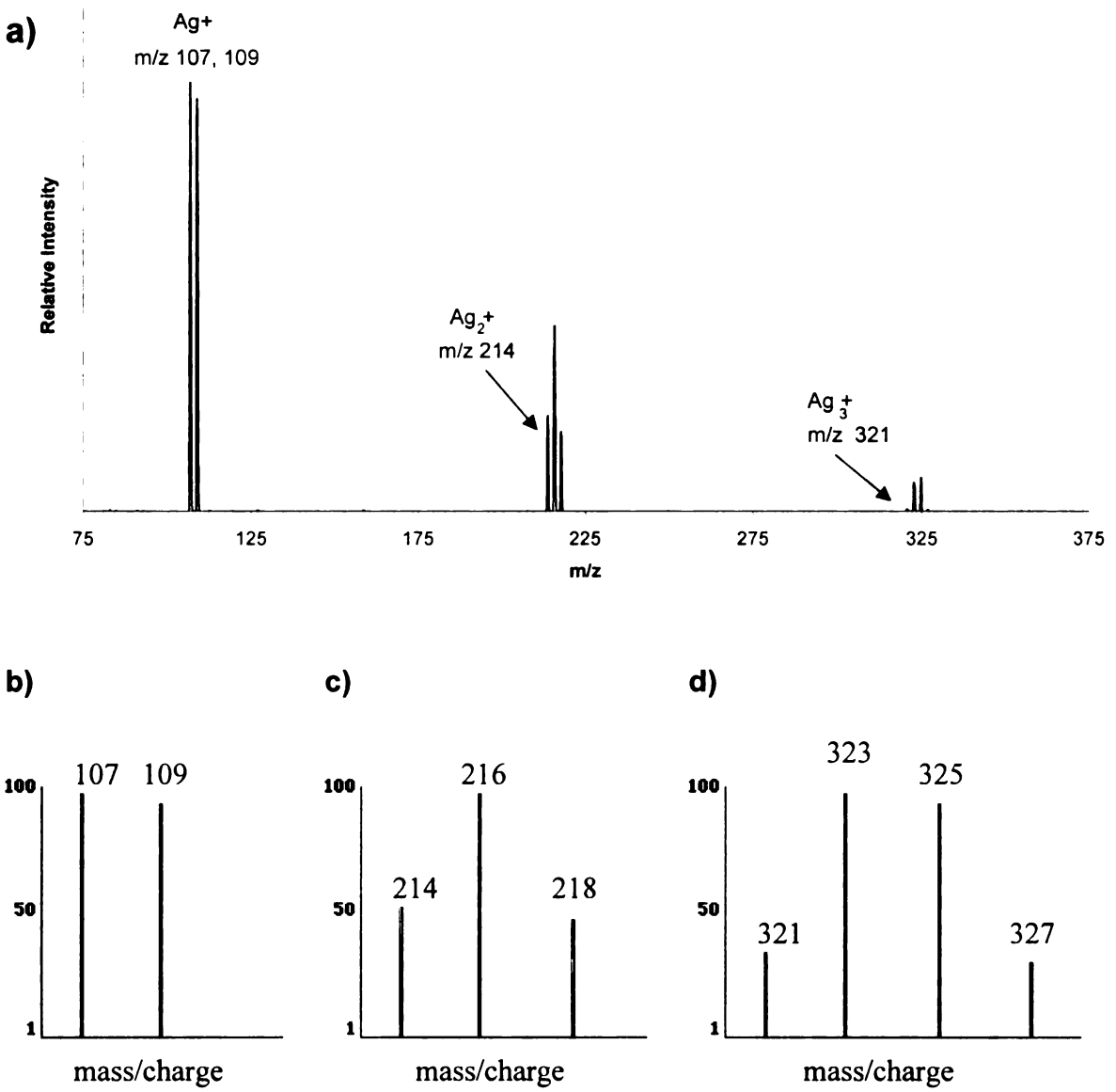

Figure 2.1: a) Positive-ion LD mass spectrum of a photograph developed in 2001, b) theoretical isotope distribution of silver monomer ions (Ag^+), c) theoretical isotope distribution of silver dimer ions (Ag_2^+), d) theoretical isotope distribution of silver trimer ions (Ag_3^+)

Silver sulfides

The spectrum shown above in Figure 2.1a was taken of a photograph developed just a few months before analysis. As easily seen, the spectrum is simple and clean, with little chemical noise. Spectra of other photographs were much more complex with more chemical noise, and unidentifiable peaks. A positive-ion mass spectrum of a black and white photograph developed in the 1950's is shown in Figure 2.2.

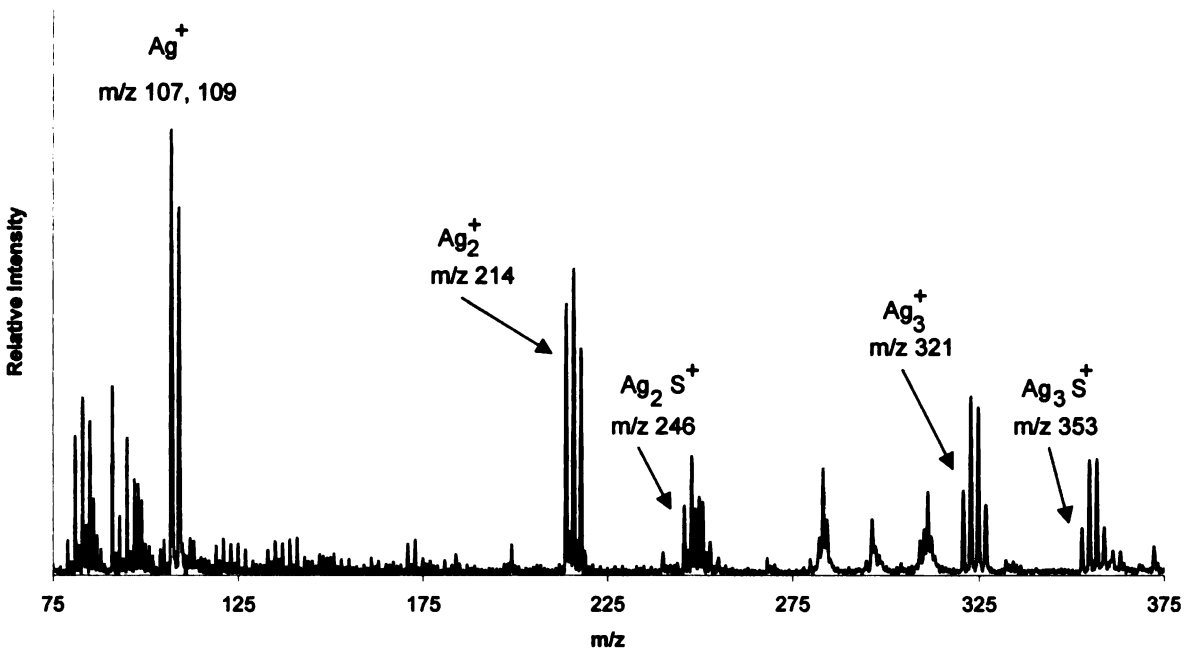

Figure 2.2: Positive-ion LD mass spectrum of photograph developed in the 1950's

Once again, peaks representing Ag^+, Ag_2^+, and Ag_3^+ feature prominently on the spectrum. Hidden amongst other peaks on the spectrum, there is a cluster of peaks at m/z 248 and another cluster at m/z 356. These peaks appear 32 mass

units higher than the silver dimer and trimer ions and represent the $(Ag_2+32)^+$ and $(Ag_3+32)^+$ ions. These ions could represent silver oxide ions ($Ag_2O_2^+$ and $Ag_3O_2^+$), however, because peaks representing Ag_2O^+ and Ag_3O^+ were not observed in the mass spectra, this assignment seemed unlikely and was rejected in favor of a silver sulfide assignment. The cluster of peaks at m/z 248 and the cluster at m/z 356 likely represent the Ag_2S^+ and the Ag_3S^+ ions, respectively. The theoretical isotope distribution for these silver sulfide ions is shown in Figure 2.3.

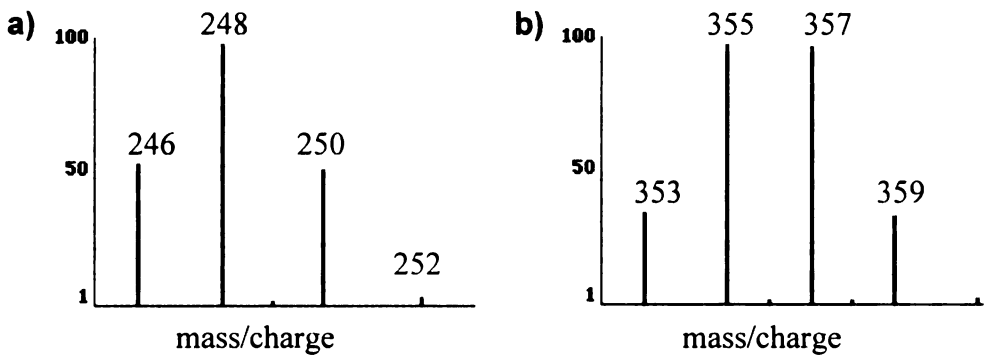

Figure 2.3: Theoretical isotope distribution of a) Ag_2S^+ and b) Ag_3S^+

Peaks representing silver sulfides appeared more often in mass spectra of older photographs than in mass spectra of newer photographs; this suggests that silver on the surface on the photographs converts to sulfides over time and that silver sulfide content could be used as a potential dating tool. We suspected that either sulfur-containing gases (such as H_2S) in the air or sulfur in the gelatin (protein network) containing the silver image was responsible for a slow conversion of

silver metal to silver sulfide. We decided to look for a correlation between the age of a photograph and its silver sulfide content (as determined by LD/MS).

Because ion intensity, listed on the mass spectrum, depends on the intensity of the irradiating laser, a simple comparison of silver sulfide peak heights from spectra of different photographs might not be a reliable indicator of silver sulfide content. Instead, the ratio of the intensity of the peak representing the silver sulfide to the intensity of the peak representing the corresponding silver cluster (i.e., ratio of Ag_2S^+ to Ag_2^+) was chosen as a more reliable point of comparison. The resulting plot of ratios versus the date of print development is shown in Figure 2.4. Some of the data points are deceptively simple; for example, the value of zero at the point representing Ag_2S^+ to Ag_2^+ ratio for 2001 actually represents 4 distinct photographs.

As seen, there is no obvious correlation between the silver sulfide content on the surface of a print and its age. The silver sulfide present in many of these prints likely did not occur slowly over time, but rather probably were formed at the time of development. The sulfides could have come from a variety of sources. Nearly every print-developing solution contains sulfites and sulfates as solution preservatives. The developing solutions and conditions are an important variable with a considerable effect on the final chemical composition of the surface of the print. In addition, some photographs, may have intentionally been "silver sulfide toned"[3]. This is a process in which some of the surface silver is intentionally

converted into (the browner) silver sulfide for aesthetics. This technique could explain why some of the photographs have strikingly high sulfide content.

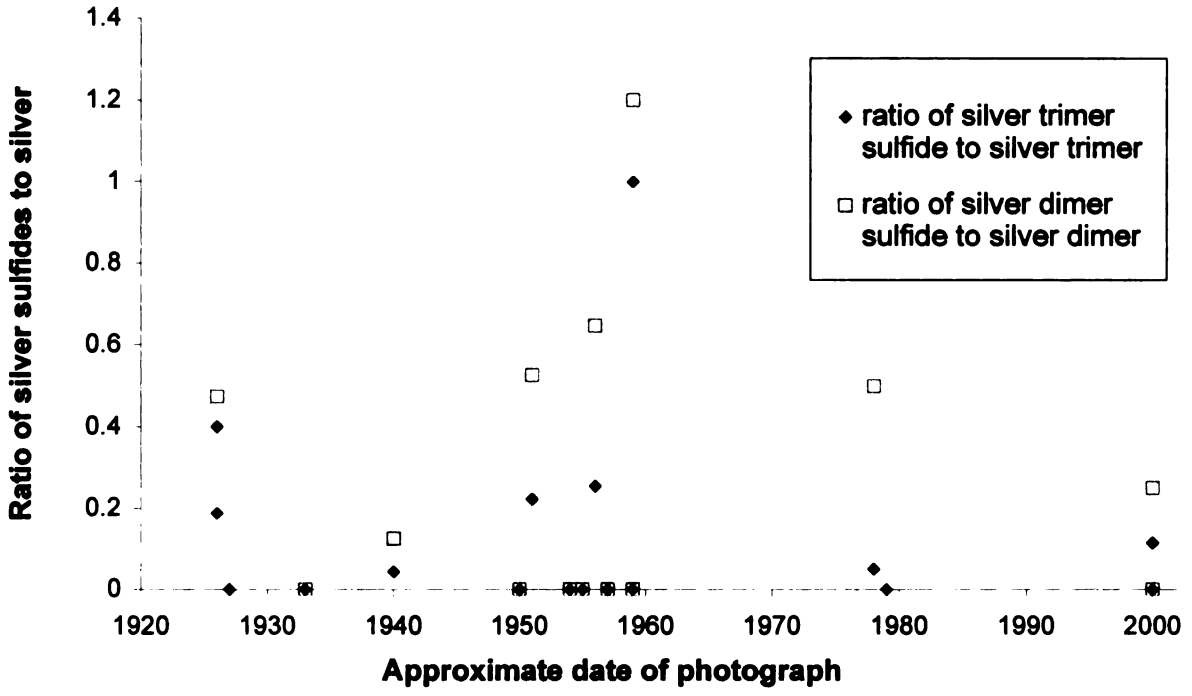

Figure 2.4: Graph of ratio of silver sulfides to silver vs. the approximate date of printing of the photograph

Halide detection and content

The presence of halides (chlorine, bromine, and iodine) was occasionally observed in positive-ion mass spectra such as the one shown below in Figure 2.5 and were an even more noticeable feature in spectra obtained in negative-ion mode.

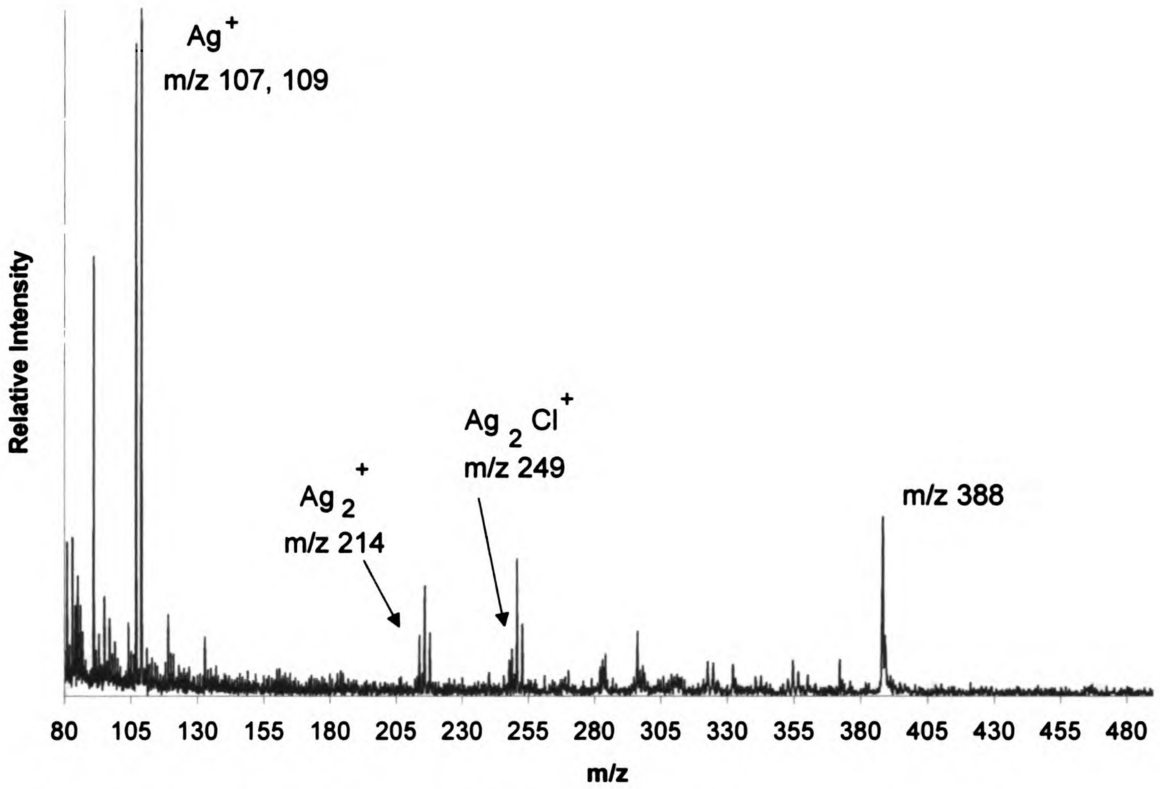

Figure 2.5: Positive-ion LD mass spectrum of a photograph. The presence of chlorine is noted on the spectrum at m/z 251.

The silver halides were a prominent feature of the negative-ion mass spectra and could be tied to the history of the photographic paper. Light sensitive silver halides coat the photographic paper before exposure to light; silver metal produced through the reduction of these silver halides forms the silver image of the print. By recognizing and following the pattern of $Ag_nX_{(n+1)}^+$ (where X is Cl, Br, or I), it was possible to assign elemental compositions to a majority of peaks in spectra such as that shown in Figure 2.6.

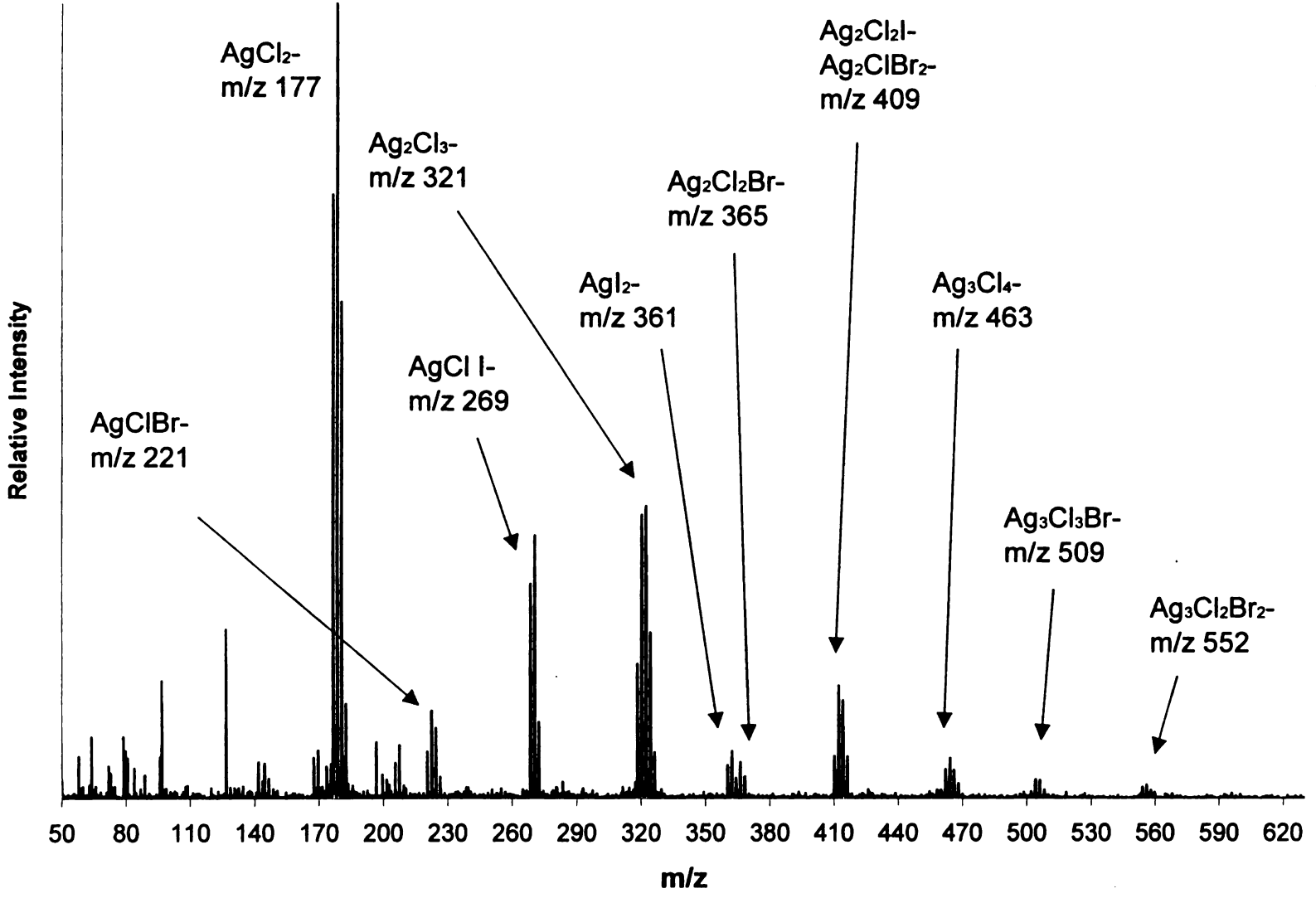

Figure 2.6: Negative-ion LD mass spectrum of a photograph. The presence of several silver halide ion clusters is noted on the spectrum

Some spectra were dominated by one halogen. Below, Figure 2.7a shows high levels of chlorine detected, while Figure 2.7b shows high levels of iodine.

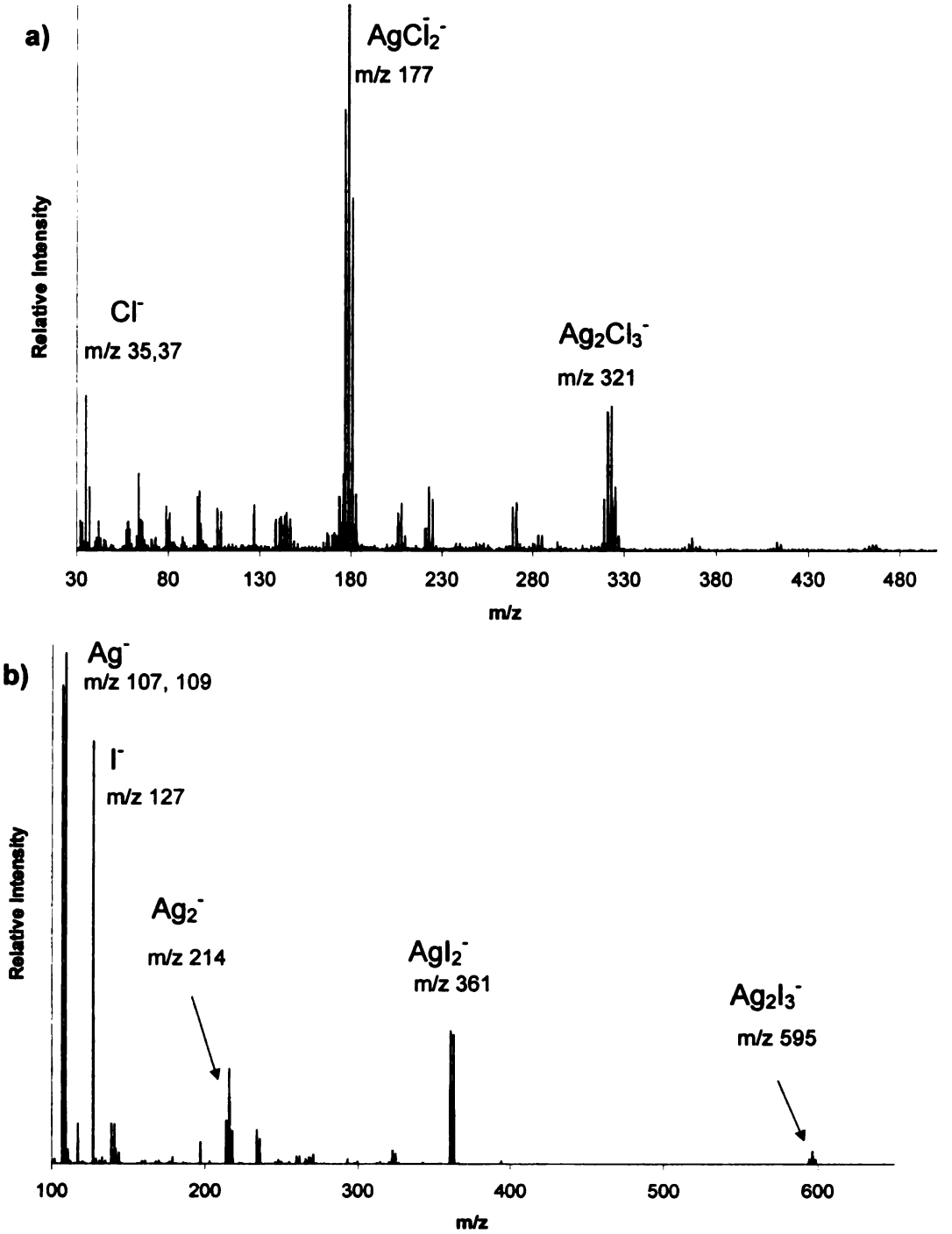

Figure 2.7: Negative-ion LD mass spectra of photograph in which a) silver chloride cluster ions produce the dominant peaks on the spectrum and b) silver iodide cluster ions produce the dominant peaks on the spectrum.

Since it's established that different silver halides have different reactivity toward light and development[4], we were interested in trends or shifts in the composition of photography paper through the years. For example, because of primitive printing techniques, the less light-sensitive silver bromide papers (a.k.a. "gas-light papers") were popular with home developers in the 1920's[1].

Again, the absolute peak height and peak intensity of the silver halides will vary depending on the intensity of the laser used to form the ions. To compensate for this, the ratio of the halides to one another (i.e., Cl:Br), rather than the individual peak intensity was plotted with respect to the date of development of the prints. Each halide was calculated by including the halide present as monoatomic ions (i.e., Cl^-) as well as the halide present in the silver halides (i.e., $AgCl_2^-$ $AgClBr^-$). For example, if the only peaks on the mass spectrum of a photograph developed in 1938 were $AgCl_2^-$, $AgBr_2^-$, and $AgClBr^-$, the halide ratio would be calculated as follows:

Table 2.1: Calculation of relative content of chlorine and bromine from negative-ion LD mass spectrum of photograph

Ion	Peak intensity (compared to most intense peak on mass spectrum)	"relative content of Cl"	"relative content of Br"
$AgCl_2^-$,	58%	2(58) =116	0
$AgBr_2^-$,	35%	0	2(35) = 70
$AgClBr^-$	14%	1(14) = 14	1(14) = 14

Total Cl represented on the mass spectrum = (116 + 14) = 130
Total Br represented on the mass spectrum = (70 + 14) = 84
Ratio of Cl to Br = (130/84) = 1.55
On the graph of Cl:Br, one would plot a single point:
[x = 1938 (the year of print development), y = 1.55]

The resulting plot of ratios versus the date of print development is shown in Figure 2.8.

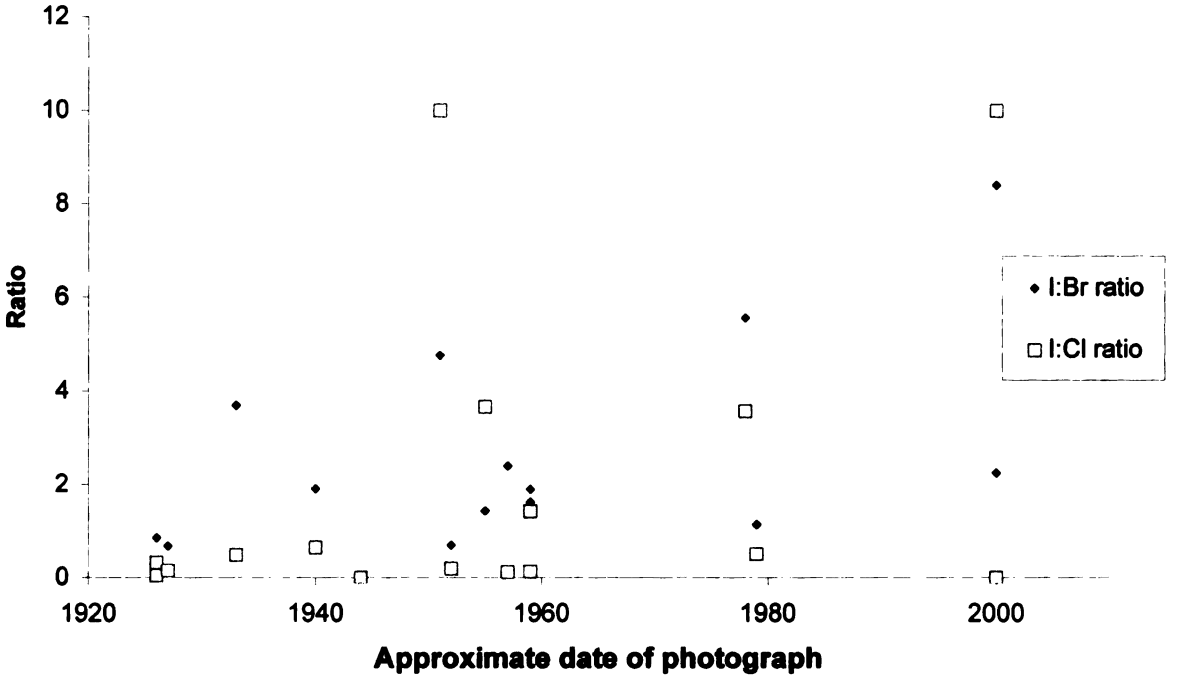

Figure 2.8: Graph of ratio of halide content vs. the approximate date of printing of the photograph.

As seen, there was no obvious trend in halide content over time. We're not sure if that is because the halide content hasn't changed in a predictable way over the years or because the technique is not accurately reflecting the change in halide content. Not all the chorine detected in the LD/MS experiments necessarily came from the silver salts. Some could have come from ordinary salt, sodium chloride, left behind from years of fingerprints on the photograph. Similarly, the bromine detected in the LD/MS experiment may also have come from sources other than

the silver salts in the paper itself. The bromine detected may have come from developing chemicals such as potassium bromide, a common anti-fogging agent, used for years[4]. While ions containing chlorine, bromine, and iodine are readily detected in LD/MS, the source of these detected halides is not controlled, making this possible dating technique unreliable.

What exactly is being detected?

Since the development process begins with a sheet of paper coated with silver salts embedded in gelatin and eventually ends with a piece of paper with regions of the dark reduced silver metal forming the image in the gelatin, we were curious to learn whether the silver peaks observed in the spectra were due to the reduced silver metal or due to residual silver salts. Positive-ion spectra taken of silver chloride powder and spectra taken of reduced silver metal powder are shown below in Figures 2.9a and 2.9b.

As shown, on both spectra, the peaks representing silver ions resemble spectra obtained from LD/MS of actual photographs. Unfortunately, this does not distinguish which species produces the observed peaks on the spectra of actual photographs. One is left with just the conclusion: "it could have been either species."

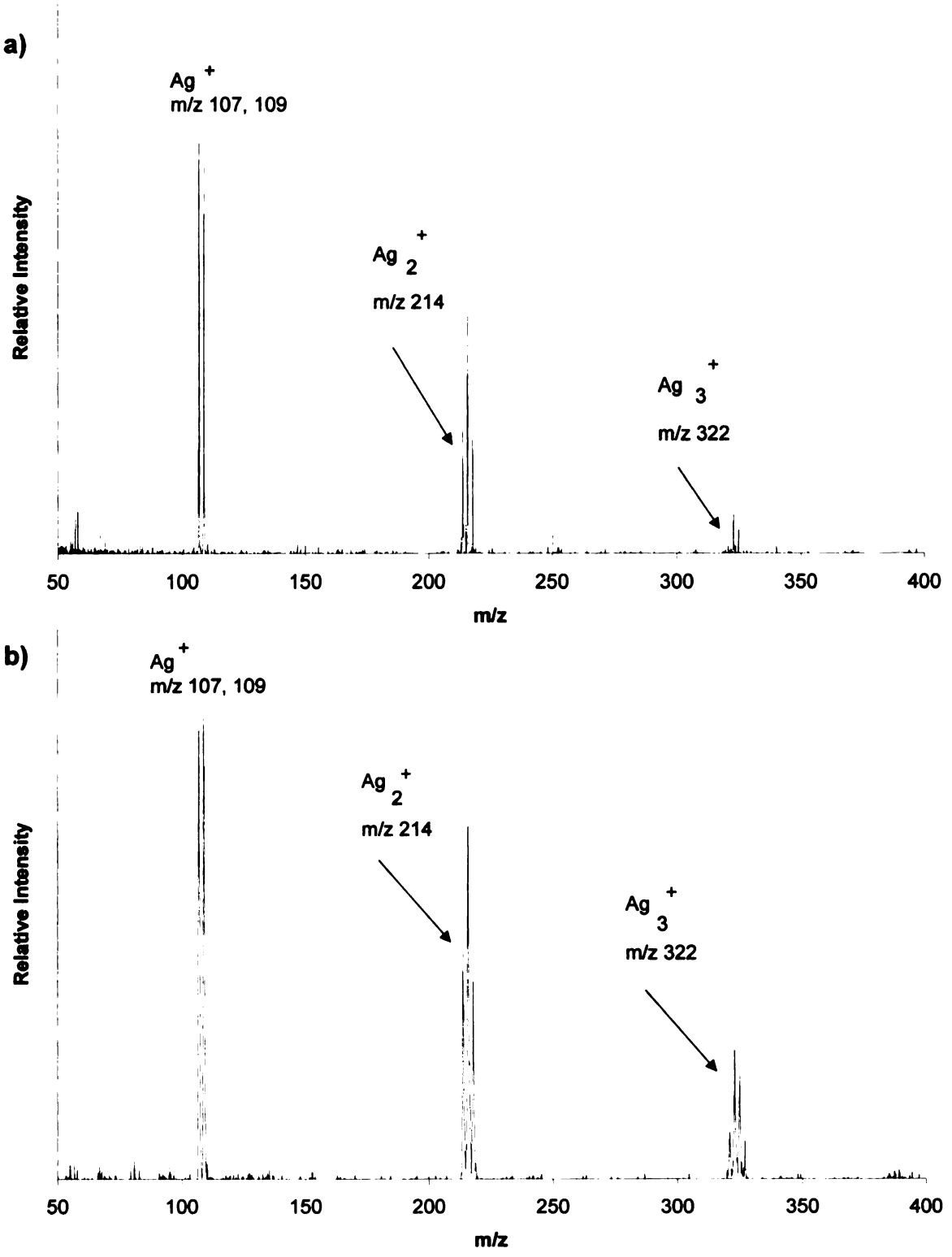

Figure 2.9: Positive ion LD mass spectrum of a) silver metal powder and b) silver chloride powder

To explore this question further, we considered the chemistry of the silver image. The lightest regions of the photographs are the areas from which all silver salt was purportedly/ allegedly washed away. The darkest regions of the print should yield the more intense peaks representing silver, because the reduced silver clusters produce the dark image. However, the spectra of these areas revealed very little intra-photograph variation. In fact, spectra taken of lighter regions and darker regions of the same photograph were often indistinguishable!

Spectra of the back of some photographs were taken in attempts to analyze various inks and stamps on the back of the print. Curiously enough, spectra of the back of the prints often mimicked the spectra from the front of the prints. Remember, the back of the print holds no image and therefore should not produce spectra with peaks representing silver and silver halides. It is possible that the front of one photograph may have rubbed against the back of another while stored in a stack. However, the lack of intra-photograph variation was remarkable (spectra taken of the back of a photograph looked much more like spectra taken of the front of that same photograph rather than the front of others) and combined with the consistency between spectra obtained from dark and light regions of the prints, a new theory emerged.

During the print development process, the prints are fully immersed and washed in several developing solutions. As the print is transferred from solution to solution, it carries along a history of its processing. Could it be the chemicals in

the developing solutions that were being detected, not the chemicals exclusive to the paper?

It's a surface technique

A piece of non-photographic paper was immersed in a set of used developing solutions and subsequently washed. When the photograph is removed from the final developing solution, it is still wet with a thin film of the final wash bath. As the photograph dries, residual amounts of chemicals from the developing and wash solutions remain on the surface of the print. Spectra taken of this paper had peaks representing silver and its halides. This suggested the theory that the LD/MS experiment was only detecting species on the very surface of the photographs.

The chemistry of the developing process occurs in a gelatin. The gelatin is a network of protein. It is permeable and swells when in solution. So regardless of how many times the photograph is rinsed, the silver salts and other chemicals intricately infused into the gelatin layer of the printing paper may slowly "leech" out of the complex gelatin network. This observation reveals the surface sensitivity of the technique of LD/MS and reveals a key challenge with this type of analysis. The surface is the part of the photograph which is most affected by external, environmental conditions.

The "surface analysis only" theory is supported by how quickly an area on the photograph appears to become "depleted" of ions during laser ablation. Similarly, FAB analysis of the photographs yielded silver cluster peaks initially; while a short time later, masses consistent with amino acid residues were observed. These amino acid residues could be fragments of the gelatin used on one side of the print to "hold" the silver image.

Usefulness, feasibility of the analysis of organic additives

The analyses described above show halide and sulfide dating strategies by LD/MS as inconclusive and ineffective. Identifying developing chemicals used in printing the photograph could aid in narrowing down the time frame of development of a print. Although "contemporary" photograph development has been around since approximately 1850[1], certain developers and additives were introduced at later dates. To explore this avenue, we analyzed various photographs (provided by the Detroit Institute of Art) printed using different developers such as those shown in Figure 2.10.

No distinguishing peaks were observed on spectra taken of these photographs. Concentrated amounts of developers were analyzed neat (commercially available developing solutions pipetted directly onto the sample plate).

Ultra-violet absorption spectra of metol and hydroquinone show that these compounds are not strong UV absorbers around 337 nm (the wavelength of laser

irradiation). Based on proposed mechanisms of direct laser desorption, we concluded that these developers are not able to absorb enough energy to desorb and ionize.

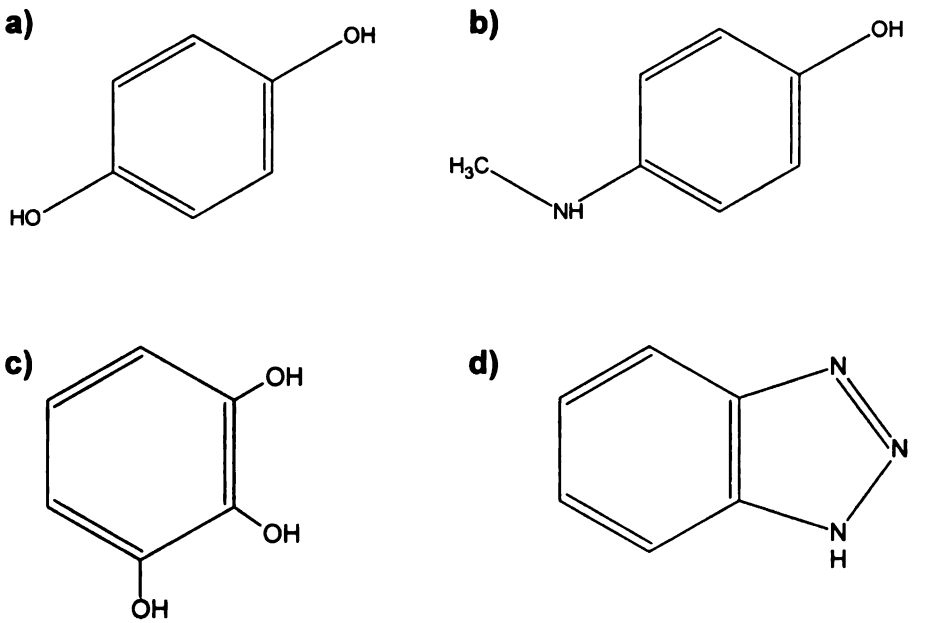

Figure 2.10: Structures of some organics encountered in print developing: a) hydroquinone (developer); b) metol (developer); c) pyrogallol (developer); d) benzotriazole (restainer)

While it is possible to look for a specific additive (i.e., a developer), organic compounds (compounds containing carbon, hydrogen, nitrogen, and oxygen) have the same general isotope pattern. Many different combinations of these elements could produce a peak at, for example, m/z 321. In response to this, we can consider the lower mass regions of the spectra, for elemental ions, or we

focus on detection of compounds with more complex isotope distribution patterns.

Analysis of photographs treated with toners

Toners are an easy way to alter the appearance of a photograph and could be used to convert the silver metal image to different colors and tints. For example, the "standard chromium intensifier" uses potassium dichromate as a key reactant to convert the reduced silver image into a "more opaque combination of silver and chromium"[3] Another toner, "copper brown toner" combines copper sulfate and potassium ferricyanide to produce red-brown hues[3].

Selected photographs were treated with each of these toners and washed thoroughly after processing. A positive ion mass spectrum of the photograph treated with the "standard chromium intensifier" is shown in Figure 2.11. The peak at m/z 52 represents chromium ions; no peaks suggested the presence of the dichromate ion (an ion with charge of –2).

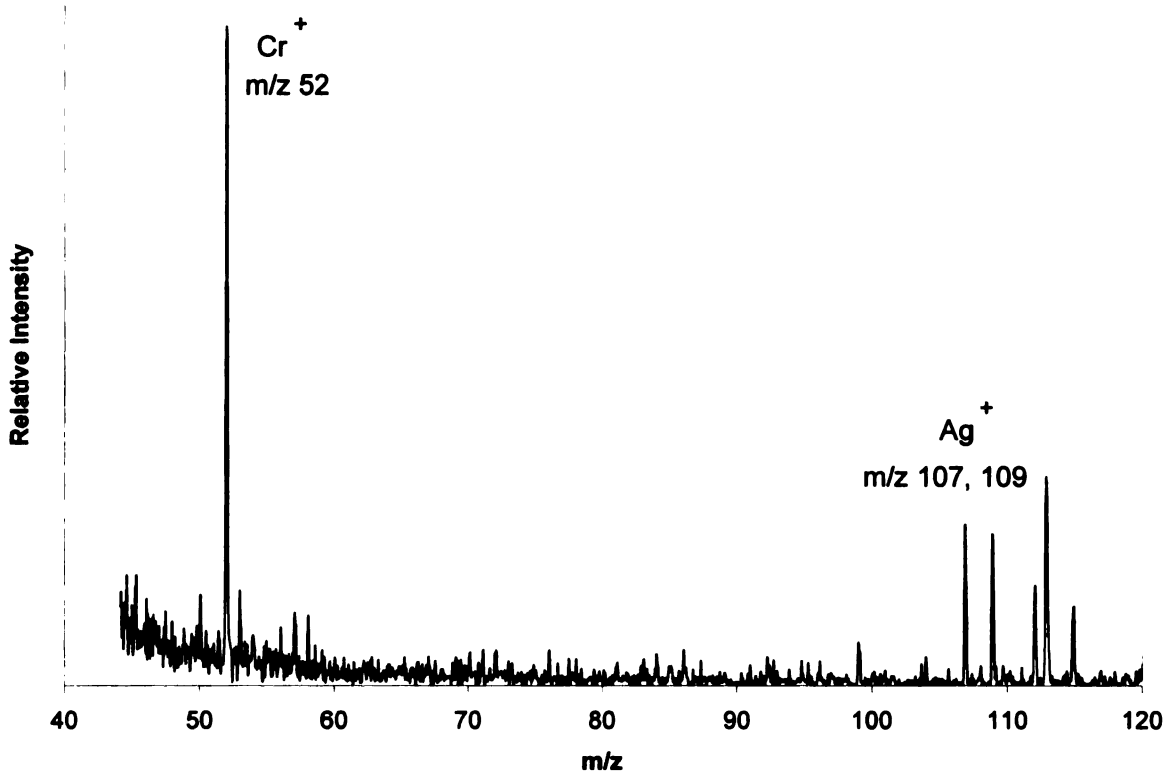

Figure 2.11 Positive-ion LD mass spectrum of a photograph treated with the "standard chromium intensifier" toner as described in reference 3

A negative-ion mass spectrum of the photograph treated with "copper brown toner" is shown in Figure 2.12. A set of copper-cyanide combinations is observed ranging from m/z 115 to m/z 386. Each ion contains one more cyanide group than copper. The peaks at m/z 115 and 117 represent the $Cu(CN)_2^-$ ion, the peaks at m/z 204 and 206 represent the $Cu_2(CN)_3^-$ ion, the peaks around m/z 295 represent the $Cu_3(CN)_4^-$ ion, and the peaks around m/z 384 represent the $Cu_4(CN)_5^-$ ions. Notice the peak pattern get more complex with the addition of each subsequent copper because copper has two isotopic forms. ^{63}Cu (69%) and ^{65}Cu (31%).

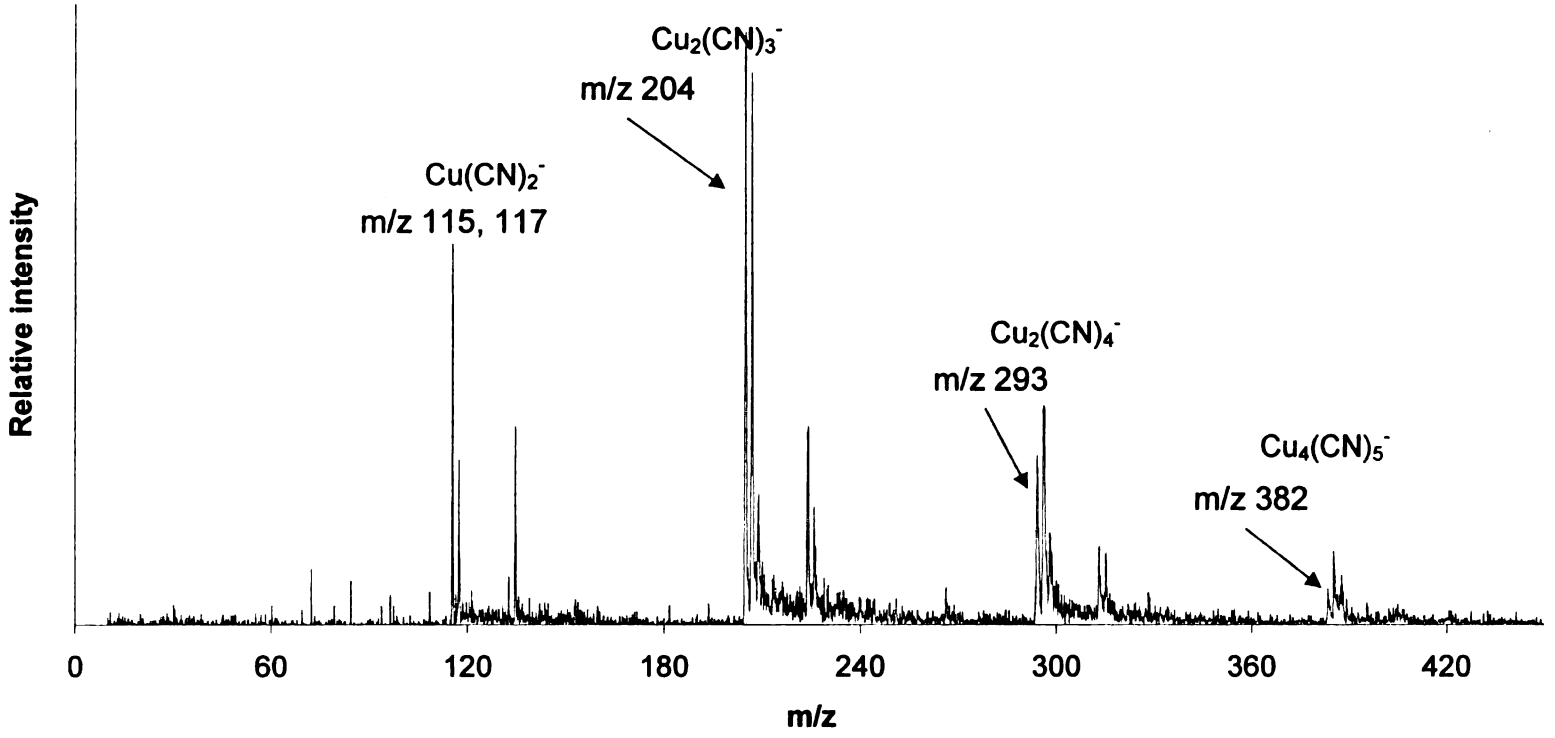

Figure 2.12: Negative-ion LD mass spectrum of a photograph treated with "copper brown" toner as described in reference 3

Summary and application

LD/MS is extremely useful in the detection and identification of species found on the surface of photographs, but we were not able to develop a systematic, quantitative application of LD/MS to the dating of prints. However, LD/MS can still be useful in the forensic analysis of prints. The presence of certain chemical species on the surface of a print (such as toners) can mark the earliest possible date of development of a print. We also noted that just a sliver of the white margin of a print could be used for analysis, thus requiring minimal sample destruction of photographs too large for direct insertion into the instrument. Preliminary analysis of a dozen tintypes (silver image "photographs" printed on a metal substrate rather than on paper), common in the late 1850's through the early 1900's, yielded well-resolved spectra similar to spectra taken of paper photographs. LD/MS could be useful in characterization of the surface of tintypes (and even daguerreotypes (silver images on glass)) as well. Perhaps the most interesting aspect of the mass spectra presented in this chapter is that results were obtained at all. It is pretty incredible that one can directly irradiate a photograph (even a 100-year old print) and obtain a well-resolved mass spectrum containing peaks representing species on the surface of the print.

References

(1) O. Wheeler, Photographic Printing Processes, American Photographic Publishing, Boston, 1930.

(2) M. Falkenstein, "*The Hine Question*," Art News, May 2000.

(3) C. Graves, The Elements of Black and White Printing Focal Press, Boston, 2001.

(4) C.E. K. Mees, The Theory of the Photographic Process, 3rd edition, The MacMillian Co, New York, 1966.

Chapter 3: Watercolor pigments

Introduction and methods

Two pigments PR 122 (Pigment Red number 122) and PV 23 (Pigment Violet number 23) were each noted in the *Wilcox Guide to the Best Watercolor Paints*[1] as having poor lightfastness. In this book, these two pigments were given a rating of III on the American Society of Testing and Materials (ASTM) lightfastness scale. This scale ranges from ASTM I ("excellent lightfastness") to ASTM V ("pigments will bleach very quickly"). The poor lightfastness of these pigments prompted us to investigate the use of LD/MS as a possible tool for studying the degradation of these pigments.

Identifying a pigment used in a painting can help pinpoint the time period when the artist painted the piece. Identifying the pigments used to create a painting can help establish the authenticity of a painting[2]. Chemical identification of an artist's materials is also of social and cultural interest[3]. X-ray fluorescence[3, 4] and Raman analysis[5] have been used to analyze watercolors, but relatively few analytical techniques have been applied specifically to the analysis of watercolor pigments (particularly for fear of damaging the paper substrate of the painting).

Two commercial paints were purchased for analysis. The pigments were analyzed neat (directly off a gold sample plate) for confirmation of the paint's pigment content. The paints were then diluted and painted onto watercolor paper. Portions of the "painting" were inserted in the ion source and the watercolor

paper was directly irradiated; this simulates the application of LD/MS for direct analysis of pigments in a painting. For all samples, cesium iodide was used for calibration.

Structure of Pigment Red 122

The structure and theoretical isotope distribution of Pigment Red 122 are shown in Figure 3.1.

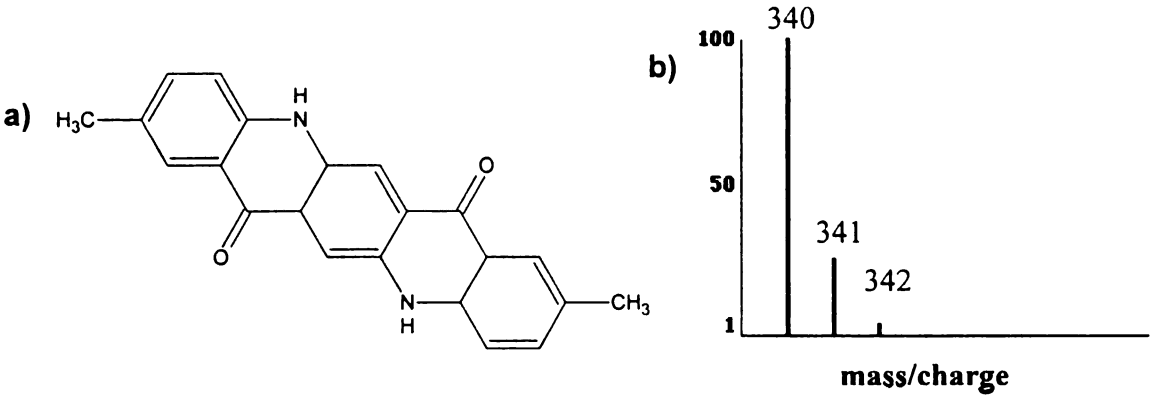

Figure 3.1: Pigment Red 122: a) structure and b) theoretical isotope distribution

PR 122 is a neutral dye (of the quinacridone class) and is detected in both the positive ion and negative ion modes. A positive-ion laser desorption mass spectrum of the paint taken directly off the sample plate is shown in Figure 3.2 and a negative-ion laser desorption mass spectrum of the paint taken directly off the sample plate is shown below in Figure 3.5.

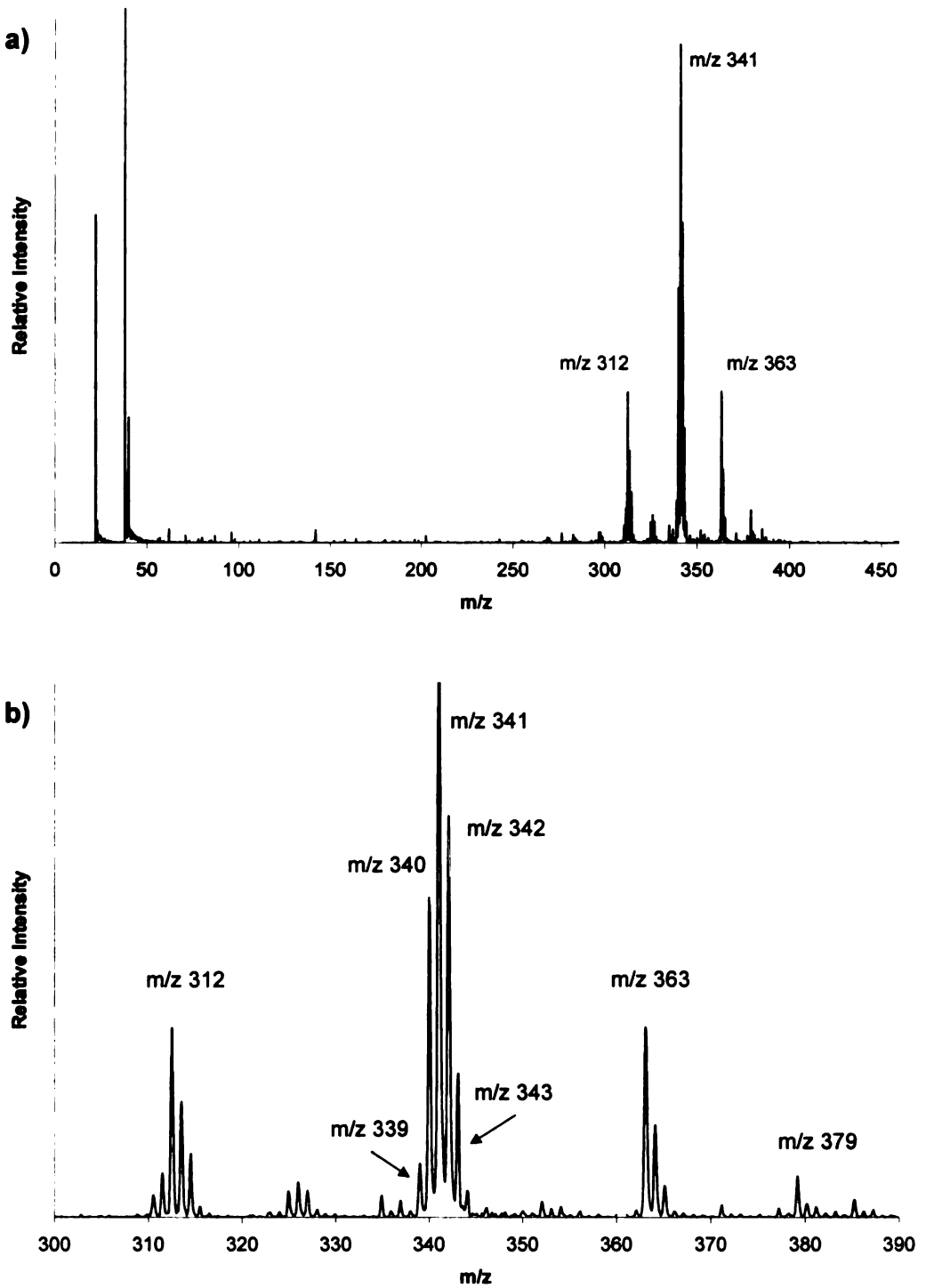

Figure 3.2: Positive ion LD mass spectrum of PR 122 obtained directly off the gold sample plate: a) m/z 0-460; and b) m/z 300-390

Interpretation of the positive-ion mass spectrum of PR 122

The peak at m/z 340 represents the molecular ion. One expects the ^{13}C isotopes at m/z 341 and m/z 342. The peak at m/z 339 most likely represents the molecular ion minus a hydrogen, $(M-H)^+$, and once again, one expects ^{13}C isotopes (m/z 340 and m/z 341). The theoretical isotope distribution for the deprotonated molecule is shown in Figure 3.3a.

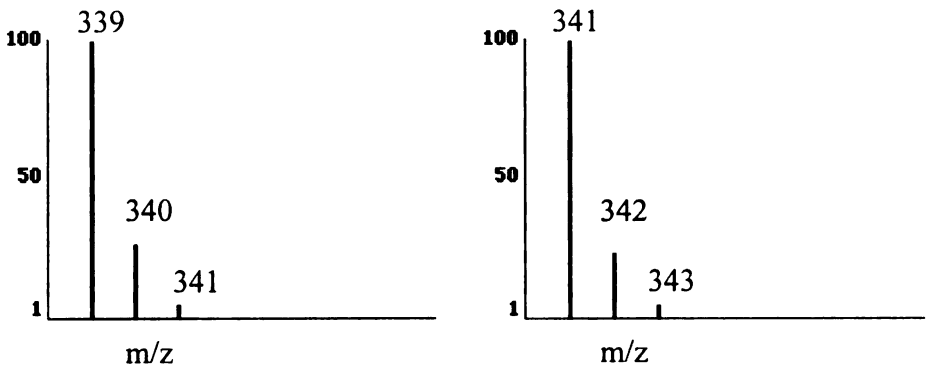

Figure 3.3: Theoretical isotope distribution of a) deprotonated PR 122 $(M-H)^+$ and b) protonated PR 122 $(M+H)^+$

The dye has an extended aromatic structure and is capable of supporting the loss of a proton and electron ($H^{\cdot}$). This dye is similarly capable of supporting the addition of a proton (H^+). It is not possible to determine whether the m/z 341 peak represents exclusively an isotope of M^+ or whether this peak represents to some degree the $(M+H)^+$ ion. The presence of the small peak at m/z 343, however, is likely an isotope of the $(M+H)^+$ ion. The theoretical isotope distribution for the $(M+H)^+$ ion is shown in Figure 3.3b.

The presence of at least two (and possibly three) ionic species representing the molecule (and their overlapping mass spectral peaks) reconciles the expected (theoretical) mass spectrum of the dye (based on its chemical formula) with the observed spectral peaks.

Additional evidence for this phenomenon is observed slightly further up the spectrum. The peak at m/z 363 likely represents sodium adducts of the m/z 339 ion: $(M+Na)^+$. Adding a salt (Na_2CO_3) to the paint as it was applied to paper for analysis led to an increase in the peak height at m/z 363, confirming that this peak represents sodium adducts of the original dye molecule. The peak at m/z 379 similarly represents a potassium adduct of the m/z 340 ion: $(M+K)^+$.

The peak cluster around m/z 312 represents the demethylated pigment. This is a distinct compound and likely an impurity in the pigment mixture. The structure of this molecule is shown in Figure 3.4.

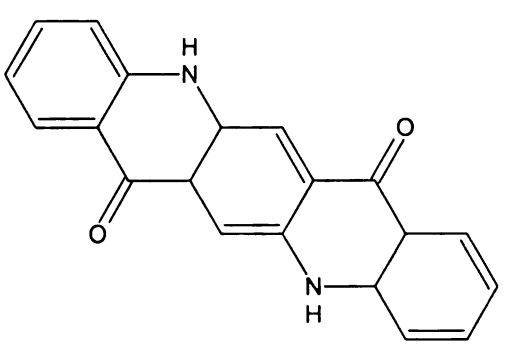

Figure 3.4: Structure of demethylated PR 122

This $(M-2CH_3+2H)^+$ ion is structurally similar to the molecule of interest (PR 122), however the two methyl groups present on PR 122 have been replaced with hydrogens, yielding an ion mass 28 mass units lower than the expected molecular ion, M^+. Because the m/z value of these peaks corresponds to hydrogen substituted in place of the methyl groups, rather than simply the loss of methyl groups (without substituted hydrogens), we conclude that these peaks represent impurities in the pigment mixture, and are not fragments formed in the ion source.

Interpretation of the negative-ion mass spectrum of PR 122

A negative-ion laser desorption mass spectrum of the dye is shown below, in Figure 3.5.

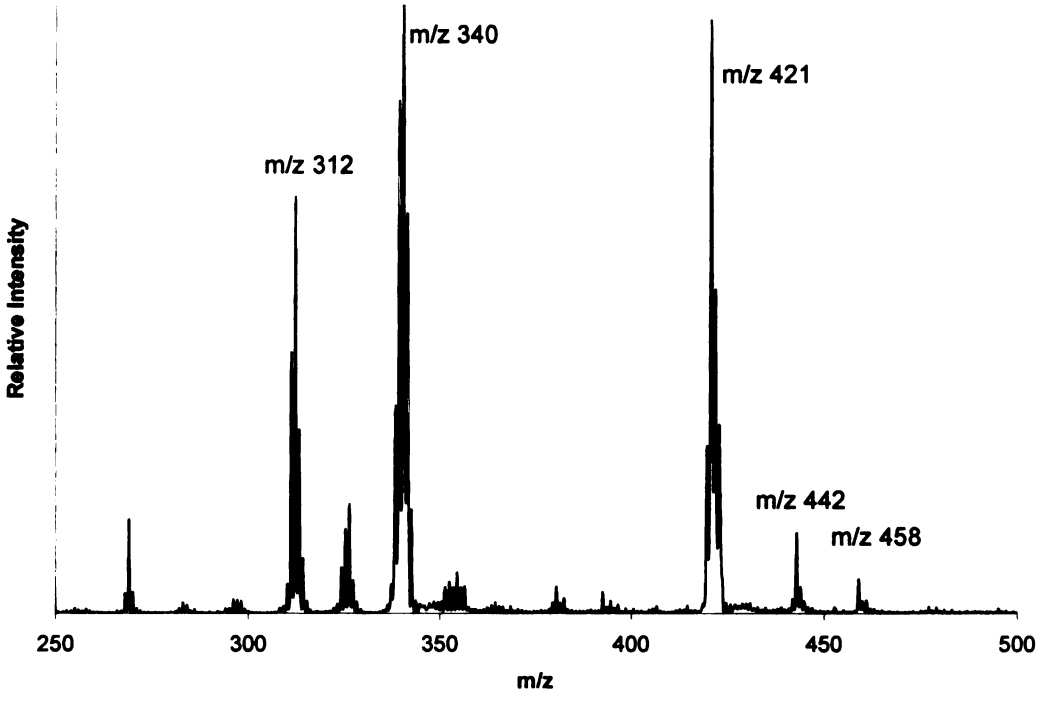

Figure 3.5: Negative ion LD mass spectrum of PR 122 obtained directly off the gold sample plate

Again, peaks representing the dye molecule are dominant on this mass spectrum. The peak at m/z 340 represents the molecular ion, M^-, the peak at m/z 339 represents the deprotonated ion $(M-H)^-$, and the peak at m/z 338 likely represents the dye molecule stripped of two hydrogens, $(M-2H)^-$.

The peak at m/z 312 represents the demethylated dye molecule $(M-2CH_3+2H)^-$. The peak at m/z 311 represents a similar ion, $(M-2CH_3+H)^-$. The peaks near m/z 326, observed to a lesser degree on the positive-ion mass spectrum, likely represent partially demethylated dye molecules $(M-CH_3+H)^-$. These would be molecules for which one methyl has been replaced by a hydrogen and one methyl group is present. The structure for one such molecule is shown in Figure 3.6.

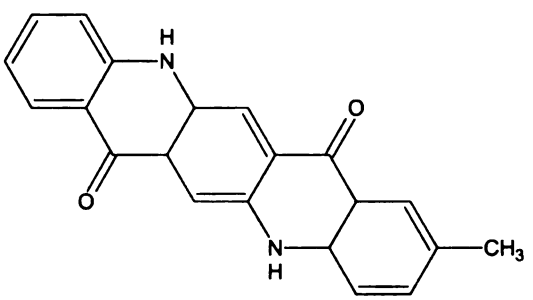

Figure 3.6: Structure of partially demethylated PR 122

An additional prominent feature of the negative-ion mass spectrum is a peak cluster around m/z 420. While this peak is not yet identified, it is 80 mass units above the peaks representing the molecular ion. This suggests the presence of a negatively-charged adduct. There are numerous unspecified resins, binders, and starches present in the watercolor paint in addition to the dye. One of these compounds might attach to the dye molecule. This compound might be detected

independent of the dye molecule and could be represented by the peak at m/z 81. Sodium and potassium ion adducts to the ion at m/z 420 are also observed (at m/z 442 and m/z 458 respectively).

Structure of Pigment Violet 23

The structure of PV 23 (a dioxazine pigment) and theoretical isotope distribution are shown in Figure 3.7.

a)

b)

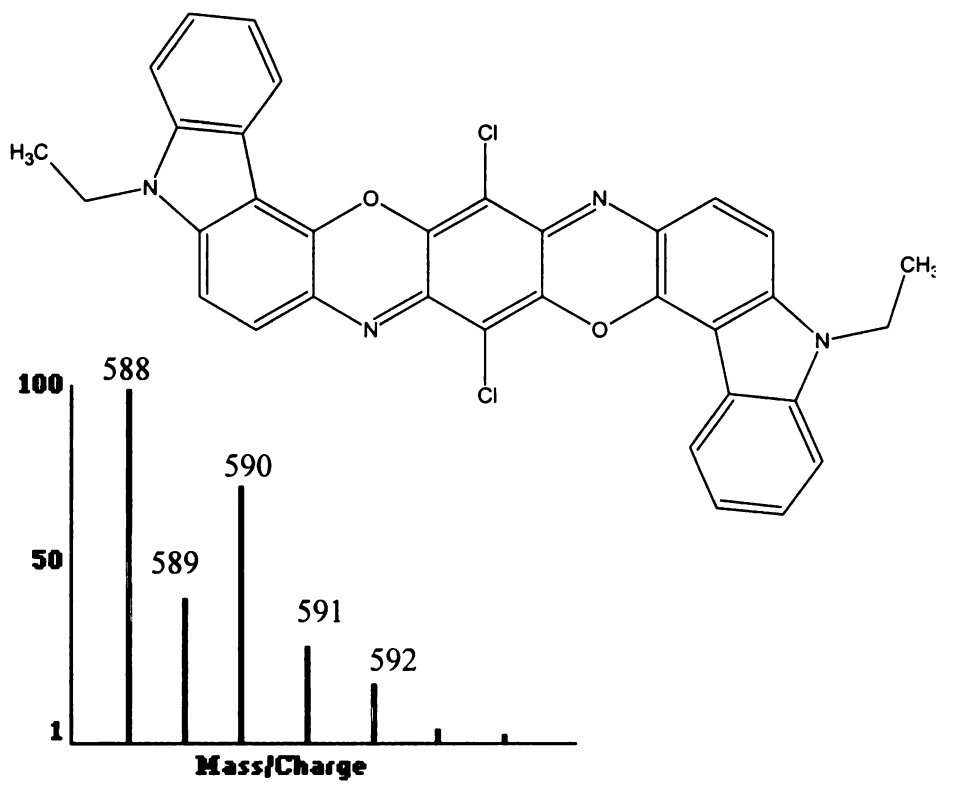

Figure 3.7: Pigment Violet 23: a) structure and b) theoretical isotope distribution

A positive-ion laser desorption mass spectrum of the dye taken directly off the sample plate is shown in Figure 3.8 and a negative-ion laser desorption mass spectrum of the dye taken directly off the sample plate is shown in Figure 3.12.

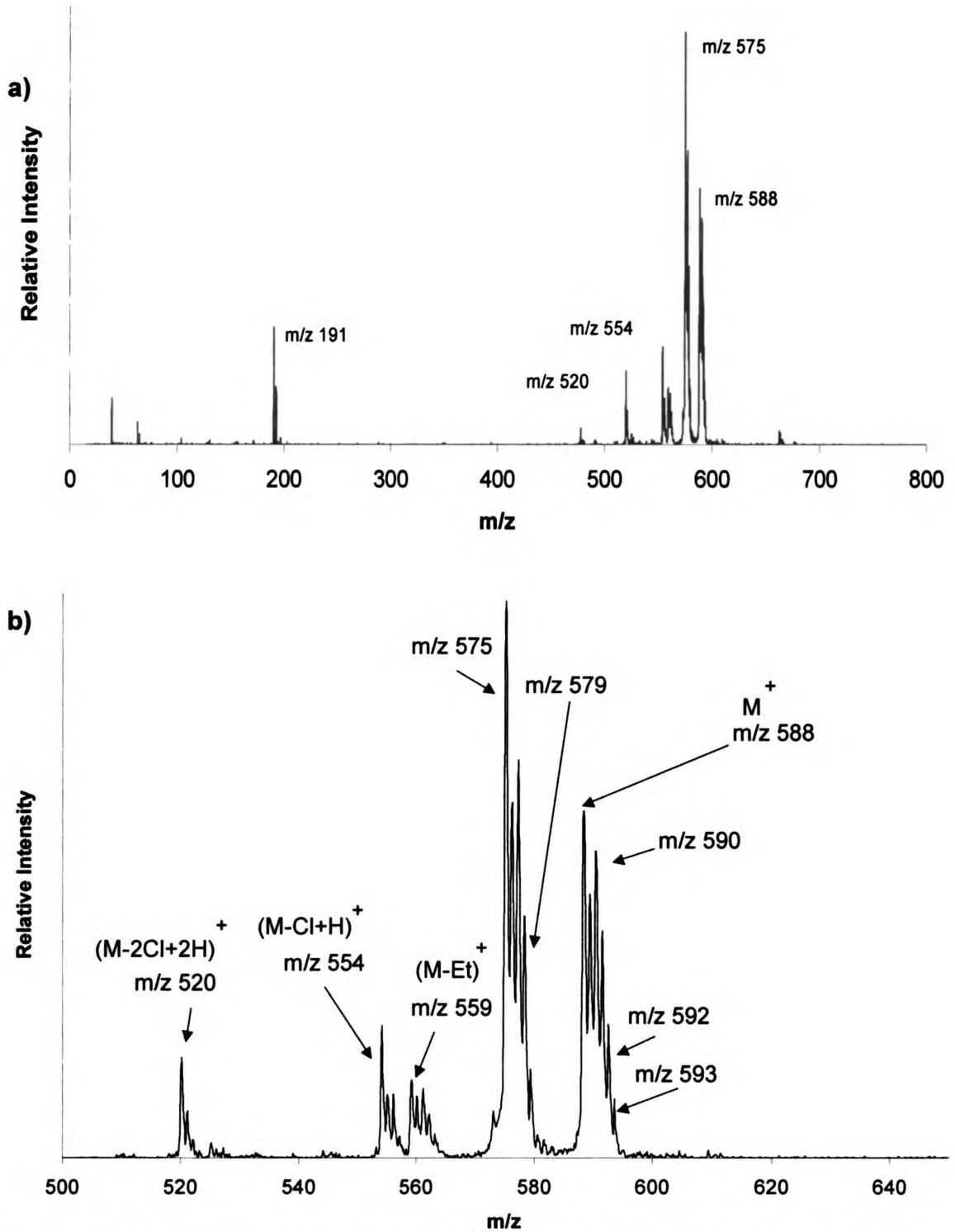

Figure 3.8: Positive-ion LD mass spectrum of PV 23 obtained directly off the gold sample plate: a) m/z 0-800 and b) m/z 500-650

Interpretation of the positive-ion mass spectrum of PV 23

The peak at m/z 588 represents the monoisotopic molecular ion. The peaks from m/z 588 through m/z 593 represent the isotope distribution of molecular ion. Note that the experimentally obtained spectrum (Figure 3.8) corresponds well with the theoretical isotope distribution of the molecule (Figure 3.7). The peaks around m/z 554 represent ions of the dye molecule where one chlorine atom has been replaced by a hydrogen: $(M\text{-}Cl+H)^+$. A possible structure of this ion and its theoretical isotope distribution are shown in Figure 3.9. Notice that the loss of a chlorine atom from the molecular ion yields a much different isotope distribution for this ion than distribution of the original molecule.

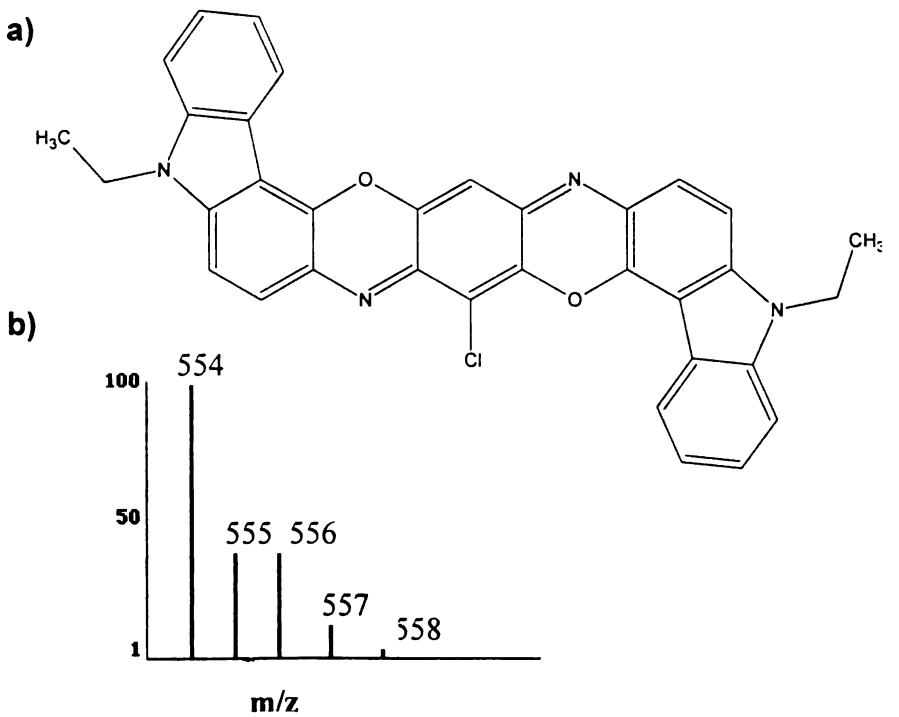

Figure 3.9: Partially dechlorinated Pigment Violet 23: a) structure and b) theoretical isotope distribution

The peaks around m/z 520 similarly represent ions of the dye molecule where both chlorine atoms have been replaced by hydrogens: $(M-2Cl+2H)^+$. The mass of these ions, (the substitution of a hydrogen in place of each chlorine, rather than simply the loss of each chlorine), suggests these are manufacturing impurities found in the pigment mixture. The isotope distribution for this ion is shown in Figure 3.10a. Notice the isotope distribution change with the loss of each chlorine.

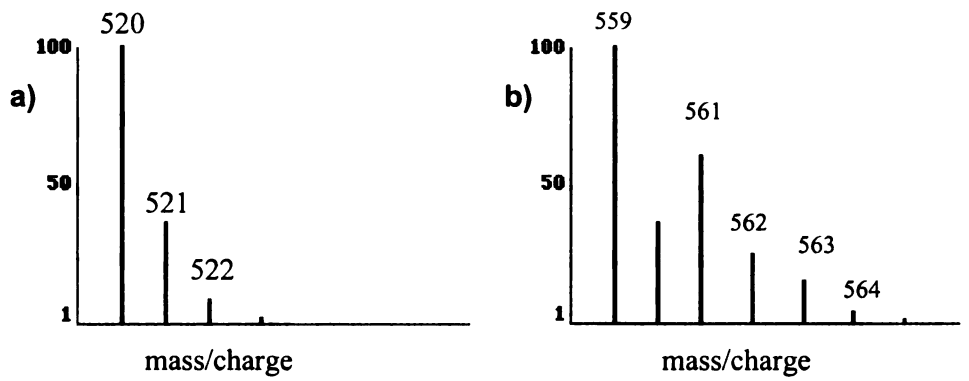

Figure 3.10: Theoretical isotope distribution of a) completely dechlorinated PV 23 and b) deethylated PV 23

The peaks around m/z 559 represent ions formed by deethylation of the original dye molecule: $(M-Et)^+$. Because this mass corresponds to the loss of an ethyl group, without a hydrogen substituted in its place, we believe this ion is formed during the desorption/ionization process. The theoretical isotope distribution of this ion shown in Figure 3.10b. The peaks from m/z 575 through m/z 579 have a similar overall pattern as the peaks representing the molecular ion. This suggests that the ions forming these peaks are somehow related to the dye molecule. If the peaks were 14 mass units lower than the molecular ion, they could be

explained as dye molecules which have a methyl where an ethyl group is expected. However, on the actual mass spectrum, the second set of peaks is 13 mass units lower than the molecular ion peaks; the compound represented by these peaks could not be related to the molecular ion peak in a simple relationship. Upon closer examination, the peak patterns are actually slightly different. While there is an expected peak at m/z 593 (5 mass units higher than the monoisotopic ion) as part of the peak cluster representing the molecular ion, there is no corresponding peak at m/z 580 (5 mass units higher than the peak at m/z 575).

Additional pigment detected in paint

Although the paint tube claims that the only pigment contained in the paint is PV 23, it appears that another common dye, copper phthalocyanine is also present in this watercolor paint. This blue dye (PB 15) is a widely used commercial pigment. The structure of this compound and its theoretical isotope distribution are shown in Figure 3.11.

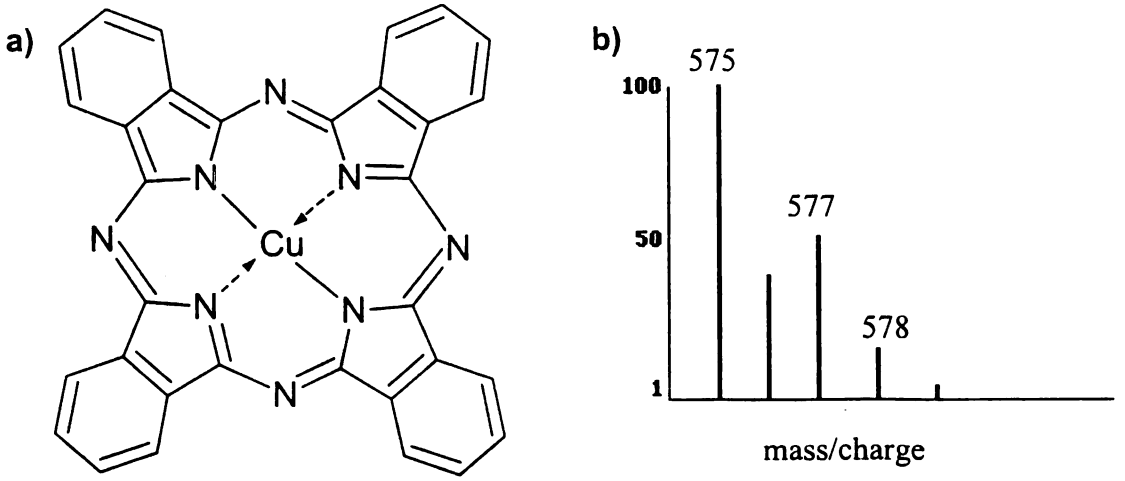

Figure 3.11: Pigment Blue 15 (Copper Phthalocyanine) a) structure and b) theoretical isotope distribution

Peaks at m/z 63 and m/z 65 are observed in the lower mass region of the positive-ion mass spectrum of the paint; these peaks represent elemental copper and support the proposal of copper phthalocyanine.

Interpretation of the negative-ion mass spectrum of PV 23

A negative-ion laser desorption mass spectrum of the dye taken directly off the sample plate is shown in Figure 3.12. The peak at m/z 588 represents the monoisotopic molecular ion, M^-. The peaks from m/z 588 through m/z 593 represent the isotope distribution of molecular ion. Note that the experimentally obtained spectrum (Figure 3.12) corresponds well with the theoretical isotope distribution of the molecule (Figure 3.7).

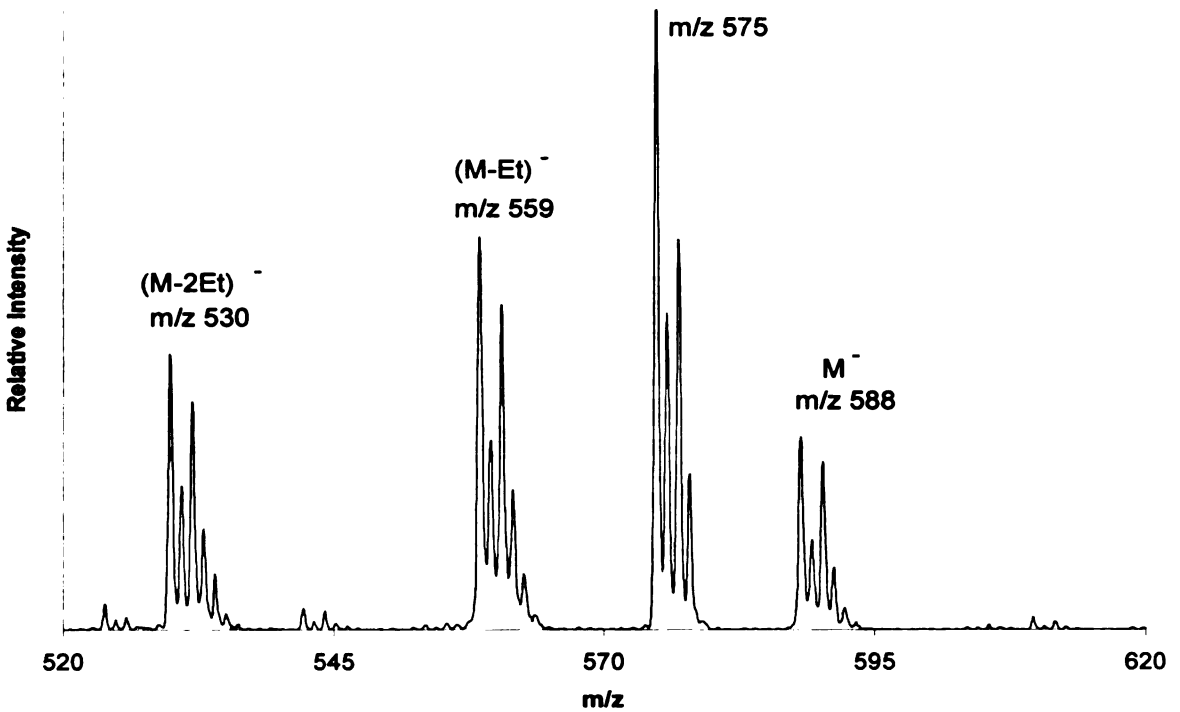

Figure 3.12: Negative ion LD mass spectrum of PV 23 obtained directly off the gold sample plate. The molecular ion is noted as M^- at m/z 588.

The peaks around m/z 559 represent ions formed by deethylation of the original dye molecule: $(M-Et)^{-}$. The theoretical isotope distribution of this ion shown in Figure 3.15.The peaks around m/z 530 represent completely deethylated ions of the dye molecule $(M-2Et)^{-}$. And again, the peaks around m/z 575 represent copper phthalocyanine ion.

Direct analysis of paints on watercolor paper

These dye molecules are as readily desorbed and ionized from a paper substrate as they are from the metallic sample plate. Laser irradiation of the painted watercolor paper produced spectra that were indistinguishable from spectra taken of the neat pigment. While laser irradiation of unpainted watercolor paper itself produces peaks in both positive-ion and negative-ion mode, these peaks do not interfere with detection of the pigments. There are two reasons: (1) some of the species producing these peaks have a higher threshold energy and are detected at much higher laser intensities than the pigments are and (2) the species which are detected simultaneously with the pigment peaks appear at much lower masses.

Summary

In harmony with other LD/MS analyses of ionic pigments[6] LD/MS successfully produces both postive-ion and negative-ion spectra from laser irradiation of watercolor paper painted with paints containing neutral pigments. As described above, each of the spectra contain peaks representing compounds related to the

pigment of interest. These peaks could be impurities from the pigment manufacturing process or degradation products formed from the original pigment. These spectra are forensically useful because they can further characterize the batch of a pigment (i.e., the peaks could reflect starting materials used to synthesize the pigments).

References

(1) M. Wilcox, The Wilcox Guide to the Best Watercolor Paints, School of Colour Publications, England. 2001-2002 Edition.

(2) M. Large, *Science Spectra*, **10** (1997) 14-20.

(3) J. H. Carlson, J. Krill, *Journal of the American Institute for Conservation* **18** (1978) 19-32.

(4) V. F. Hanson, *Advances in Chemistry Series.*, **193** (1981) 143-168.

(5) K. J. Smith, J. G. Barabe *Microscope,* **49(3)** (2001) 159-170.

(6) D. Grim, J. Siegel, J. Allison, *Journal of Forensic Science*, **46** (2001) 1411-1420.

CHAPTER 4: Stamp inks

Introduction and motivation

Like most types of forgeries, counterfeit postage stamps can be mistaken for valuable genuine stamps. Microscopy is the primary method used to analyze possible counterfeit stamps. Identifying the inks on the stamp can help distinguish genuine from fake.

As with each sample in this research, LD/MS was used to analyze inks used to print postage stamps. Along the edge of a sheet of postage stamps, a printer often prints test dots of each of the 3-5 colors used to print every shade and hue on the actual stamp. These test spots were particularly useful for our analysis, because they allowed us to analyze each color of ink individually. The stamp randomly chosen for analysis is the U.S. 37-cent 2002 "teddy bear" self-adhesive stamp.

Magenta ink region

No peaks characteristic of mid-weight (150-800 g/mol) dyes (cationic or anionic) were observed in spectra of the magenta region of the stamp.

Light yellow ink region

Both the positive-ion and negative-ion mass spectra of this ink contained peaks exclusive to the yellow ink. On the positive ion spectrum (Figure 4.1), one of the most intense peaks occurred at m/z 250.

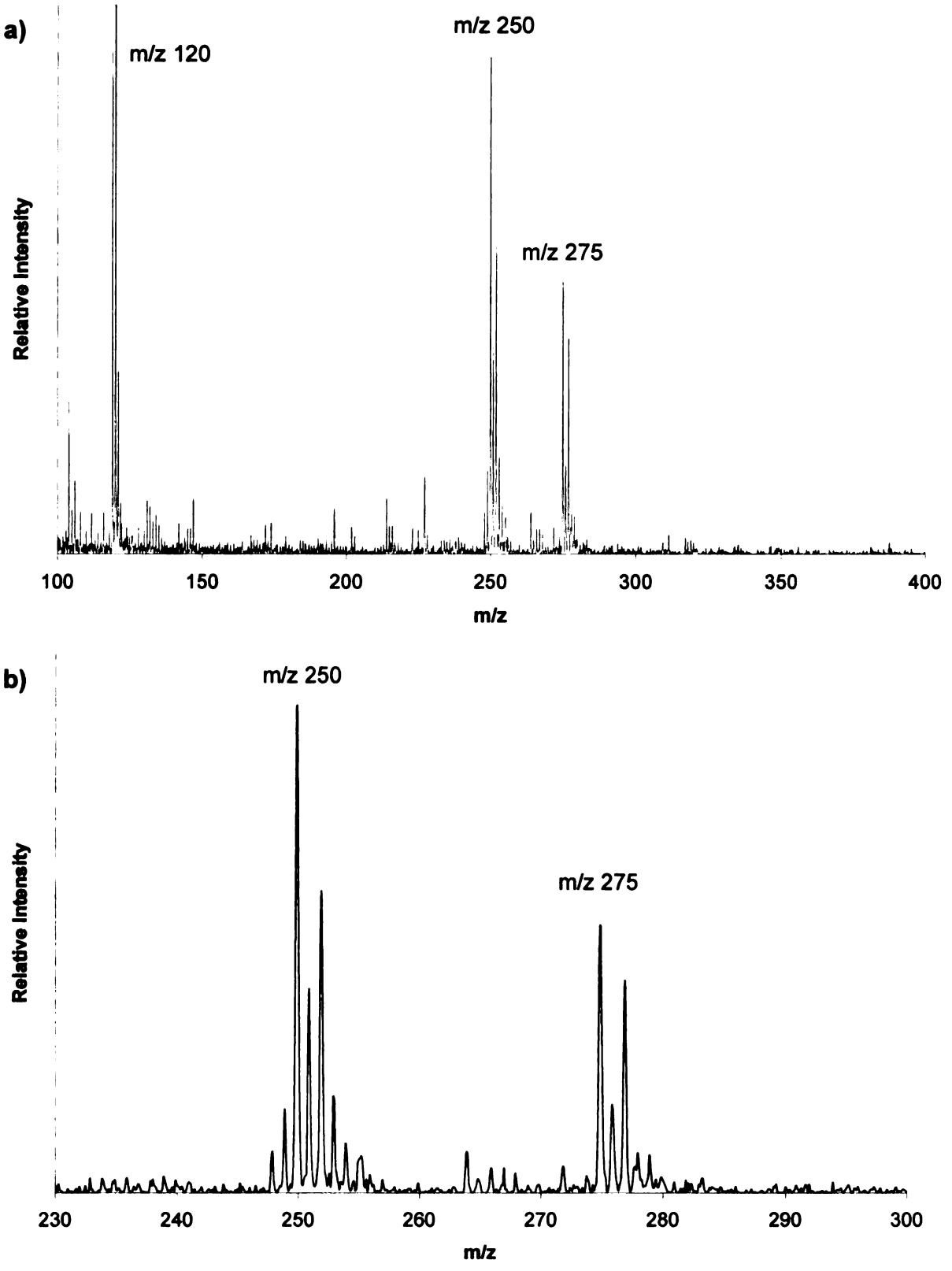

Figure 4.1: Positive ion LD mass spectrum of yellow ink region of stamp a) m/z 100- 400; and b) m/z 230-300

A likely assignment for these peaks is dichloroazobenzene, structure and theoretical isotope distribution shown in Figures 4.2. A number of structurally similar azobenzene pigments (with various alkyl-group, hydroxyl-group, and halide substitutions) produce desirable, colorfast yellow pigments. The structure shown in Figure 4.2a was chosen because it corresponds well with the observed mass and isotope distribution observed in the mass spectrum.

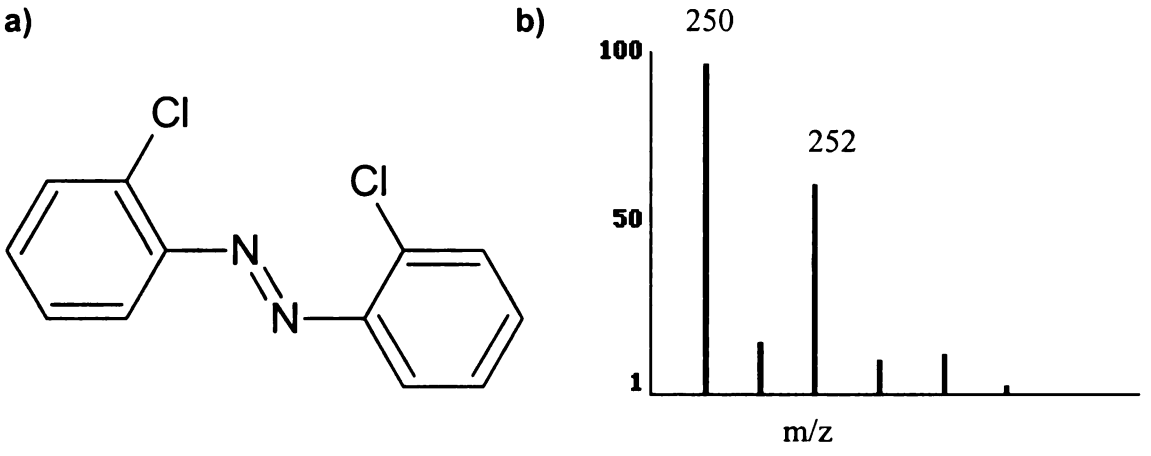

Figure 4.2: Dichloroazobenzene: a) structure and b) theoretical isotope distribution

The peaks at m/z 275 is not identified, but appears to also contain two chlorines. The mass difference could be due to the substitution of a group to one of the phenyl groups of dichloroazobenzene, or the peaks could represent an entirely different compound.

In the negative ion mass spectrum (Figure 4.3), there was a similar pattern of peaks starting at m/z 250 also representing the compound whose structure is shown above in Figure 4.2.

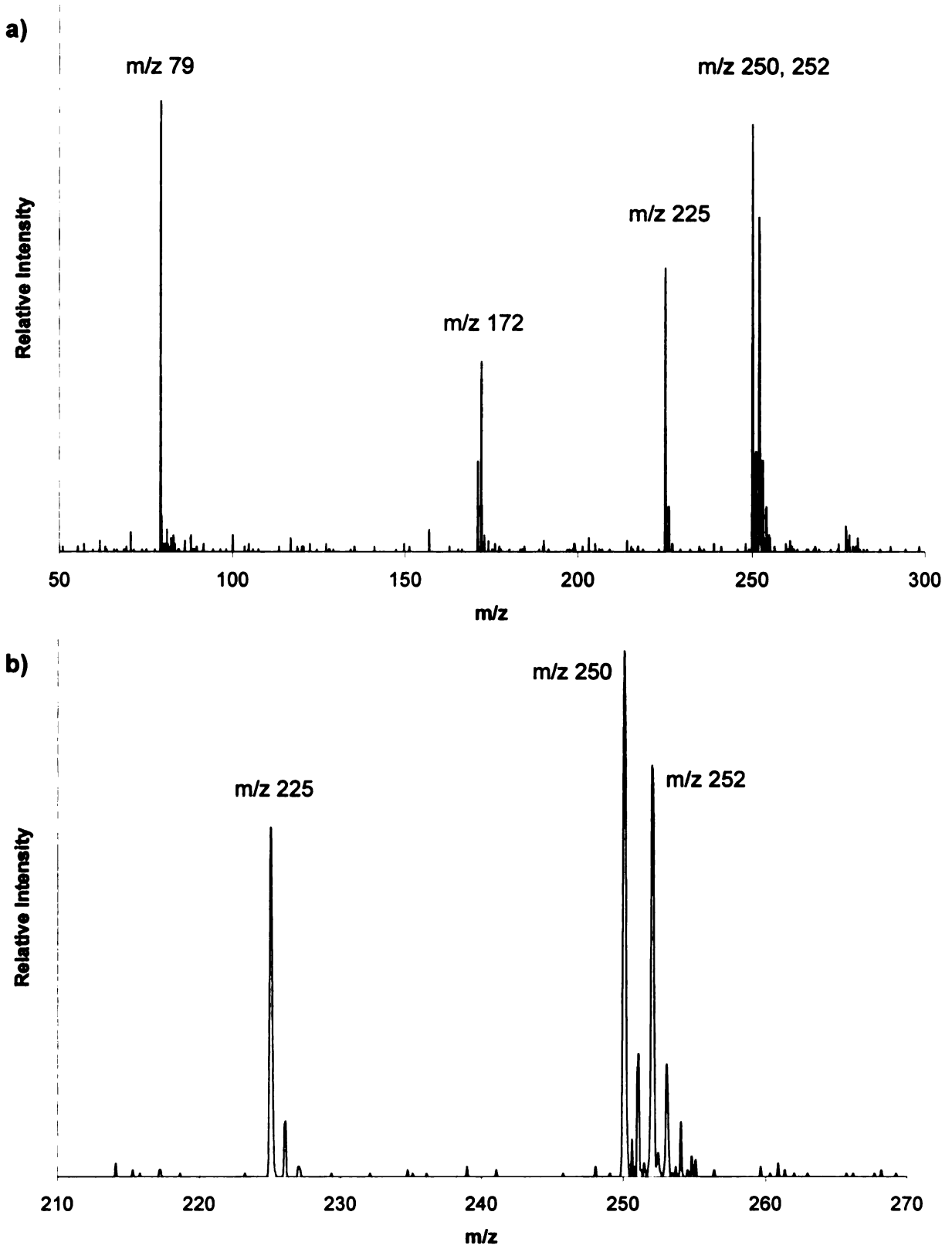

Figure 4.3: Negative ion LD mass spectrum of yellow ink region of stamp: a) m/z 50-300 and b) m/z 210-270

This compound is a neutral dye, and is expected to be detected in both positive and negative ion mode. Additional peaks in the negative ion mass spectrum at m/z 172 and m/z 225 appear to be not immediately related to the structure of dichloroazobenzene. The dechlorinated azobenzene structure and theoretical isotope distribution are shown in Figures 4.4.

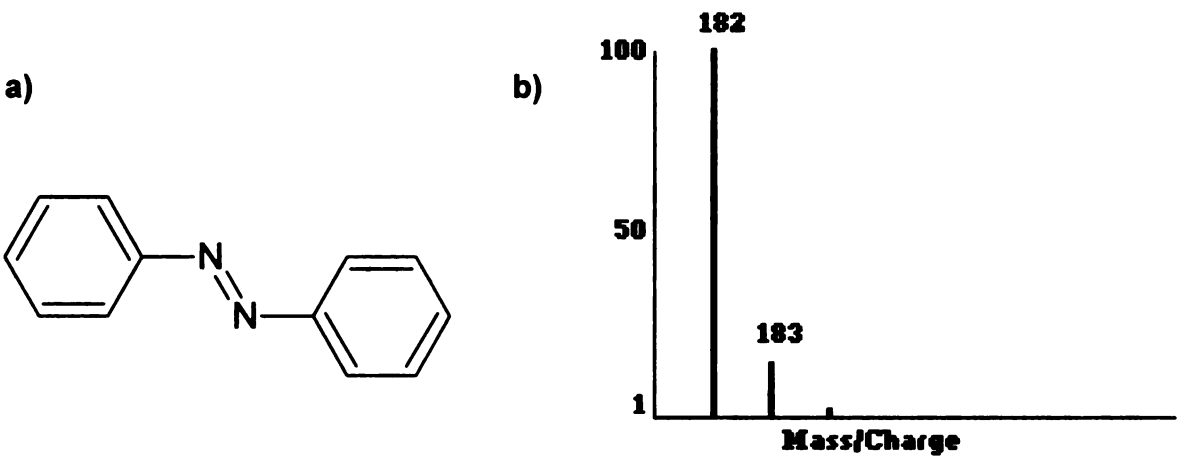

Figure 4.4: Azobenzene: a) structure and b) theoretical isotope distribution

The peaks at m/z 172 have a unique isotope pattern, not similar to the isotope pattern of the dechlorinated dye. The peaks at m/z 225 could be of an azobenzene with (alkyl) groups substituted onto a phenyl group. One possible structure is shown in Figure 4.5. This structure could be detected in the negative ion mode as the deprotonated alcohol.

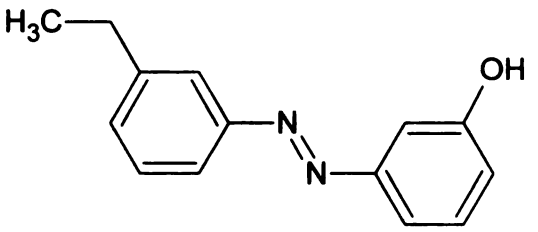

Figure 4.5: Structure of ethyl- and hydroxyl- substituted azobenzene

Teal ink region

In the positive-ion mass spectrum (Figure 4.6), the ever-popular copper phthalocyanine is observed at m/z 575.

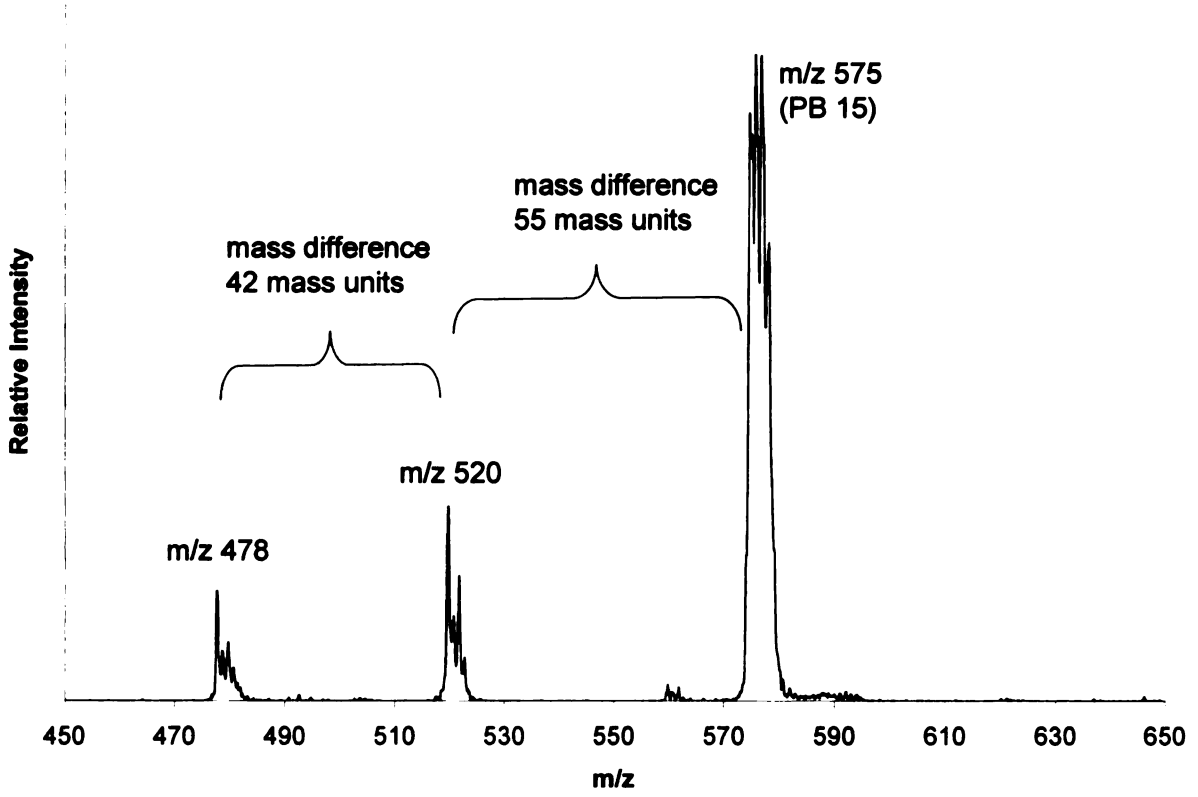

Figure 4.6: Positive-ion LD mass spectrum of teal ink region of stamp

The peaks clusters at m/z 478 and m/z 520 appear to have the same isotope pattern, suggesting that both of these compounds contain copper. These lower mass peaks are not yet identified; they may or may not be related to one another or to copper phthalocyanine. It is interesting and confusing to note that each of these peak clusters is not evenly spaced. The mass difference between m/z 478 and m/z 520 is 42 mass units while the mass difference between m/z 520 and m/z 575 is 55 mass units.

In the negative ion mass spectrum (Figure 4.7), peaks representing copper phthalocyanine are again observed.

Additionally, peaks near m/z 654 and m/z 733 represent copper phthalocyanine with bromine substituted in place of one or two hydrogen atoms. A curious peak is observed 16 mass units up from each of these three phthalocyanine peaks. These peaks likely represent the presence of oxygen on the phthalocyanine structure.

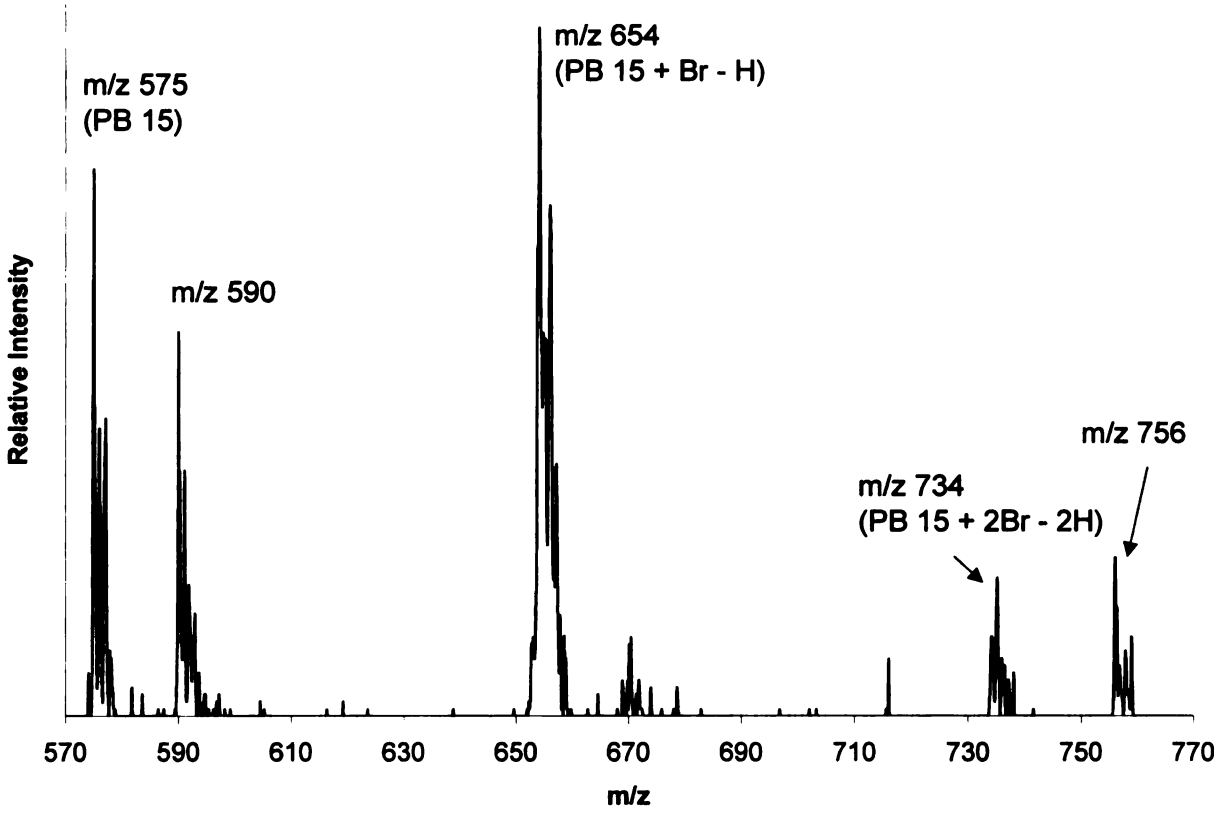

Figure 4.7: Negative ion LD mass spectrum of teal ink region of stamp

Orange ink region

The positive ion mass spectrum (Figure 4.8) of the orange ink region contained one intense set of peaks at m/z 334. These peaks have no distinguishing peak characteristics suggesting the presence of an element with a distinctive isotope distribution (e.g., copper, titanium, or chlorine). These peaks likely represent a compound containing only carbon, hydrogen, nitrogen, and oxygen.

The negative ion mass spectrum (Fig. 4.9) of this ink similarly contained one set of peaks at m/z 425. Again, these peaks have no distinguishing pattern characteristics and likely represent an organic ion.

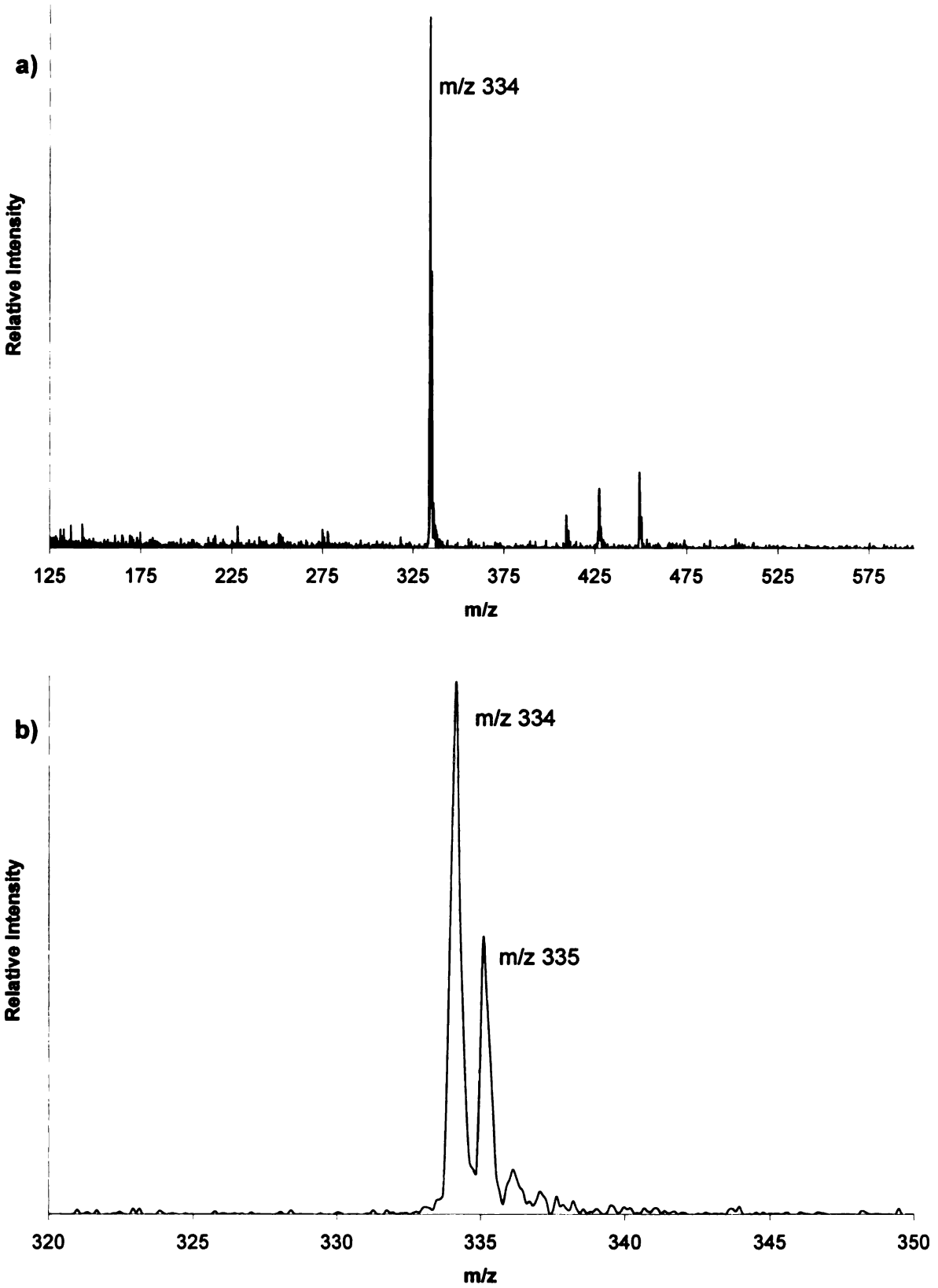

Figure 4.8: Positive-ion LD mass spectrum of orange ink region of stamp a) m/z 125- 600 and b) m/z 320-350

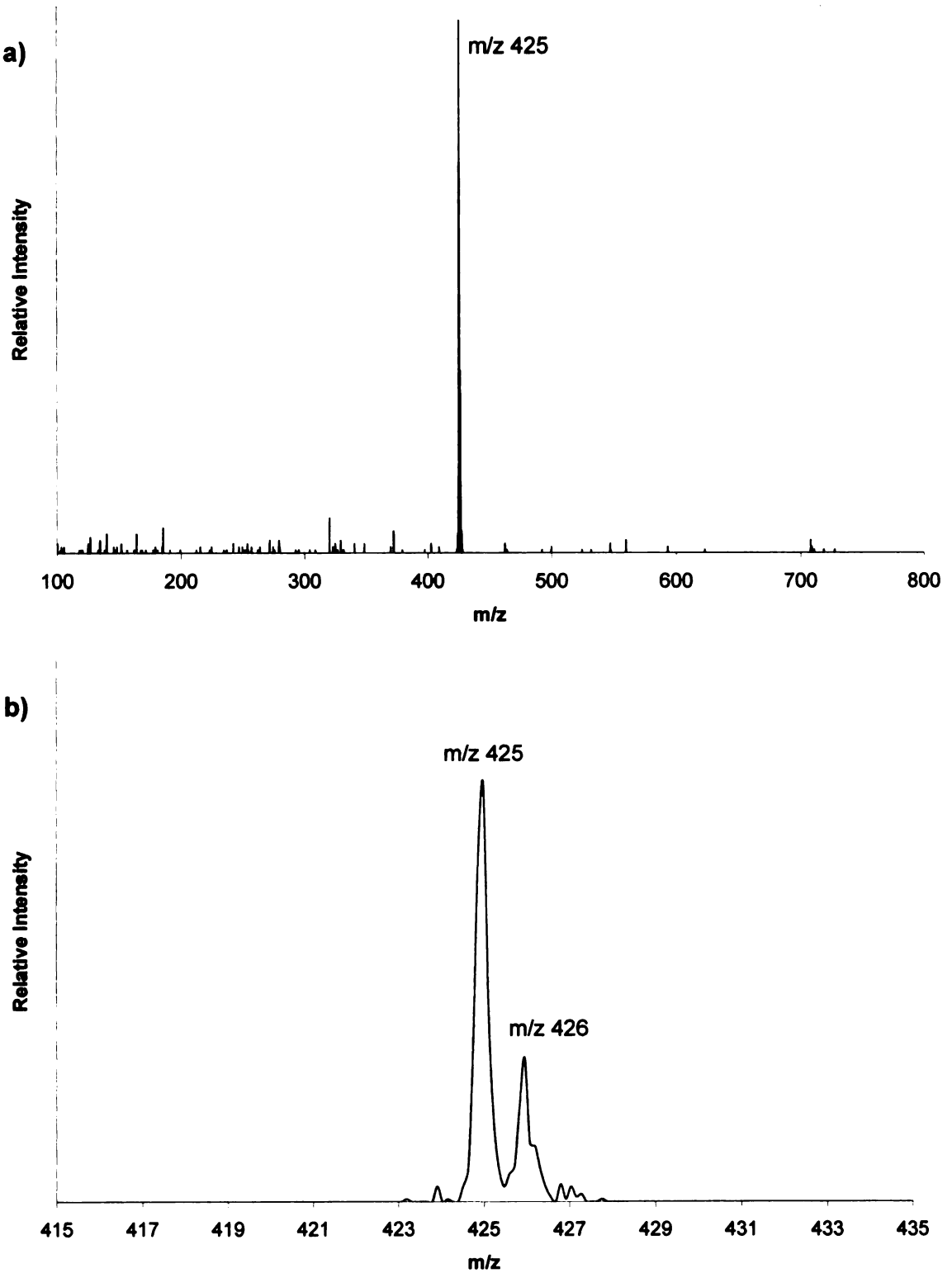

Figure 4.9: Negative ion LD mass spectrum of orange ink region of stamp a) m/z 100-800 and b) m/z 415-435

These peaks could represent the same dye (that fragments in positive-ion mode by losing a functional group that weighs approximately 92 Daltons) or the peaks could represent two distinctive dyes (one cationic and one anionic). Examples of neutral, cationic, and anionic orange dyes are shown in Figure 4.10.

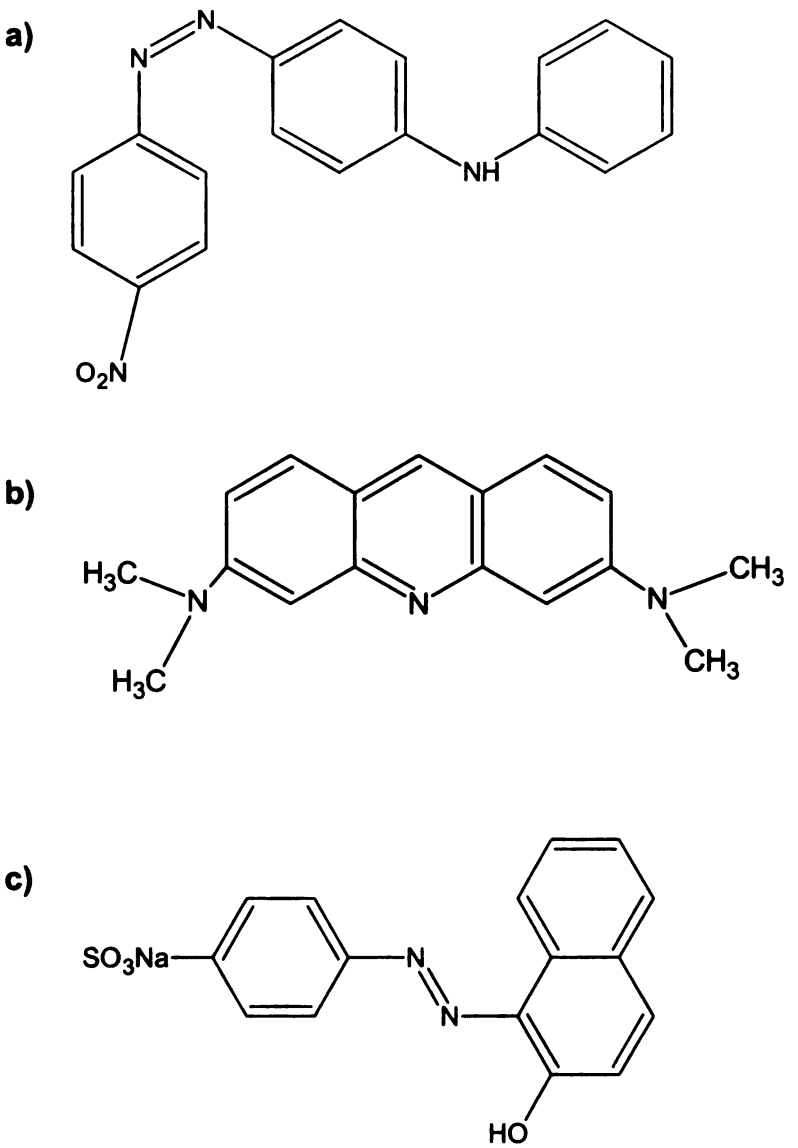

Figure 4.10: Representative neutral, cationic, and anionic orange dyes: a) Disperse Orange 1; b) Basic Orange 14; c) Acid Orange 7

Summary

Because of their small size, postage stamps are appropriate for analysis by LD/MS. As shown, direct laser irradiation of the stamps produced well-resolved mass spectra of several printing inks. Mass spectra (not shown) of the magenta region of the stamp curiously did not contain any distinctive peaks exclusive to that color. Mass spectra (positive-ion shown in Figure 4.11) of the black region of the stamp produced a large number of peaks that we could not make mass assignments for.

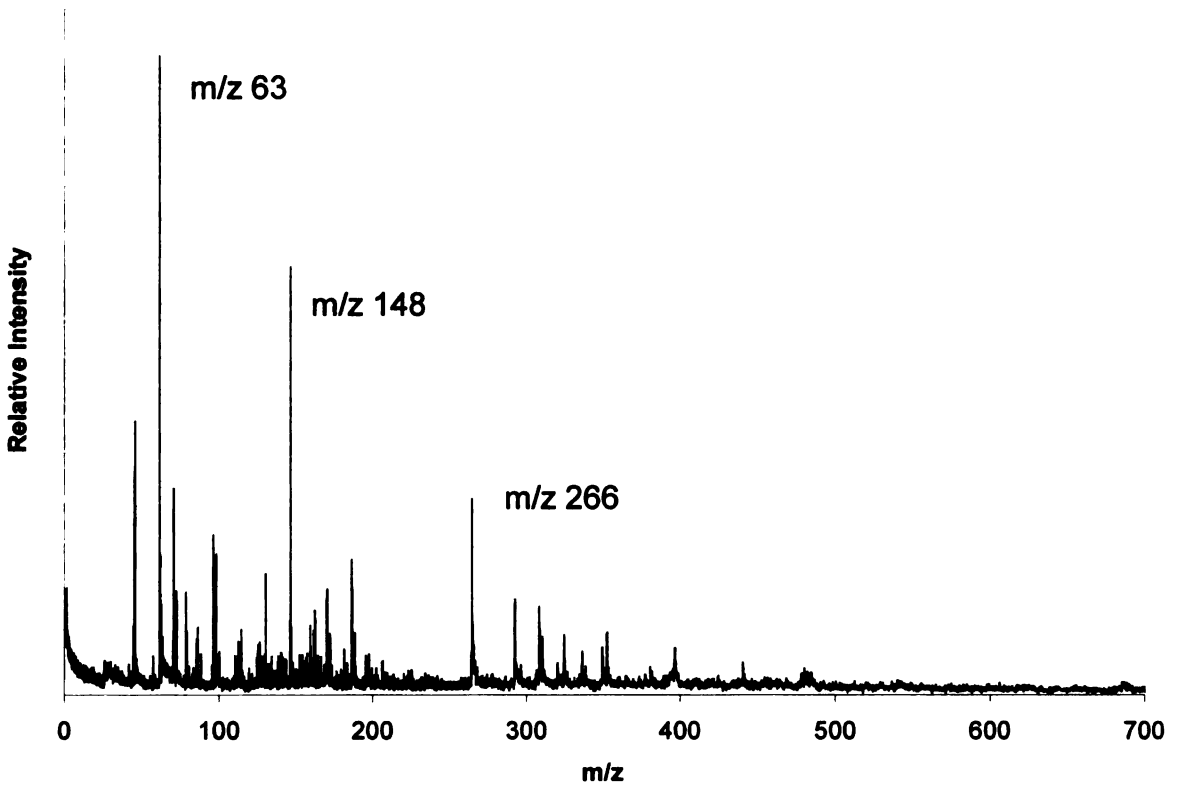

Figure 4.11: Positive-ion LD mass spectrum of black ink region of stamp

While some black inks contain distinct organic pigments (e.g., the anionic dye solvent black 29), some do not. For example, carbon black is a mixture of 90%+ elemental carbon (the "pure pigment") and numerous organic impurities containing chemically bound hydrogen, oxygen, nitrogen, and sulfur. Because the desorption/ionization of molecules depends on their structure, these impurities may be the dominant species observed.

While actual peak assignment is optimal, it is not always forensically necessary. Mass spectra that contain unidentified peaks can be compared even when the exact chemical identity of the species producing the peaks is not known. As a trivial example, compare the mass spectrum shown in Figure 4.1 (positive-ion mode, yellow ink) and the mass spectrum shown in Figure 4.8 (positive-ion mode, orange ink). Without even identifying the chemical composition of the inks, we can easily see that the spectra represent different chemical species. If Figures 4.1 and 4.8 were the mass spectra obtained from the same corner of two stamps alleged to be from the same printing, a scientist would be able to confidently (and correctly) conclude that different inks produced the spectra.

The technique of LD/MS can be very valuable in the identification of pigments used to print postage stamps and even when identification of the actual pigment isn't ascertained, spectra can still be compared.

Chapter 5: Currency inks

Introduction and methods

Counterfeit currency costs the U.S. (and other countries) enormously each year. Detection of forged bills often relies on the fine detail in the designs on the bills produced by the intaglio printing process used to print the currency. As the quality and resolution of home printers increases, characterizing the ink used to print currency is obviously desirable. Some work in the area of elemental analysis of different regions of currency using x-ray fluorescence has been done[1]. Chemical characterization of the inks is desirable because it may help distinguish between forged and genuine bills. The ink formulas used in intaglio printing vary and their disclosure isn't exactly promoted by the Bureau of Engraving and Printing (the printing division of the U.S. Department of the Treasury). Some intaglio ink formulations are described vaguely in patents: "for the printing of security documents, especially currency, the preferred pigments are black iron oxide, yellow iron oxide, carbon black, Pigment Green 7, Pigment Green 36, Pigment Blue 15, Pigment Red 146, Pigment Red 224, and mixtures thereof."[2] Representative formulae[3] are shown below in Tables 5.1 and 5.2:

Table 5.1: Green intaglio printing ink composition as described in U.S. Patent # 5,723,514

Pigment Green 7	Chlorinated copper phthalocyanine	2.3 % of base
Pigment Black 7	Carbon Black	0.8 % of base
Pigment Yellow 42	Iron oxide hydrate	12.2 % of base
Pigment Blue 15:3	Copper phthalocyanine	0.1 % of toner
Pigment Violet 23	Carbazole Violet (MW 588+)	0.1% of toner

Table 5.2: Black intaglio printing ink composition as described in U.S. Patent # 5,723,514

Pigment Black 7	Carbon Black	1.5 % of base
Pigment Black 11	Iron oxide (black)	27.3 % of base
Pigment Blue 15:3	Copper phthalocyanine	0.3 % of toner
Pigment Violet 23	Carbazole Violet (MW 588+)	0.1% of toner

For the LD/MS analysis, portions of a new bill were taped to the sample plate for analysis. These portions included blank regions (areas without any green or black ink) as well as portions with a high density of green and black printing ink.

Analysis of blank region of bill

A positive-ion mass spectrum of the blank region of U.S. $1 bill is shown in Figure 5.1.

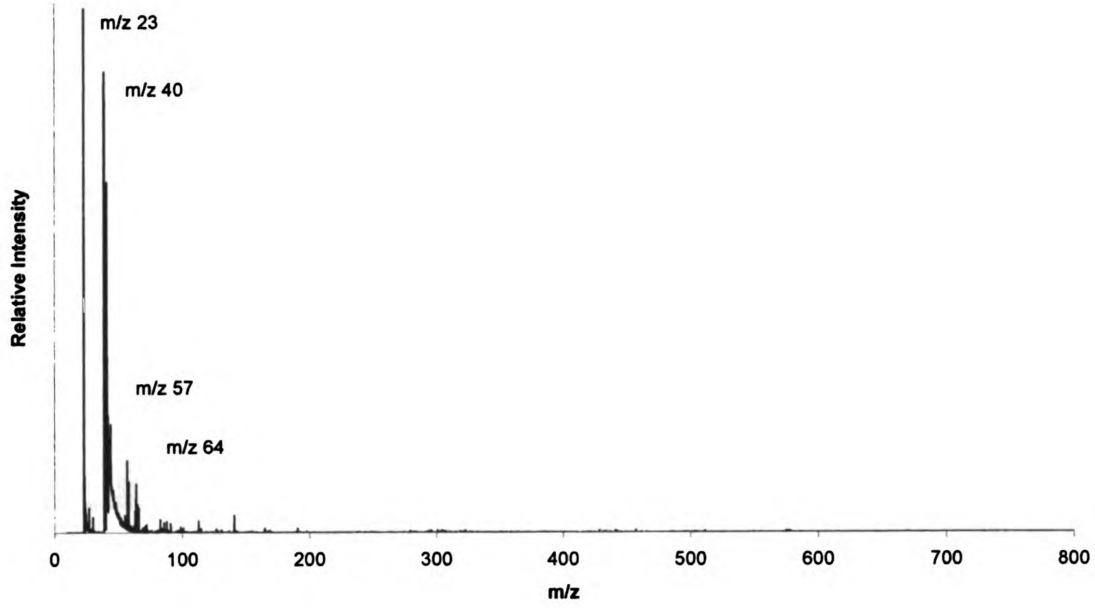

Figure 5.1: Positive-ion LD mass spectrum of blank region of currency (Laser power = 2700)

Peaks at m/z 23 and m/z 40 represent sodium and potassium ions respectively. The peaks at m/z 57 likely represents an organic fragment ion (possibly produced by laser irradiation of the cellulose-based paper). The peak at m/z 64 could represent another organic fragment ion or it could represent the TiO^+ ion (a species present due to paper bleaching agents). Notice however, that there are no distinct peaks higher mass peaks.

A negative-ion mass spectrum of the blank region of U.S. $1 bill is shown in Figure 5.2.

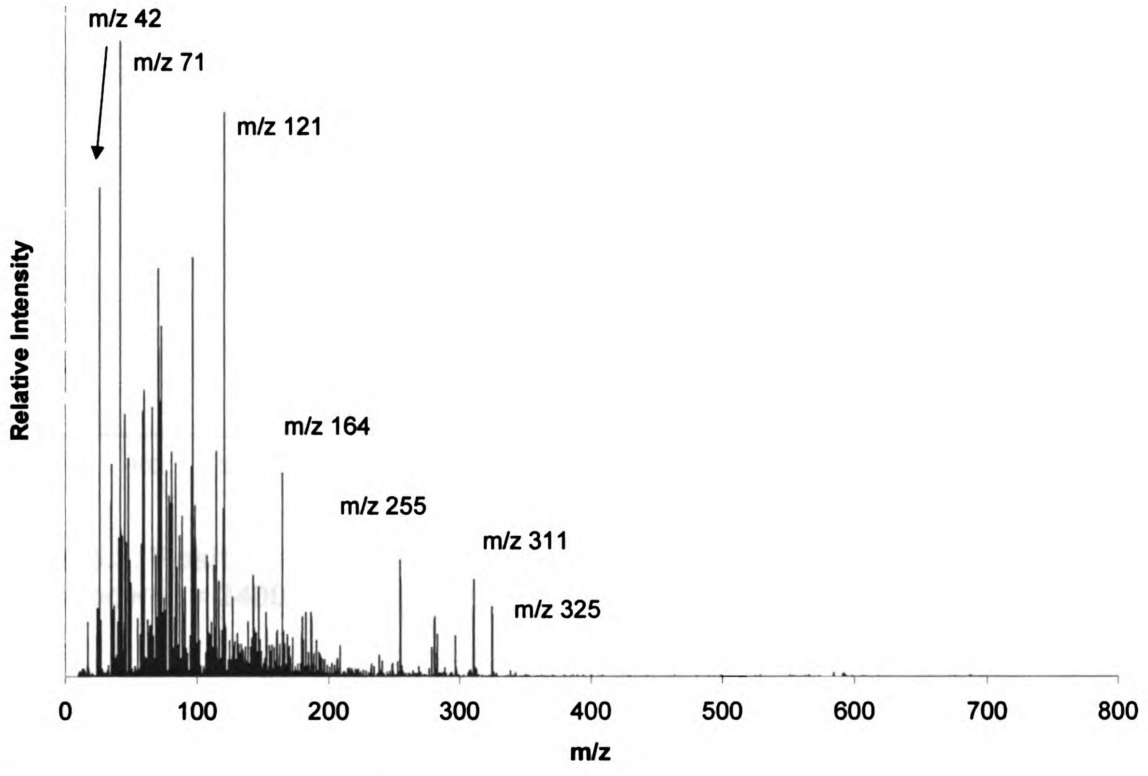

Figure 5.2: Negative-ion LD mass spectrum of blank region of currency (Laser power = 2700)

The numerous well-resolved peaks in the negative-ion mass spectrum likely represent organic fragment ions. These ions could represent fragments produced by laser irradiation of the actual paper or could represent chemicals the paper was treated with prior to printing.

Analysis of black ink region of bill

Positive-ion mass spectra (Figure 5.3) of the black ink region of the bill had consistent peaks at m/z 23 and m/z 575.

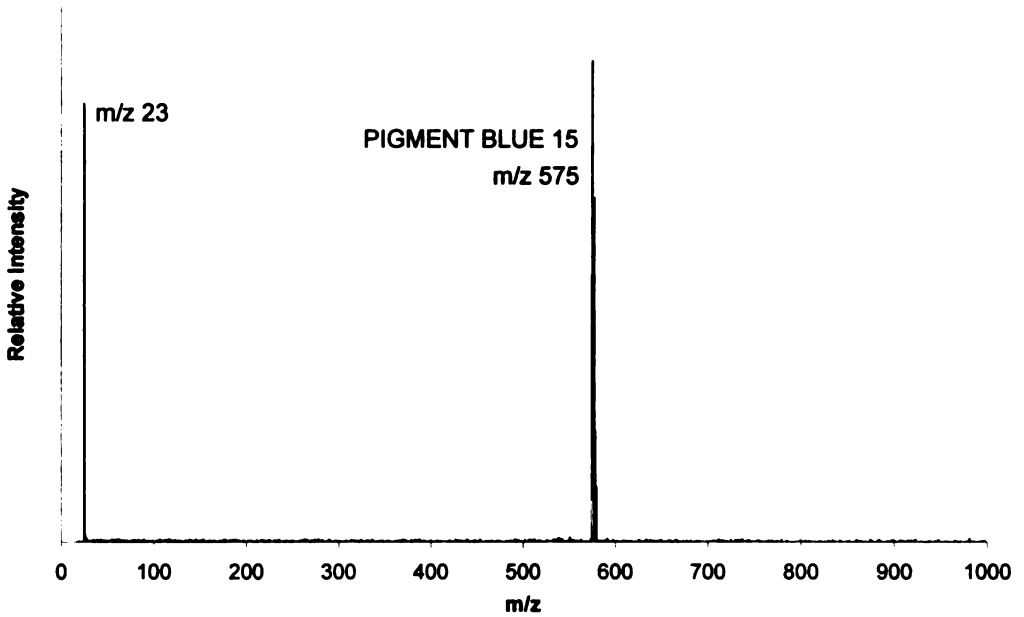

Figure 5.3: Positive-ion LD mass spectrum of black ink region of currency (Laser power = 2400); m/z 0-1000

The first of these peaks represented Na^+. The "peak set" beginning at m/z 575 was identified as copper phthalocyanine (Pigment Blue 15) and is shown in more detail in Figure 5.4. The structure and theoretical isotope distribution of Pigment Blue 15 are shown in Figure 5.5.

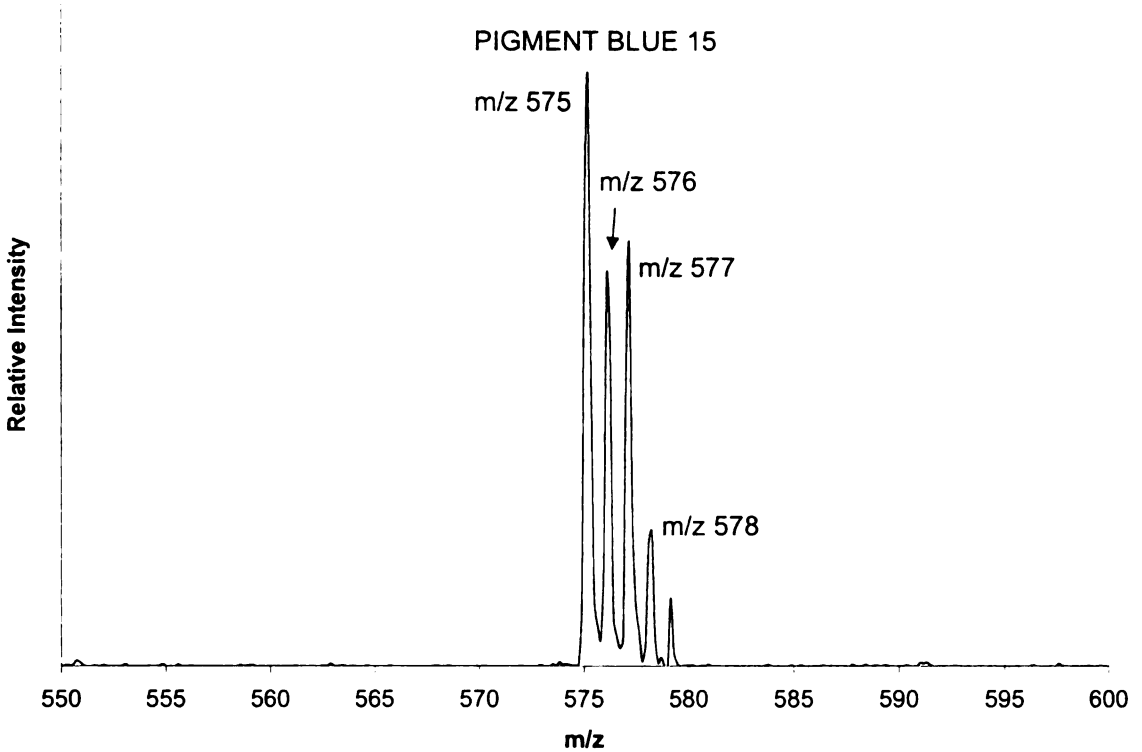

Figure 5.4: Positive-ion LD mass spectrum of black ink region of currency (Laser power = 2400); m/z 550-600

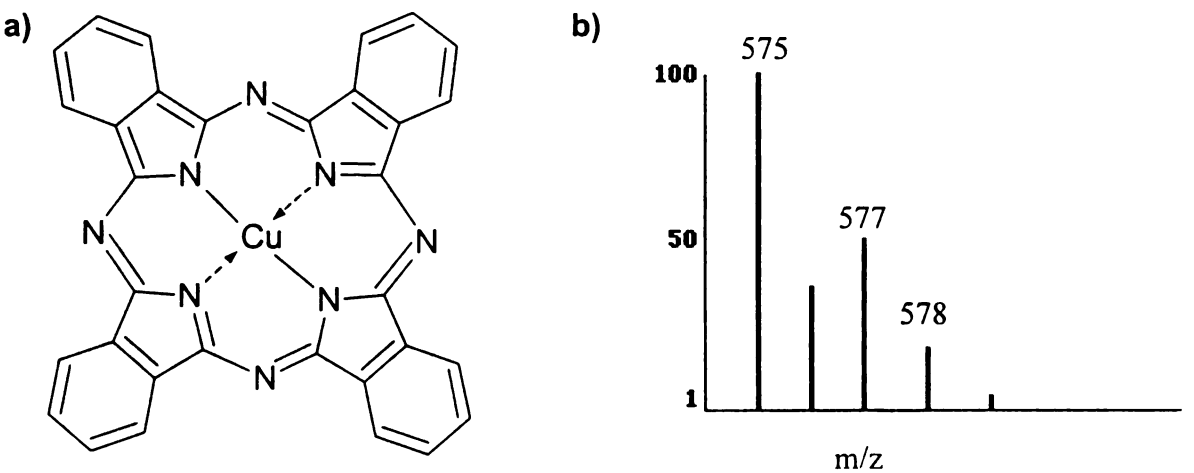

Figure 5.5: Pigment Blue 15 (Copper phthalocyanine): a) structure and b) theoretical isotope distribution

Peaks representing copper phthalocyanine were also observed in negative-ion mass spectra (Figure 5.6) of the black ink region. A few other peaks which appear in this spectrum were also observed in Figure 5.2 (the negative-ion mass spectrum of the blank paper), so these peaks represent compounds which are not exclusive to the ink.

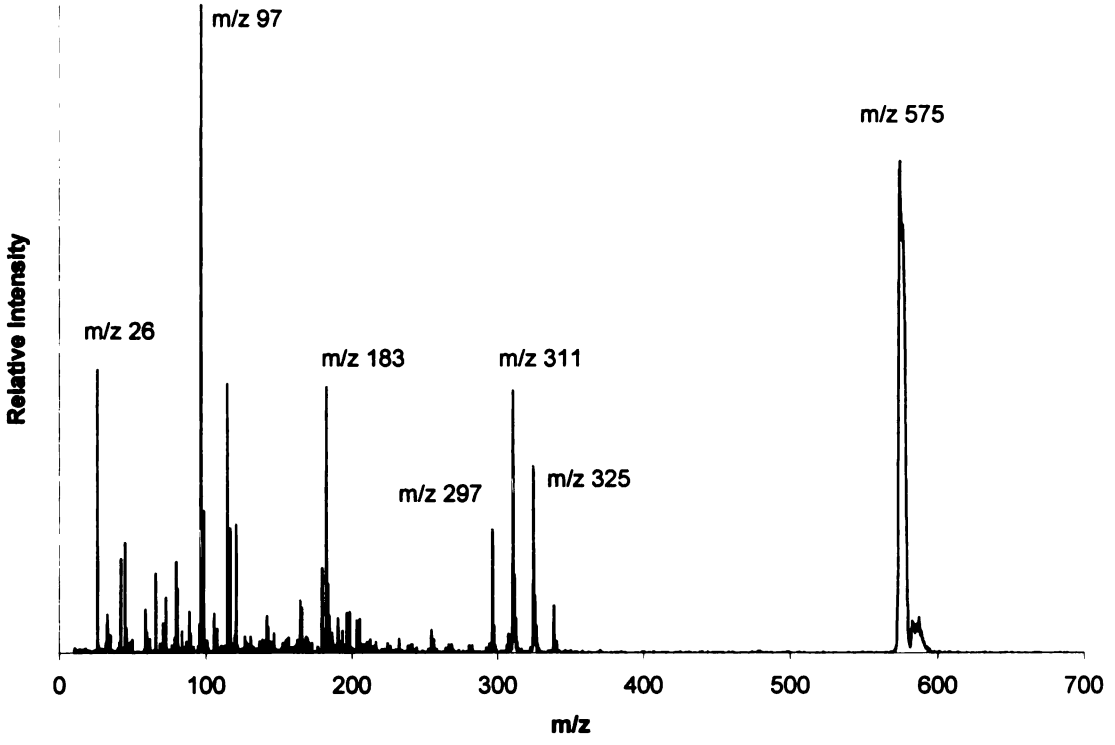

Figure 5.6: Negative-ion LD mass spectrum of black ink region of currency (Laser power = 2700)

Analysis of green ink region of bill

Similar to the black ink region of the bill, positive-ion mass spectra (Figure 5.7) of the green ink region of the bill had consistent peaks at m/z 23, m/z 39, and m/z 575. These peaks again represent Na^+, K^+, and copper phthalocyanine. In addition, these spectra contained a set of higher mass peaks (above m/z 1000), shown enlarged in Figure 5.7b. These peaks are related to chlorinated copper

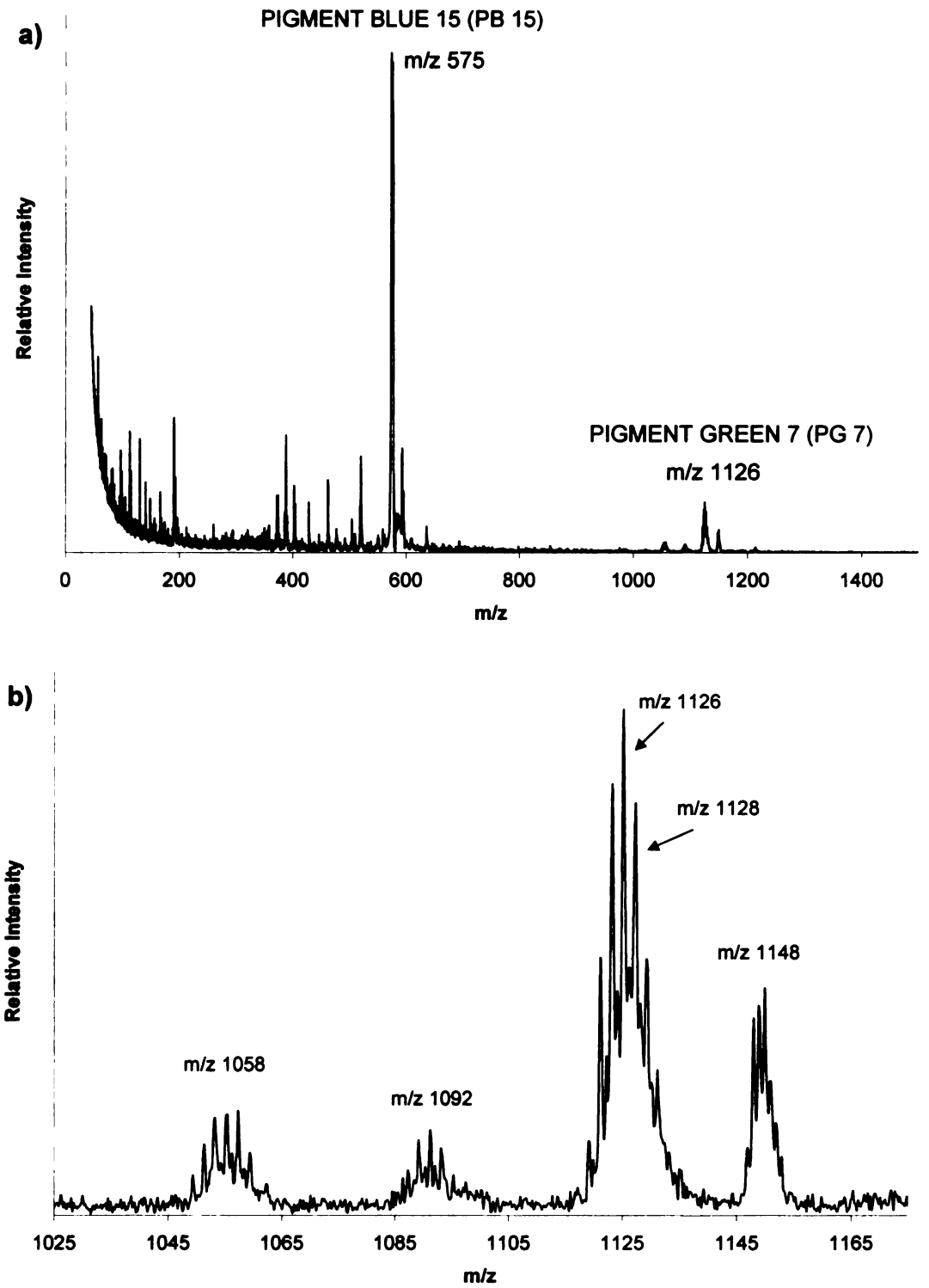

Figure 5.7: Positive-ion LD mass spectrum of green ink region of currency (Laser power = 2700); a) m/z 0-1500 and b) 1025-1175

phthalocyanine (Pigment Green 7). The structure and theoretical isotope distribution of this compound are shown in Figure 5.8. The peak cluster around m/z 1126 represents the molecular ion. The peaks at m/z 1126 and m/z 1128 are labeled in preference to the monoisotopic peak to show the resolution of the peaks (and because the monoisotopic peak is small in comparison due to the large number of chlorines in each ion).

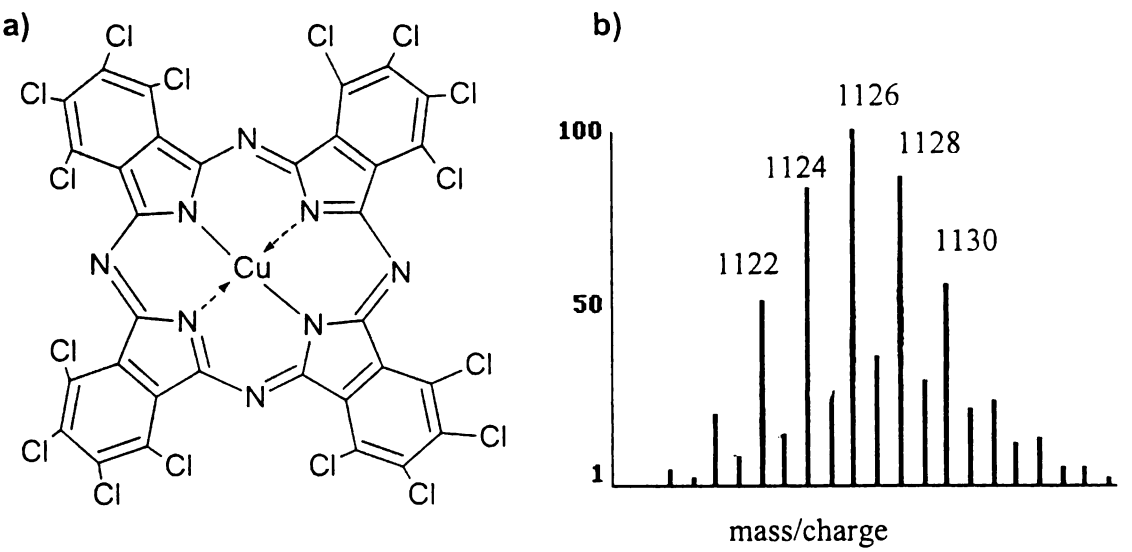

Figure 5.8: Pigment Green 7 (Chlorinated copper phthalocyanine): a) structure and b) theoretical isotope distribution (inescapable text overlap caused by isotope calculator)

The peak cluster around m/z 1092 represents chlorinated copper phthalocyanine ions in which a single chlorine has been replaced by a hydrogen. The theoretical isotope distribution for this molecule is shown in Figure 5.9. Similarly, the peak cluster around m/z 1058 represents chlorinated copper phthalocyanine ions in which two chlorines have been replaced by hydrogens. The peak cluster around m/z 1148 represents the sodium adduct of chlorinated copper phthalocyanine $(M+Na)^+$.

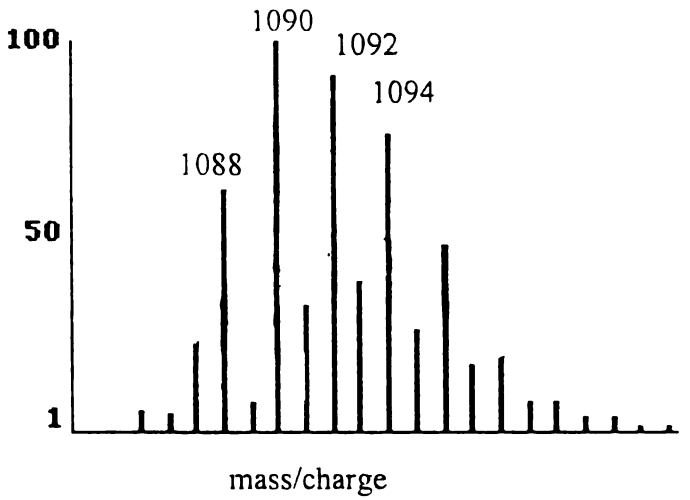

Figure 5.9: Theoretical isotope distribution of chlorinated copper phthalocyanine (with one hydrogen in place of a chlorine)

The negative-ion mass spectrum (Figure 5.10) of the green ink region of the bill contains peaks similar to those observed in the positive-ion mass spectrum. At first glance there appears to be a metal adduct to chlorinated copper phthalocyanine at m/z 1171. This peak actually represents chlorinated copper phthalocyanine ions in which a single chlorine has been replaced by a bromine, this is likely an impurity from the manufacturing process.

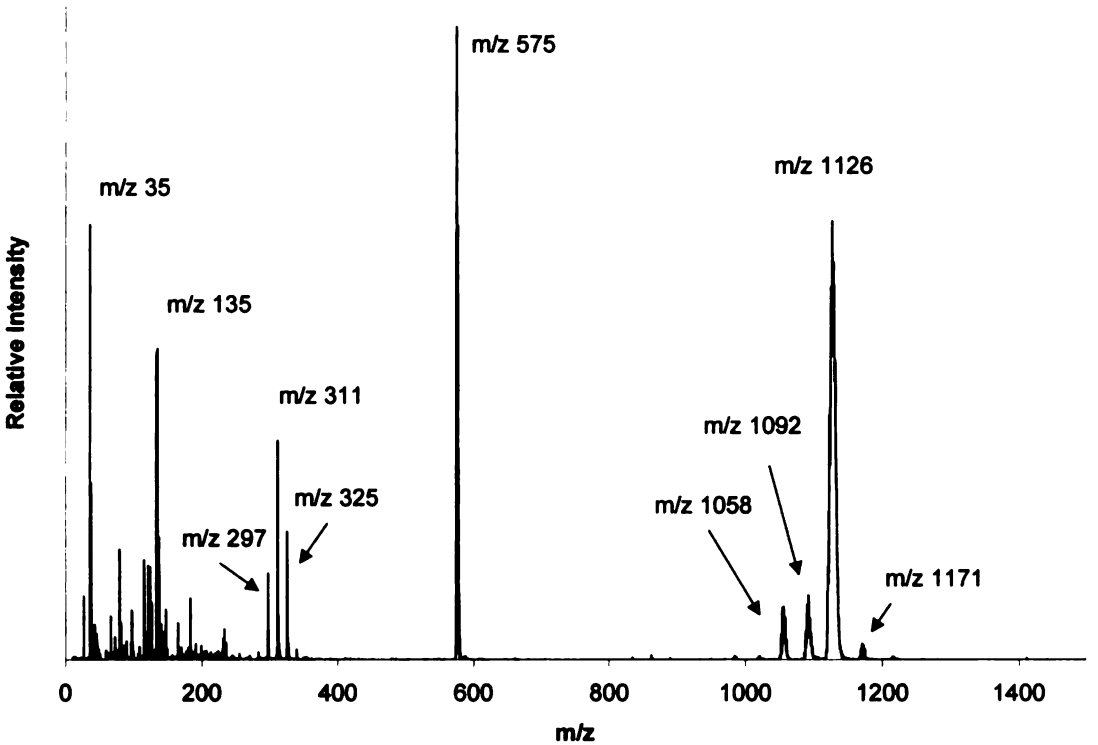

Figure 5.10: Negative-ion LD mass spectrum of green ink region of currency (Laser power = 2700)

Summary

As demonstrated in related work[4], LD/MS is a useful tool in the analysis of inks directly off of paper. In this chapter, we've presented an example of how LD/MS can be used to generate mass spectra containing peaks representing known inks used in printing currency and could be a tool in the detection of counterfeit currency.

References

(1) V. F. Hanson, *Advances in Chemistry Series.*, **193** (1981) 143-168.

(2) W. J. Glesias, (Sun Chemical Corporation) U.S. Patent 5,100,934 (1991).

(3) S. J. Nachfolger; H. Babij, J. Malanga, R. H. Reiter, W. J. Glesias, (Sun Chemical Corporation) U.S. Patent 5,723,514 (1995).

Chapter 6: Cationic dyes in security dye packs

Introduction, motivation and methods

Explosive dye packs and security inks are a common way to protect large amounts of currency. These inks might be found in currency cassettes in ATM machines. These security devices can be activated (released) if the ATM machine is tampered with, staining stolen money, making it unattractive to the perpetrator. Hopefully some of the security ink might also stain the perpetrator as well. Identifying these dyes on money or clothing can connect an individual with a crime. An investigator might also be interested in the ink's color fastness (resistance to washing): Can the ink be removed by simply "laundering" the stained money? Can the red ink be detected on a red shirt that's been washed?

Dye identification using UV-Vis spectrophotometry is common. This technique can be misleading, however, since many dyes may have similar absorbance spectra. GC/MS is useful for identifying some dyes used in dye packs (such as 1-methylaminoanthraquinone)[1], however some security inks are ionic (like the one in our study) and are therefore unsuitable for analysis by GC/MS. Techniques such as FT-IR[2] work best with pure analyte; extraction would be used to collect and concentrate the dye. The evidence a forensic scientist encounters could contain unknown impurities that would co-extract with the dye, leading to confusing and misleading IR spectra.

Analysis by LD/MS

For these analyses, samples of a commercial security ink and stained bills were generously provided by the mauufacturer (intentionally not disclosed). The security Ink is a complex mixture of solvents, dyes, optical brighteners, and rare earth tagging compounds. The exact formula is intentionally not disclosed here. The two main dye components of the ink were listed as Basic Violet 11:1 and Basic Red 1.

For the analysis of the currency, a portion of the stained (or washed) bill was taped to the sample plate and inserted directly into the instrument. The security ink was also spotted neat for analysis directly off the sample plate.

Washing of stained currency:

Strips of stained currency (approximately 1cm x 2cm) were immersed and intermittently sonicated in approximately 2 mL of solvent for up to 24 hours. The solvents used were: dichloromethane, distilled water, isopropyl alcohol, cyclohexanone, benzene, nitric acid, tetrahydrofuran, acetone, ethanol, bleach, RIT color remover (approximately 50 mg RIT® in 2 mL water), Gain® laundry detergent (approximately 50 mg detergent in 2 mL water), and non-acetone nailpolish remover (ethyl acetate- based). Three sets of stained currency were used: bills stained over 1 year ago (provided by the manufacturer), bills stained in our laboratory one week prior to washing, and bills stained in our laboratory one hour prior to washing.

Detection of the security ink on sample plate

A positive-ion mass spectrum (Figure 6.1) of the security ink spotted onto plain paper contains two dominant peaks at m/z 429 and m/z 457. The two main dye components of the security ink are listed as Basic Violet 11:1 and Basic Red 1, two common rhodamine dyes. The structures and theoretical isotope distributions of these dyes are shown in Figure 6.2. The two main dye components of the security ink are listed as Basic Violet 11:1 and Basic Red 1, two common rhodamine dyes. The structures and theoretical isotope distributions of these dyes are shown in Figure 6.2.

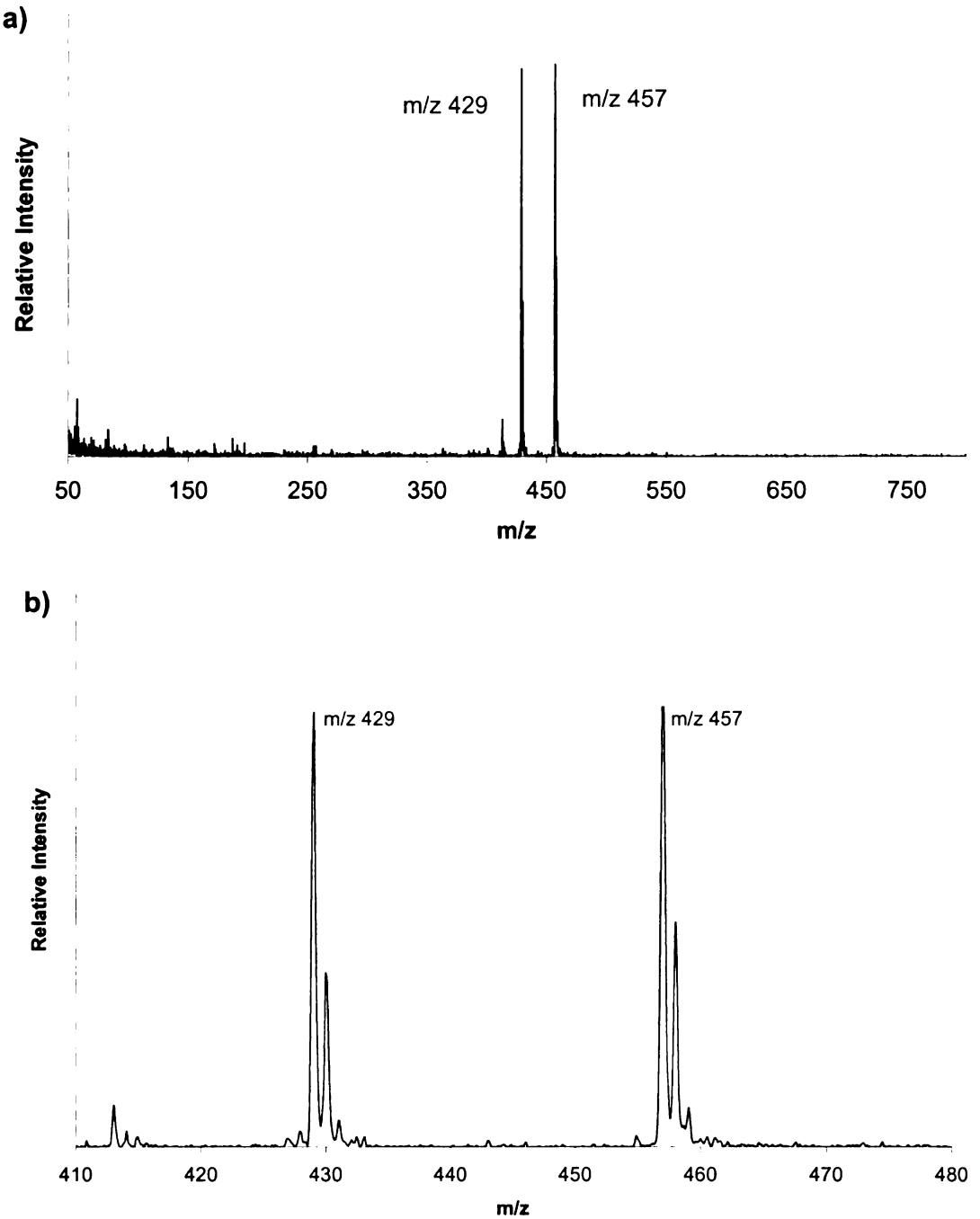

Figure 6.1: Positive-ion LD mass spectrum of security ink on sample plate a) 50-800 and b) m/z 410-480

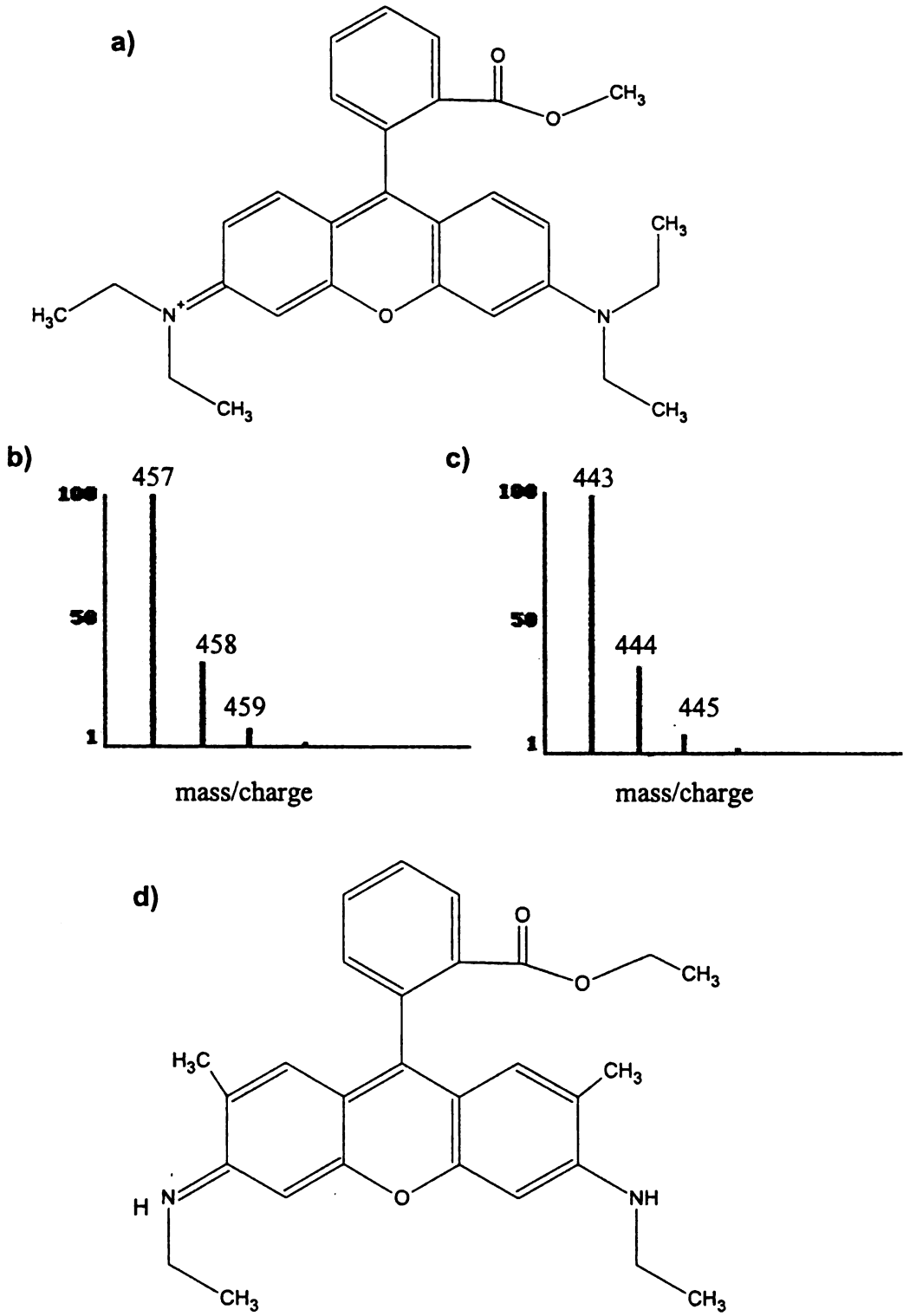

Figure 6.2: Basic Violet 11:1: a) structure and b) theoretical isotope distribution; and Basic Red 1: c) theoretical isotope distribution and d) structure

The peak at m/z 457 corresponds well with the presence of Basic Violet 11:1. For example, the peak at m/z 457 represents the monoisotopic cation of Basic Violet 11:1; this peak represents the cation in which each carbon has an atomic weight of 12, each hydrogen has a nominal atomic weight of 1, each nitrogen has a nominal atomic weight of 14, and each oxygen has a nominal atomic weight of 16. The peak at m/z 458 represents the cation of the same molecular formula; the increase in m/z value is predominantly due to the substitution of one carbon-13 isotope in place of a carbon-12. The peak at m/z 459 again represents the cation with the same molecular formula; the ions which are detected at m/z 459 could contain two carbon-13 atoms in place of carbon-12 atoms, or could contain an oxygen-18 atom in place of an oxygen-16 atom.

However, the other dominant peak at m/z 429 does not correspond with the theoretical isotope distribution of Basic Red 1. One would expect Basic Red 1 to yield ions that appear at m/z 443 and related research in our lab has confirmed that the positive-ion mass spectrum of Basic Red 1 contains peaks at m/z 443 (and not at m/z m/z 429). Notice that each of the above described peak differ in m/z value by 14 or 28 daltons (corresponding to the presence of a hydrogen in place of a methyl- or ethyl- group. The peak at m/z 429 is likely produced by a related rhodamine dye. An alternative peak assignment, Basic Red 1:1 is presented in Figure 6.3.

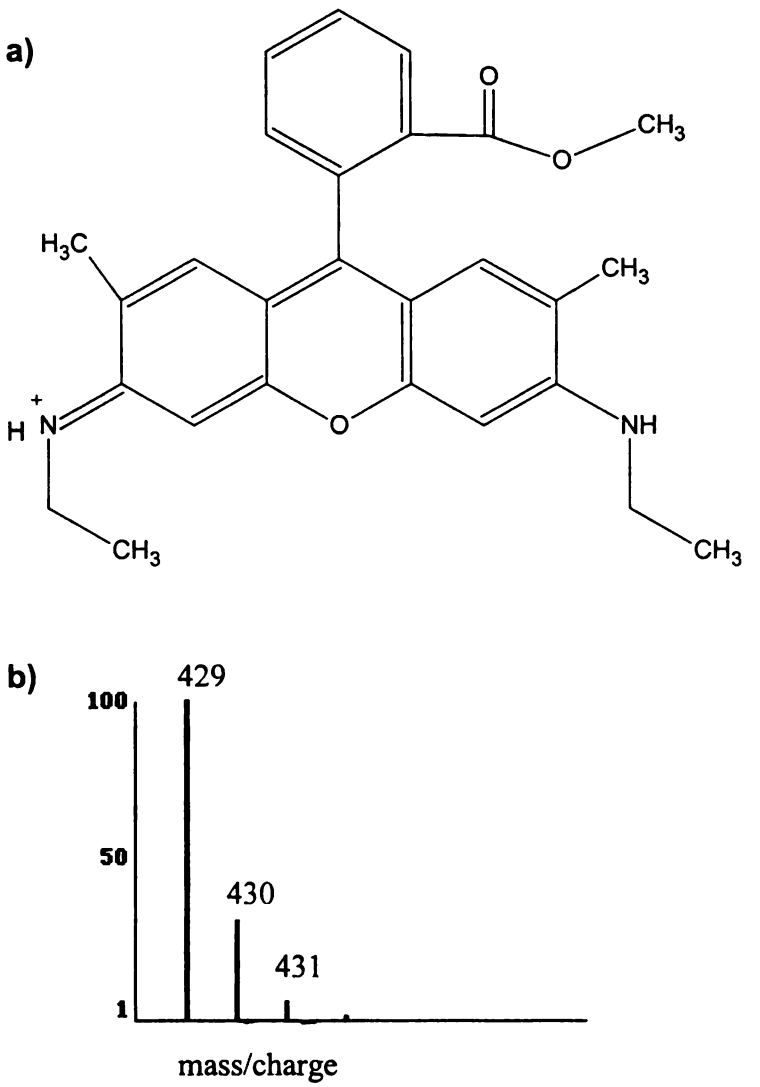

Figure 6.3: Basic Red 1:1: a) structure and b) theoretical isotope distribution

This molecule differs only slightly from Basic Red 1. Basic Red 1:1 has a methyl group attached to the carboxyl group where Basic Red 1 has an ethyl group. It is very possible that this particular batch of the security ink contained Basic Red 1:1 in place of Basic Red 1 as the formula listed. In this application (a security ink staining currency and criminal), the exact chemical structure of the rhodamine is not important, as long as the ink is bright and colorfast. On the mass

spectrometric level, however, the substitution of a methyl group for an ethyl yields significant differences. These rhodamine dyes are cationic and therefore detected only in the positive-ion mode.

Successful detection of the security ink was broadly defined as the detection of both of the two main dye components of the ink (Basic Violet 11:1 and (likely) Basic Red 1:1). This required detection of mass spectral peaks corresponding to the cation of each of the dyes and near-unit resolution of these peaks. LD/MS is a soft ionization technique, meaning that an intact molecular ion may be detected. In contrast, hard ionization techniques such as electron impact ionization (encountered with GC/MS) fragment ions substantially, and one may not be able to even detect a molecular ion. Even without an "ion fragmentation pattern," we are confident in the detection of the security ink. We weren't suggesting the presence of the security ink based on the presence of a single mass spectral peak, rather we confirmed the presence of the security ink using two sets of peak patterns.

Detection of security ink on currency

A positive-ion mass spectrum of a stained bill is shown in Figure 6.4. Similar resolution was obtained from all three sets of stained currency: currency stained over a year ago, currency stained one week before analysis and currency stained immediately before analysis.

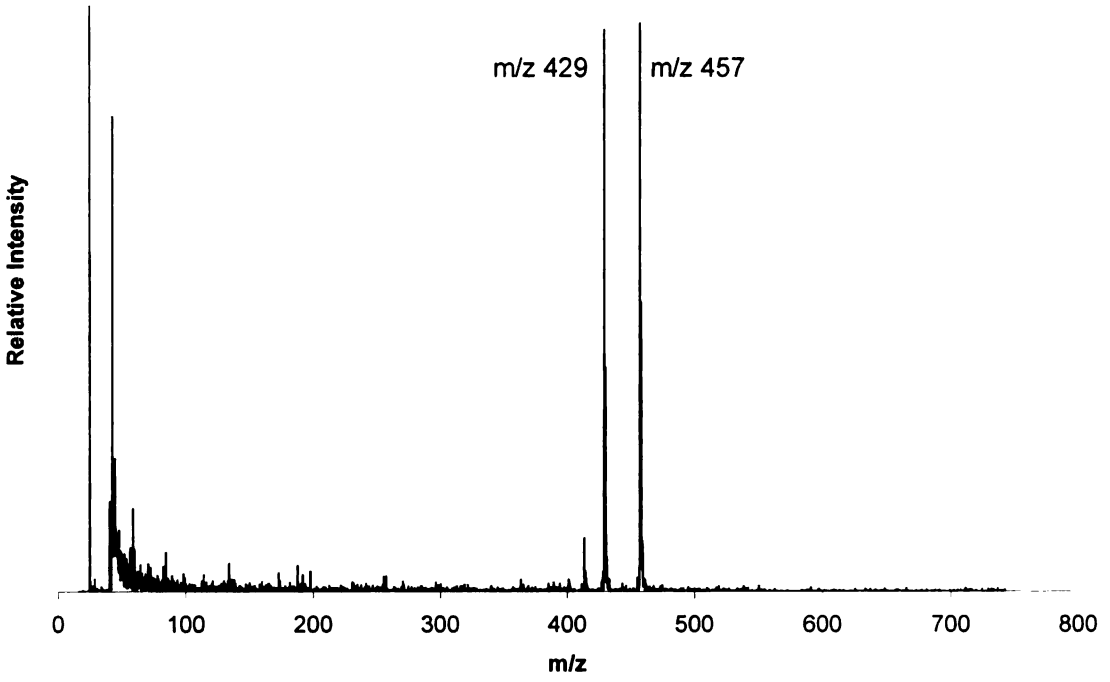

Figure 6.4: Positive-ion LD mass spectrum of stained bill

To eliminate the paper and the intaglio inks used to print the currency as sources of the peaks on Figure 6.4, mass spectra of unstained currency were also taken. Positive-ion and negative-ion mass spectra of unstained currency have been discussed in Chapter 5. Neither the paper nor the currency printing inks interfere with detection of the security ink because the currency printing inks and the security ink appear at unique masses. If a scientist was analyzing a portion of the bill that had been printed green and also stained, the printing ink and the security ink could be detected simultaneously.

An interesting observation was made regarding detection of both these inks. The security ink could be detected at lower laser powers than currency printing inks

were detected. By choosing a low laser power, one can obtain a mass spectrum representing just the security ink (absent of peaks representing the currency).

To outfox a bank robber who attempts washing stained currency, we considered whether the security ink could still be detected off currency that had been washed. As expected, slightly more ink could be extracted from the more freshly stained bills than from the bills stained one year prior to washing. Bleach, nitric acid, and the (ethyl-acetate based) nail polish remover appeared to best remove the security ink. These solvents left only a faint pink (or in the case of nitric acid, orange) color on the bills. After approximately one hour in each of these solvents, the security ink was still not fully removed, and due to the strong nature of the solvents, the paper itself started to break down. Each of the other solvents left a noticeable pink stain. Using LD/MS, it was possible to detect the security ink on all of the washed currency.

Detection of Basic Blue 7

The security ink also contained a related dye, Basic Blue 7 (structure and theoretical isotope distribution shown in Figure 6.5) This technique can detect dilute amounts of isolated Basic Blue 7. However, the 100-200 fold excess of the other dyes appears to hinder detection of Basic Blue 7 in this sample. Peaks representing this compound were observed after TLC separation of the security ink, to isolate the blue component of the ink. A positive-ion mass spectrum of the blue dye after TLC separation of the security ink is shown in Figure 6.6.

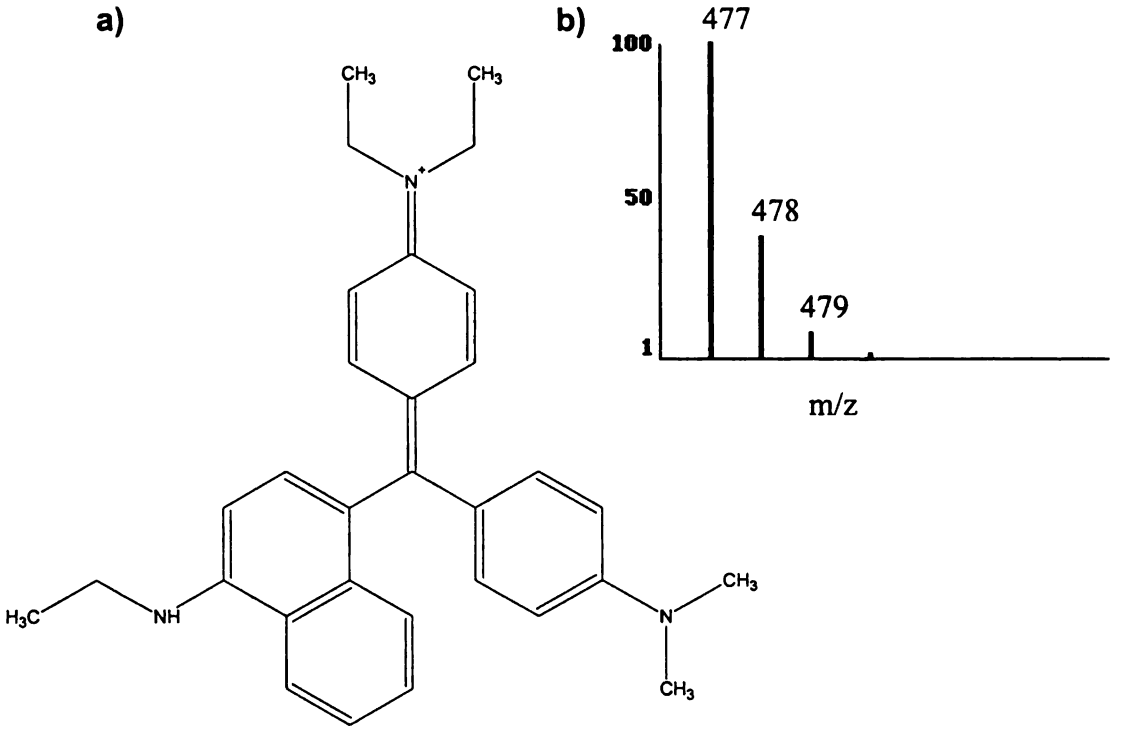

Figure 6.5: Basic Blue 7: a) structure and b) theoretical isotope distribution

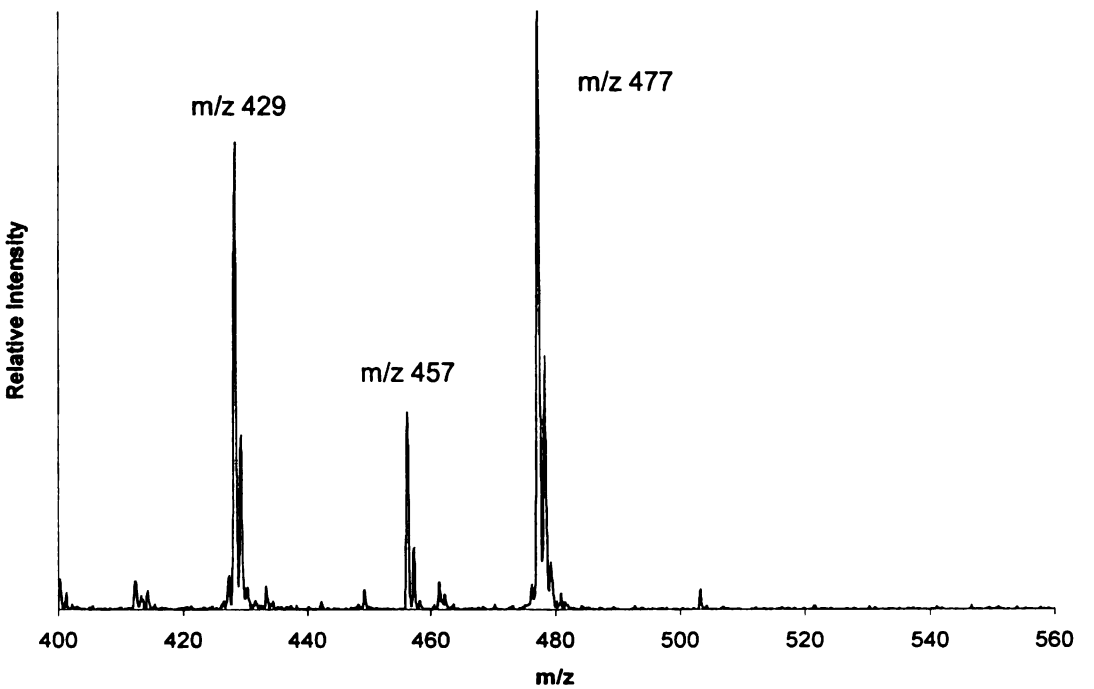

Figure 6.6: Positive-ion LD mass spectrum of blue dye (on gold plate) recovered by TLC separation of security ink. Other dye components are still present in the separation.

Analysis of other pink inks encountered on currency

Occasionally we've observed a bit of pink ink in the corners of currently circulated bills. Marks in the corners of bills are sometimes made by banks or ATM services using a highlighter or other pen. We wanted to confirm that these pinks spots would not produce spectra falsely indicating the presence of the security ink. A positive-ion mass spectrum of this region of a bill is shown in Figure 6.7. The peaks at m/z 283 and m/z 311 appear in the positive-ion mode only, suggesting that they represent cationic dyes. Also, these peaks are separated by 28 mass units; this suggests the molecules differ by an ethyl group. The m/z values are too low for these molecules to be in the rhodamine family of dye molecules. Also, these peaks do not have any characteristic isotope distribution pattern suggesting the presence of any elements other than hydrogen, carbon, nitrogen and oxygen. No identification has been made for these peaks. We note the presence of these dyes to illustrate how LD/MS can be used to analyze and distinguish between dyes that appear to be the same color.

Summary

This chapter describes a way to quickly identify one commercially available security ink. Since relatively few molecules on the surface are desorbed, this technique is not significantly destructive[3]. After using LD/MS to obtain a mass spectrum of the sample, one can continue with another analysis (such as extraction of the ink for FT-IR).

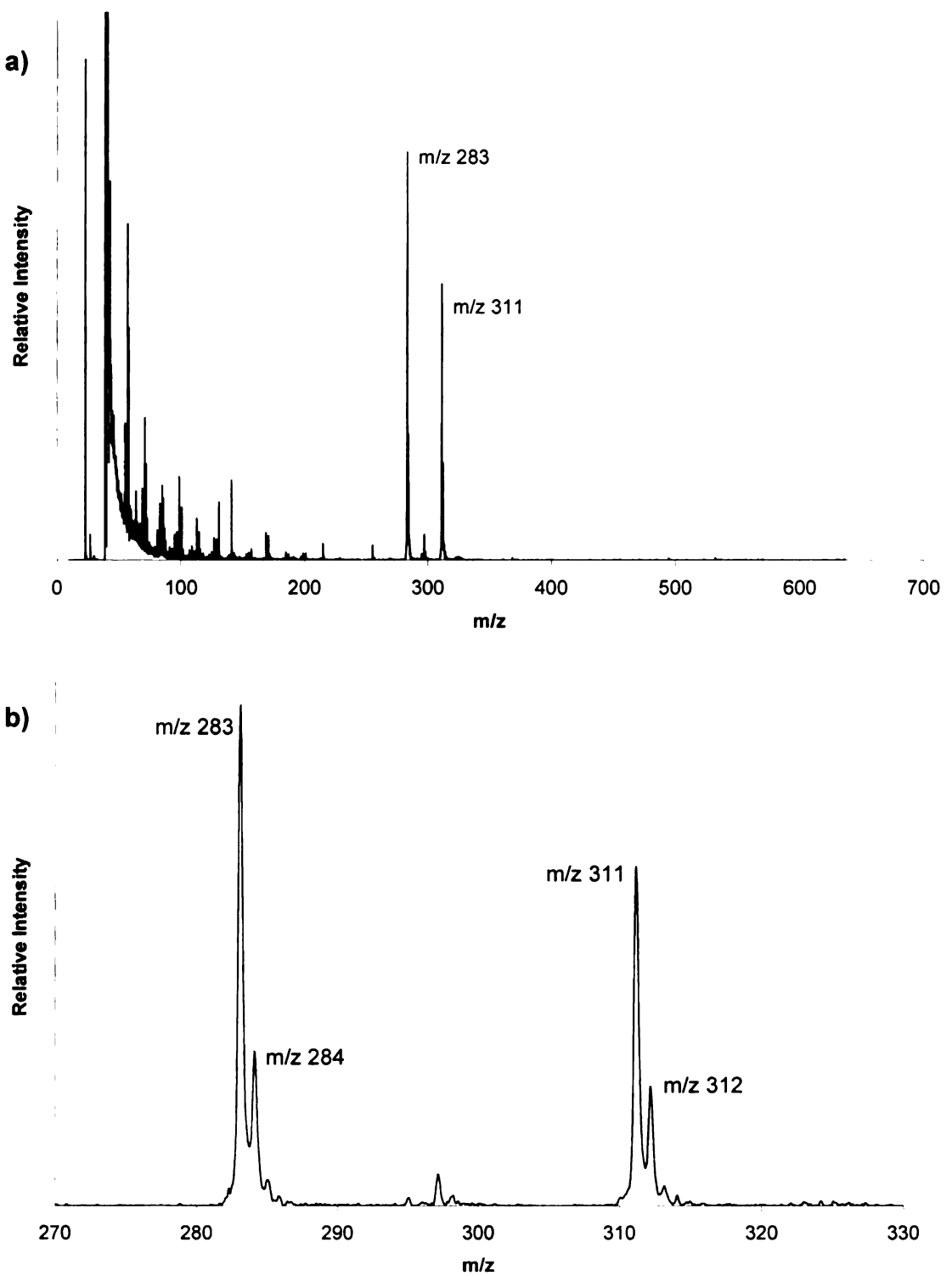

Figure 6.7: Positive-ion LD mass spectrum of pink corner of $20 bill

References

(1) R. M. Mart, D. J. Reutter, L. D. Lasswell, *Journal of Forensic Sciences,* **28** (1983) 200-207.

(2) H. Seiden, *International Journal of Forensic Document Examiners,* **2(3)** (1996) 220-225.

(3) Grim, D.M., Siegel, J., Allison, J., *Journal of Forensic Sciences,* **46** (2001) 1411-1420.

(4) Reilly, C.A., Crouch, D.J., Yost, G.S., Andrenyak, D.M., *Journal of Forensic Sciences,*. **47** (2002) 37-43.

Chapter 7: 1-Methyl aminoanthraquinone

Introduction and method

Explosive devices containing dyes are used to protect currency (and other valuables) in vaults and bags used to transport currency[1,2]. When a robbery occurs, the explosive device can be activated (read: detonated) to produce a cloud of dye. This dye can stain the stolen currency and suspect, aiding in the arrest and conviction of the criminal. These devices contain pyrotechnic chemicals (to generate the cloud of dye), an anthraquinone-based (usually) dye, and may also contain tear gas to stun a fleeing suspect[3,4]. Chromatographic techniques such as GC-MS[5] and HPLC-UV[6] have been used to detect and study smoke dyes.

A portion of a smoke pellet (provided by a security device manufacturer) was dissolved in water. This solution was "painted" onto a piece of plain printer paper for analysis. This was done to simulate the residue from an activated smoke pellet adhering to paper or other surfaces. The main/ only color component of the pressed smoke pellets is 1-methyl aminoanthraquinone (1-MAAQ), the structure and theoretical isotope distribution shown in Figure 7.1.

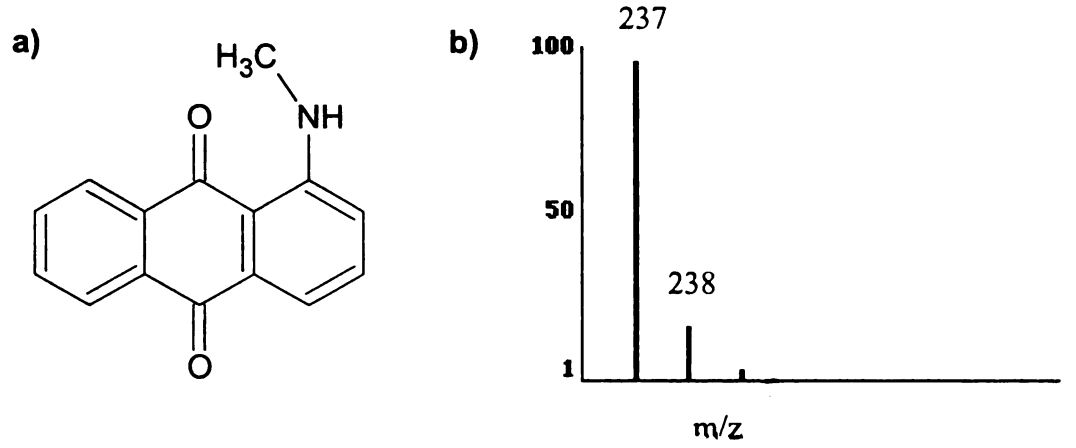

Figure 7.1: 1-Methyl aminoanthraquinone (1-MAAQ): a) structure and b) theoretical isotope distribution of 1-MAAQ

Interpretation of positive-ion mass spectrum of 1-MAAQ

As observed in the positive-ion mass spectrum (Figure 7.2), a peak at m/z 237 represents the molecular ion. The peak at m/z 238 represents both the protonated molecular ion $(M+H)^+$ and ^{13}C isotopes of the molecular ion. The peak at m/z 239 represents ^{13}C isotopes of the protonated molecular ions.

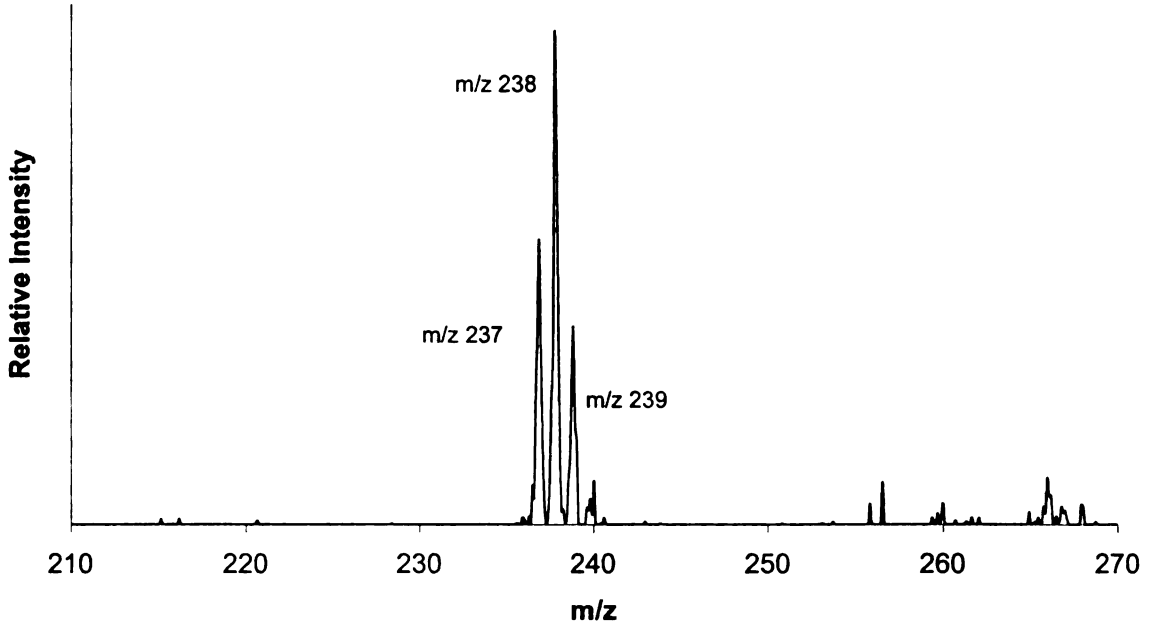

Figure 7.2: Positive-ion LD mass spectrum of paper stained with smoke pellet

Interpretation of negative-ion mass spectrum of 1-MAAQ

This neutral dye is easily detected in negative-ion mode; the negative-ion LD mass spectrum is shown in Figure 7.3. The peak at m/z 237 represents the molecular ion (M^-), the peak at m/z 236 represents the deprotonated dye molecule $(M-H)^-$.

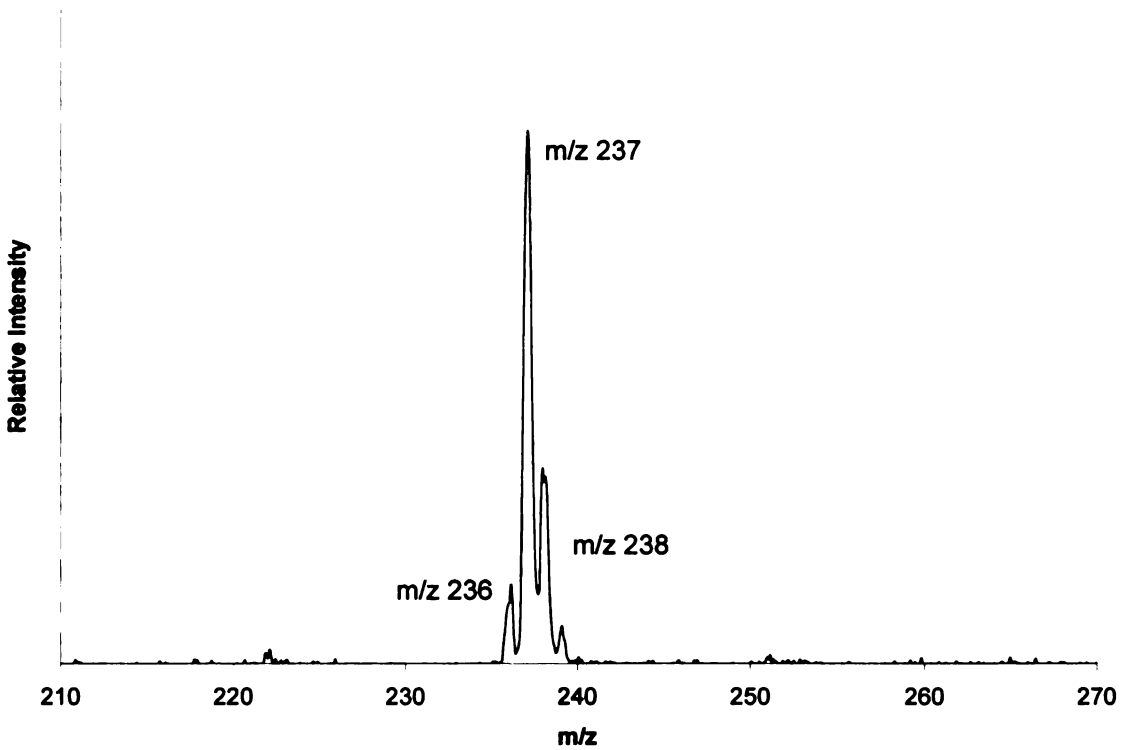

Figure 7.3: Negative-ion LD mass spectrum of paper stained with smoke pellet

Analysis of 1-MAAQ by GC/MS

This dye is detected easily using GC/MS. The EI mass spectrum is shown in Figure 7.4. GC/MS is a standard method of separating, detecting, and characterizing smoke pellet components. LD/MS allows for focused analysis of the dye components (such as 1-MAAQ) without detection of confusing and distracting fillers such as sugars and binders.

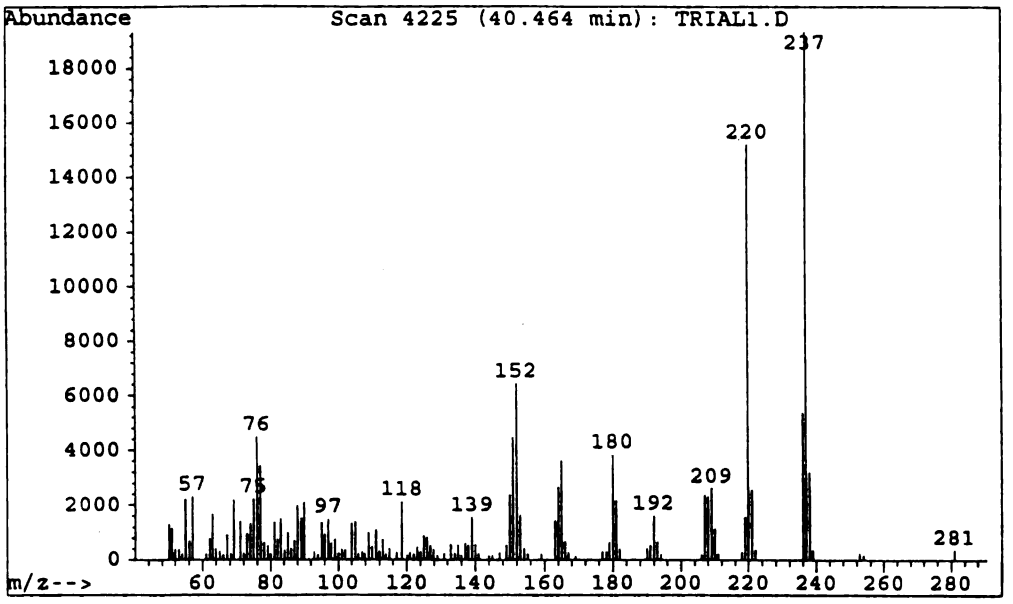

Figure 7.4: Electron impact mass spectrum of dilute CH_2Cl_2 solution of smoke pellet

PSD and "artificial aging" of smoke pellet using fluorescent light

In addition to identifying peaks on a mass spectrum as characteristic of a certain analyte, it is possible to do more confirmatory analyses using LD-MS. For example, post source decay (PSD) mass spectrometry can be used to look for characteristic fragments ions of a dye molecule. In the case of 1-MAAQ, no fragment ions were detected due to the aromaticity and stability of 1-MAAQ. Artificial aging through photodegradation may be conducted to further confirm the structure of a peak assignment. For the analysis of the smoke pellets in these experiments, samples of paper "painted" with the dye were exposed to fluorescent light for up to 120 hours. Compounds of this class are known to dimerize at the nitrogen[7,8,9]. Peaks representing the dimer of 1-MAAQ appear at above m/z 400; this region of the mass spectrum is shown in Figure 7.5.

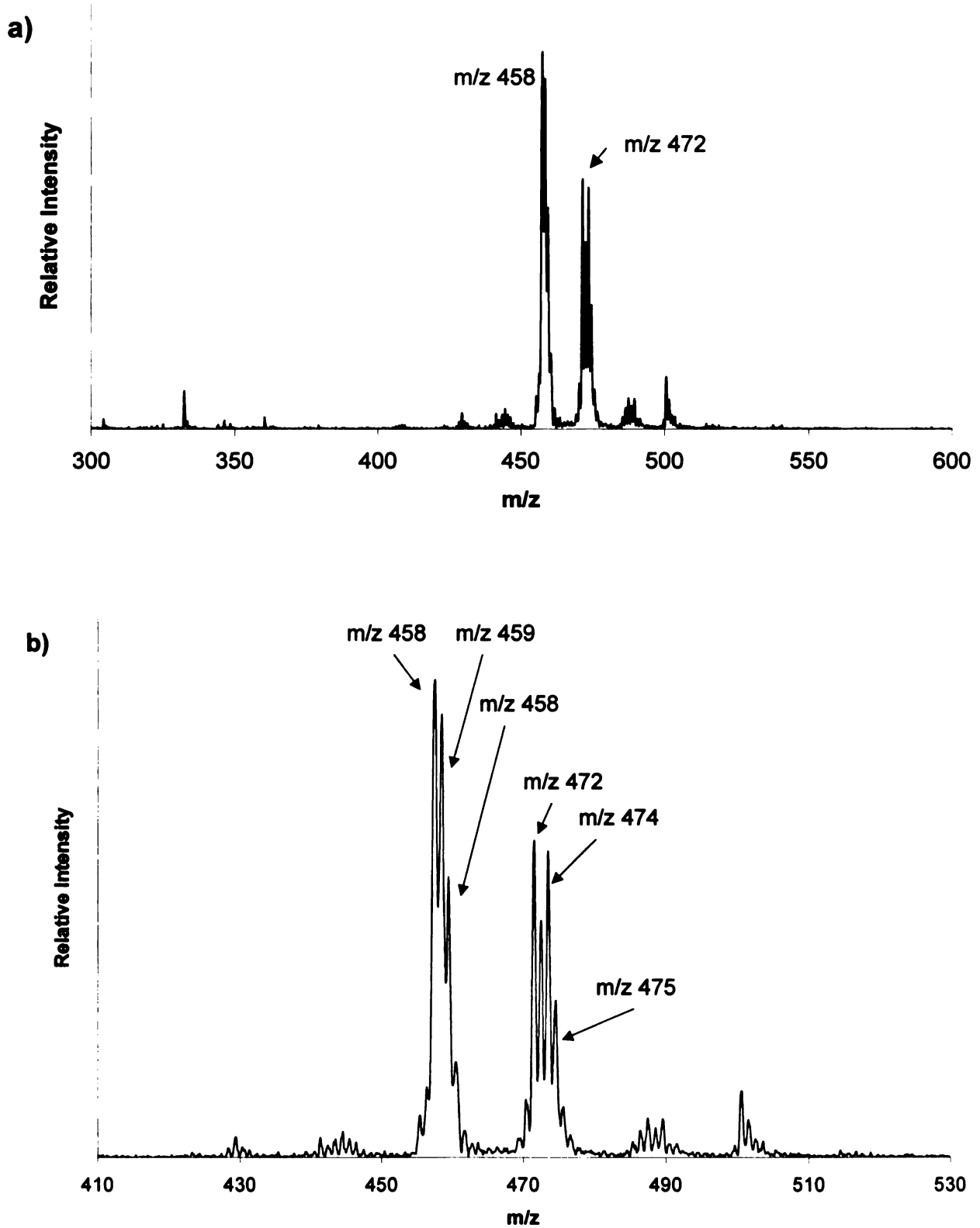

Figure 7.5: Positive-ion LD mass spectrum of paper stained with smoke pellet exposed to direct fluorescent light for 120 hours; a) m/z 300-600 and b) 410-530

Structures of two dimers and their theoretical isotope distributions are shown in Figure 7.6.

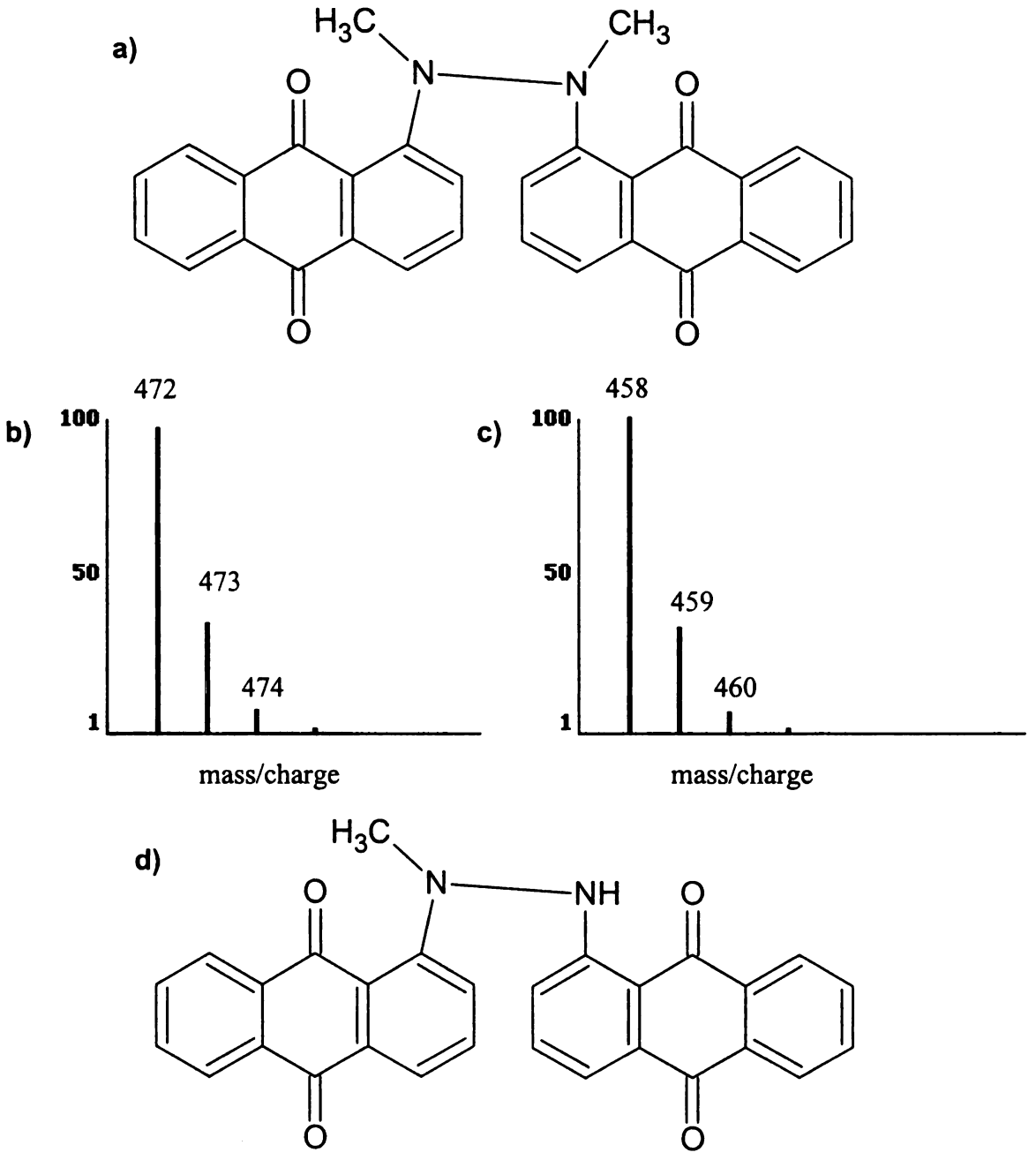

Figure 7.6: Dimer A: a) structure and b) theoretical isotope distribution Dimer B: c) theoretical isotope distribution and d) structure

Peaks representing the molecular ion of dimer A (M^+) and protonated dimer A $(M+H)^+$ are observed in the range of m/z 472 to 476. Peaks representing the molecular ion of dimer B (M^+) and protonated dimer B $(M+H)^+$ are observed in the range of m/z 458-461.

Summary

LD/MS successfully detected 1-MAAQ directly off paper in both positive-ion and negative-ion modes. Exposure to fluorescent light induced predicted dimerization of the molecules, further confirming the mass spectral peak assignments and structure of the dye molecule. As some research describes[10], during combustion, some of the dye molecules may be converted to slightly different chemical species. Based on what we've observed here (and our analysis of other dyes), we anticipate that any combustion products that contain the anthraquinone structure would be detected using LD/MS.

References

(1) F. W. Millar., US patent 4,391,203 (1981)

(2) S. E. Keniston, (U.S. Currency Protection Corp.) US Patent 5,196,828 (1993)

(3) Security ink manufacturer representative, personal communication

(4) H. Seiden, *International Journal of Forensic Document Examiners,* **2(3)** (1996) 220-225.

(5) R. M. Martz, D. J. Reutter, and L. D. Lasswell, *Journal of Forensic Sciences,* **28** (1983) 200-207.

(6) I. B. Rubin, M. V. Buchanan, J. H. Moneyhun, *Analytica Chimica Acta*, **155** (1983) 151-158.

(7) K. Orito, T. Hatakeyama, M. Takeo, S. Uchiito, M. Tokuda, H. Suginome, *Tetradehdron*, **54** (1998),8403-8410.

(8) H. R. Ellison, and B. W. Meyer, *Journal of Physical Chemistry* " **74** (1970) 3861-3867.

(9) I. Stassen, G. Hambitzer, *Journal of Electroanalytical Chemistry*, **440** (1997) 219-228.

(10) I. B. Rubin, M. V. Buchanan, J. H. Moneyhun, *Analytica Chimica Acta*, **155** (1983) 151-158.

Chapter 8: Fabric Dyes

Introduction and motivation

Fiber evidence is one type of trace evidence encountered at crime scenes. A variety of techniques such as microscopy, infrared spectroscopy[1,2] and raman spectroscopy[3] are currently used to characterize fibers. These techniques primarily identify the composition of the fiber itself (i.e., what type of polyester it is?). Comparative microscopy, thin layer chromatography, and microspectrophotometry are used to study the dye component of the fibers.[4-8] However, these techniques rely more on comparison rather than identification of dyes and do not provide much information about the chemical structure of the dye. Chemical characterization of the dye component of fibers is desirable because the more chemical information that can be garnered about two fibers, the more confidently a forensic analyst can conclude whether or not the fibers had a common origin.

Additionally, from an archeological and historical standpoint, identifying the dyes used to color fabrics (for clothing, etc.) can help researchers learn more about the culture, habits, and knowledge of a particular people group or time period. Even in the past 100 years, some of the dyes used on cotton fabrics used in quilts have changed significantly[9]. Recently, many fabric designs from 100-200 years ago are being reintroduced[10] (using improved lightfast and washfast dyes). Identification of the dyes would help distinguish genuine fabrics from contemporary imitations.

Direct Dyes

The phrase "direct dye" explains the application process of these dyes. They are applied directly to the fabric, without the use of a mordant or reactive group. The dye molecules are held to the fabric primarily through hydrogen bonding[11] and dispersion forces. Portions of a colorful, cotton fabric purchased locally were used for analysis of direct dyes.

Positive-ion and negative-ion mode mass spectra were taken of the blank (not colored) regions of the fabric (shown in Figures 8.1 and 8.2, respectively).

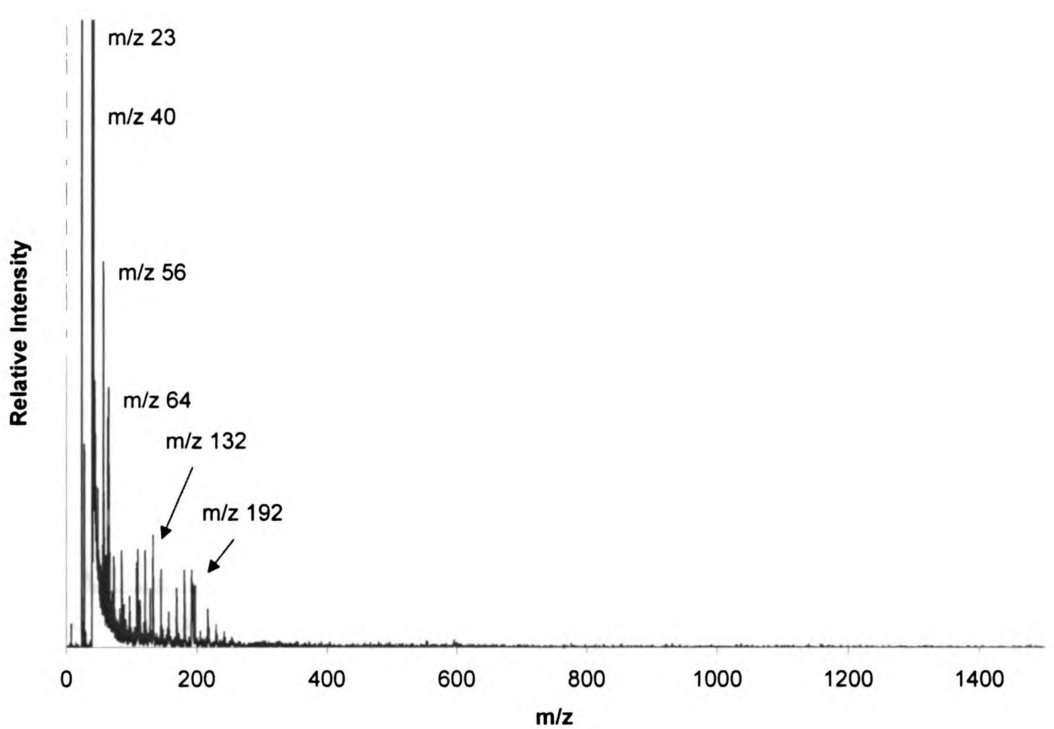

Figure 8.1: Positive-ion LD mass spectrum of unprinted region of cotton fabric (Laser power = 2680)

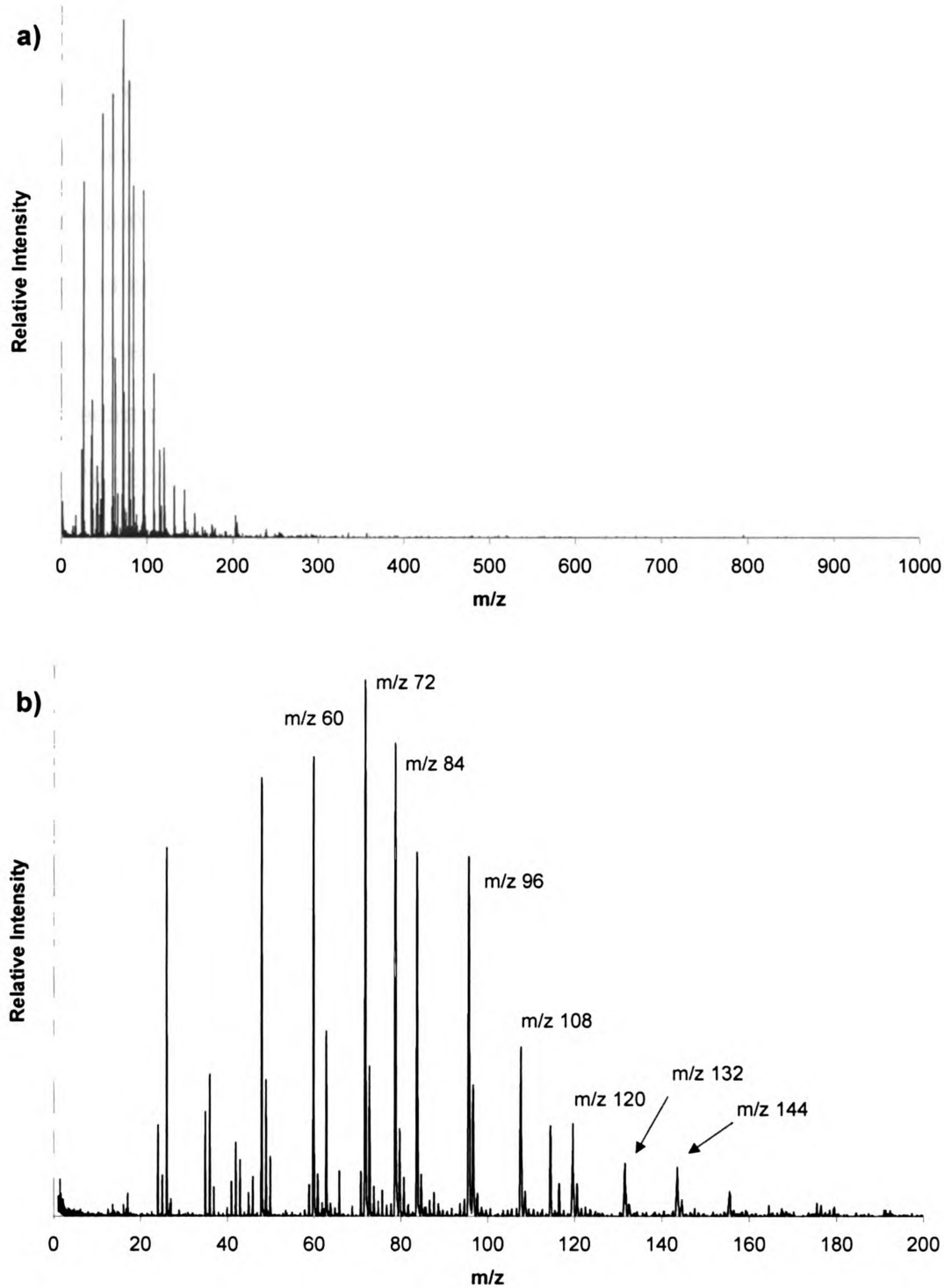

Figure 8.2: Negative-ion LD mass spectrum of unprinted region of cotton fabric (Laser power = 2680) a) m/z 0-1000 and b) m/z 0-200

No obvious assignments for these peaks were made; these peaks may be due to sizing, detergents, or other additives in the fabric. The identity of these peaks is not important for our analysis of the dyed regions of the fabric. Collecting mass spectra of the un-dyed regions of the fabric is comparable to collecting background spectra of a solvent used in UV-Vis spectrophototometry. Mass spectra of the blank regions of a fabric help a scientist isolate the peaks on the mass spectra of a dyed region of fabric representing the dye. Notice that peaks above m/z 220 appear on neither of the mass spectra. This is helpful because it assures us that peaks produced by laser irradiation of the fabric (and any chemicals the fabric has been treated with) will not obscure dye peaks appearing above m/z 220.

Positive-ion and negative-ion mass spectra of the yellow region of the fabric are shown in Figures 8.3 and 8.4.

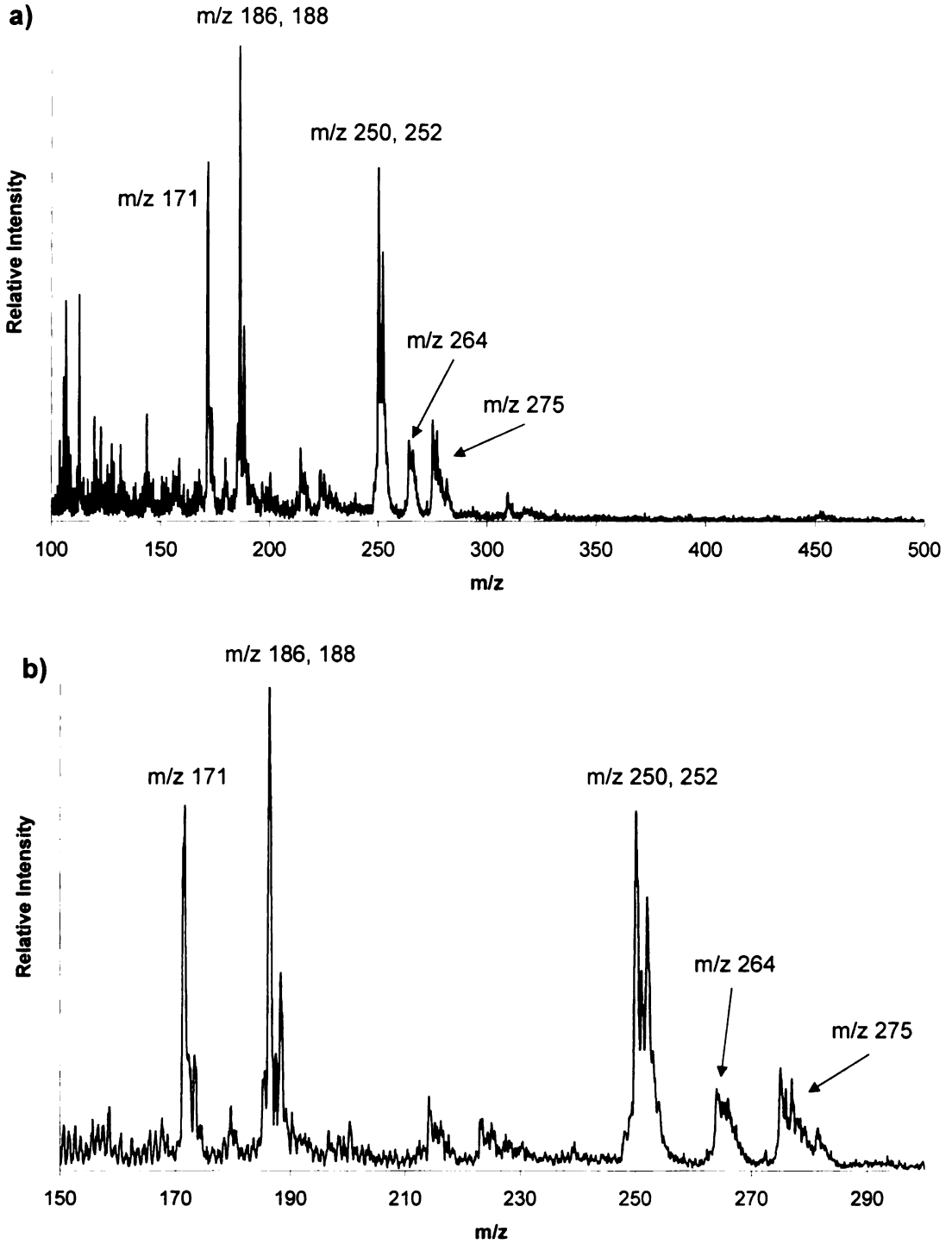

Figure 8.3: Positive-ion LD mass spectrum of yellow region of cotton fabric (Laser power = 2680) a) m/z 100-500 and b) 150-300

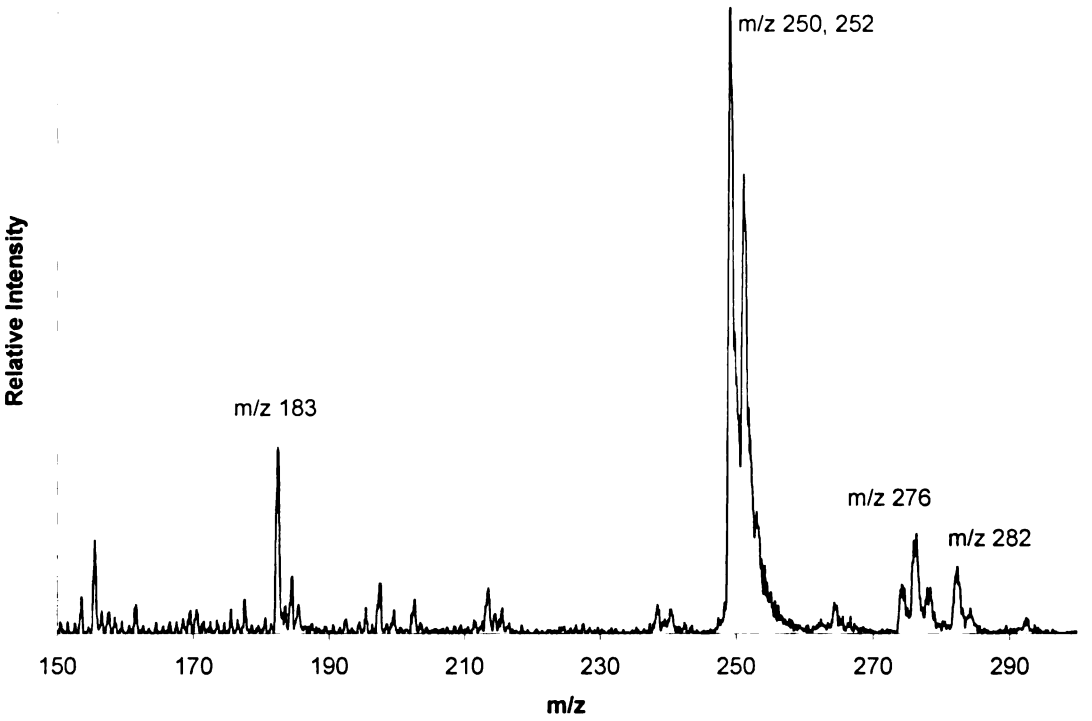

Figure 8.4: Negative-ion LD mass spectrum of yellow region of cotton fabric (Laser power = 2680)

Unit resolution was not possible for the peaks around m/z 250, however, the peaks resembled the isotope pattern observed in the mass spectra taken of the yellow region of a stamp (discussed earlier in chapter 4). Comparing the positive-ion mass spectrum taken of the stamp (Fig. 4.1) with the positive-ion mass spectrum of this region of the fabric (Fig. 8.3) allowed us to conclude that the dye on the yellow region of the fabric was likely the same dye identified in chapter 4, dichloroazobenzene. The structure and theoretical isotope distribution of this molecule are shown in Figure 8.5.

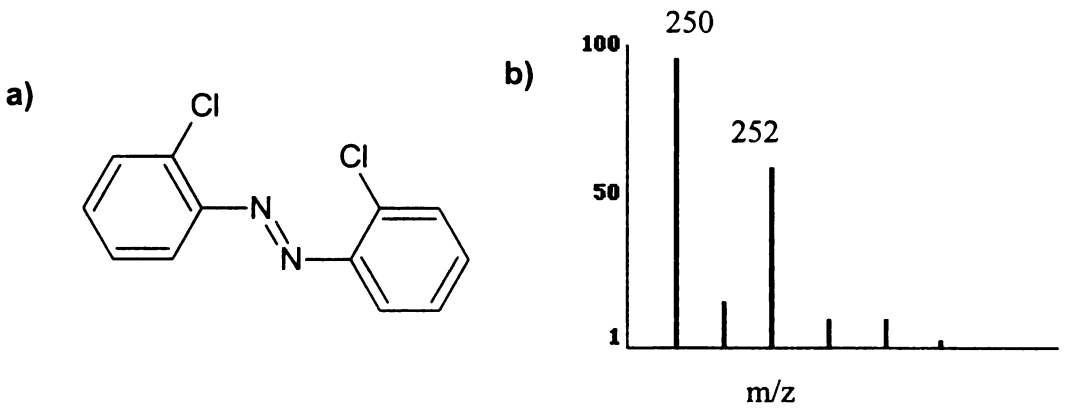

Figure 8.5: Dichloroazobenzene a) structure and b) theoretical isotope distribution

Both the positive-ion and negative-ion mass spectra (Figure 8.7) of the blue region of the spectra contained peaks representing the neutral dye copper phthalocyanine. The structure and theoretical isotope distribution of this compound are shown in Figure 8.6 and were discussed earlier in chapter 3.

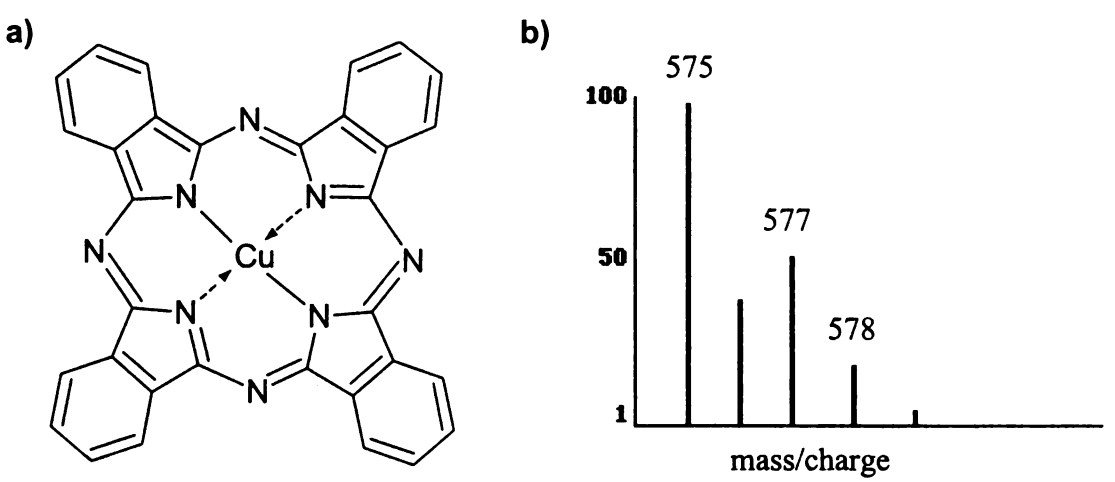

Figure 8.6: Pigment Blue 15 a) structure and b) theoretical isotope distribution

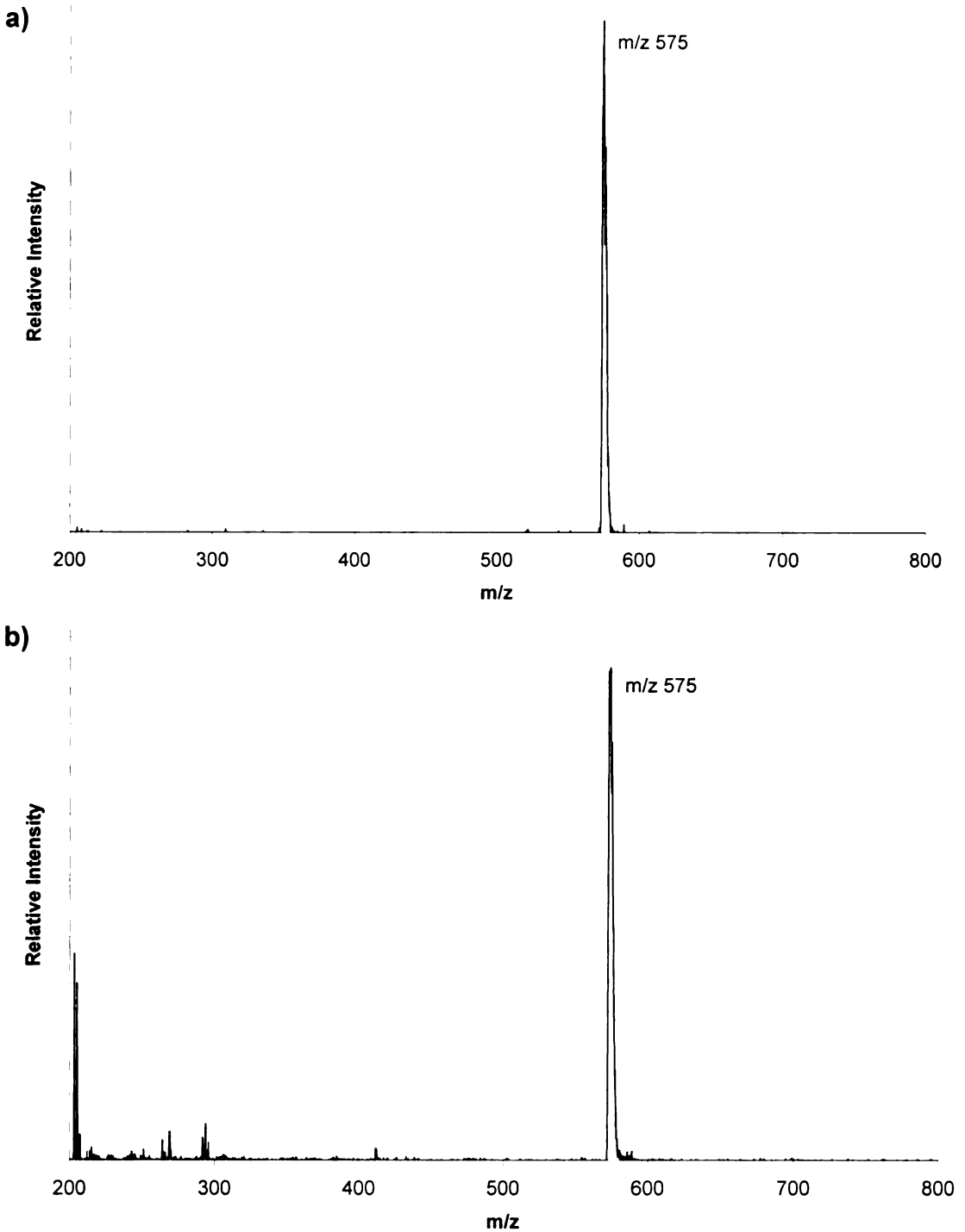

Figure 8.7: LD mass spectrum of blue region of cotton fabric: a) positive-ion (Laser power = 1780) and b) negative-ion (Laser power = 2080)

Because "yellow and blue make green," it is not surprising that mass spectra taken of the chartreuse (light yellow-green) region of the fabric contain peaks representing the dyes observed in the yellow and blue regions of the fabric. The positive ion mass spectrum of the chartreuse region of the fabric is shown in Figure 8.8.

On this spectrum, the peak at m/z 250 represents dichloroazobenzene (the yellow dye) and the peak at m/z 575 represents copper phthalocyanine (PB 15, the blue dye). Additional peaks above m/z 1000 represent chlorinated copper phthalocyanine (PG 7), a green dye discussed in chapter 5. The same peak assignments are made on the negative-ion mass spectrum (Figure 8.9) of the same region of fabric.

Peaks representing each of the dyes are observed in both positive-ion and negative-ion mode because each of the three dyes are neutral molecules. Notice however, that the ratios of the peaks vary between the spectra. For example, the ratio of the peak at m/z 1125 to the peak at m/z 575 is higher on the negative-ion mass spectrum. This is likely a feature of the molecules themselves, and possibly reveals information about the relative ease of ionization of the molecules. The ratio mentioned above suggests that the PG 7 molecule is more readily ionized than PB 15 (the unsubstituted copper phthalocyanine); the sixteen chlorines on PG 7 perhaps facilitate the formation of the M^- ion of PG 7.

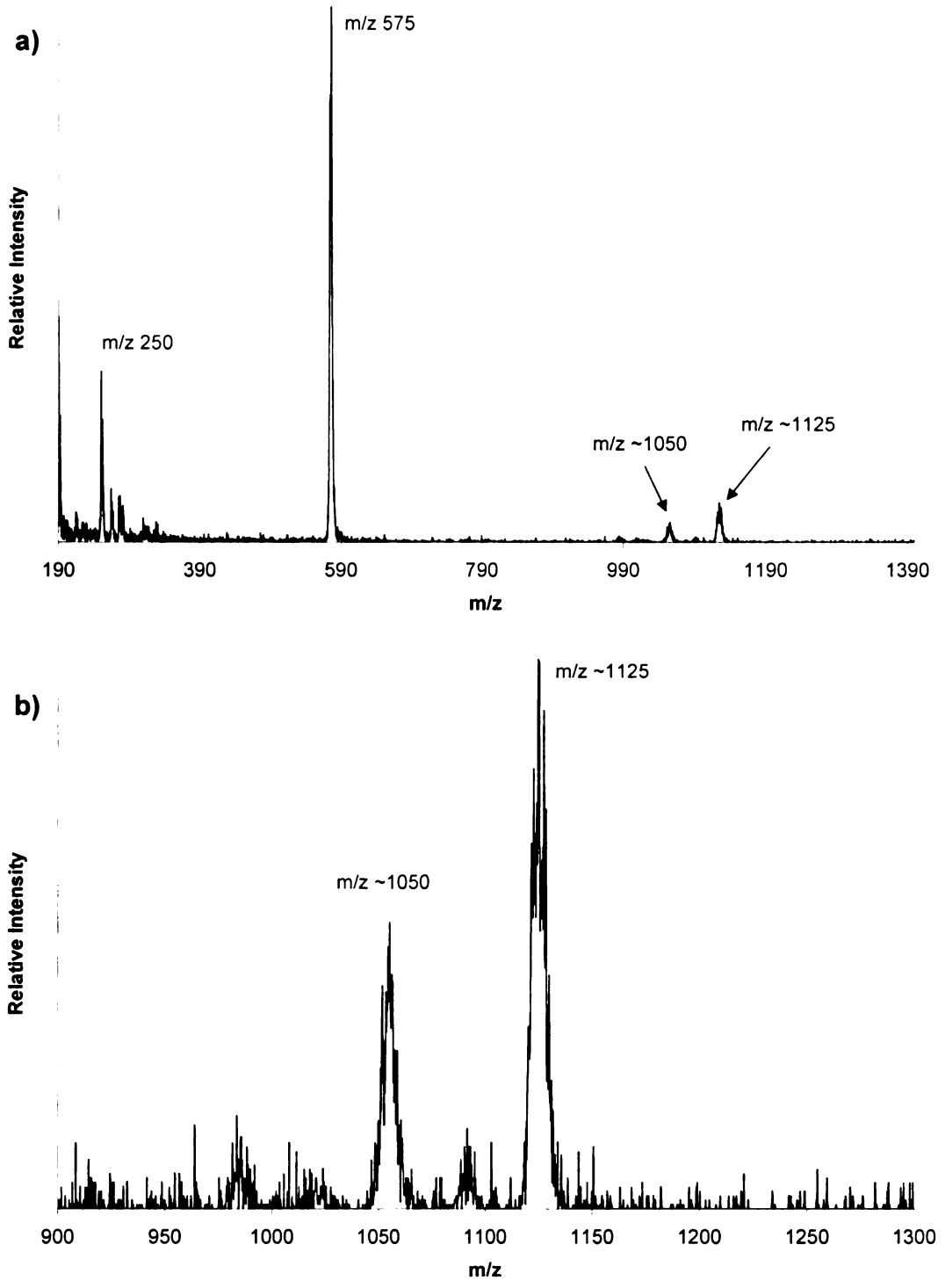

Figure 8.8: Positive-ion LD mass spectrum of chartreuse region of cotton fabric (Laser power = 2480) a) m/z 190-1400 and b) m/z 900-1300

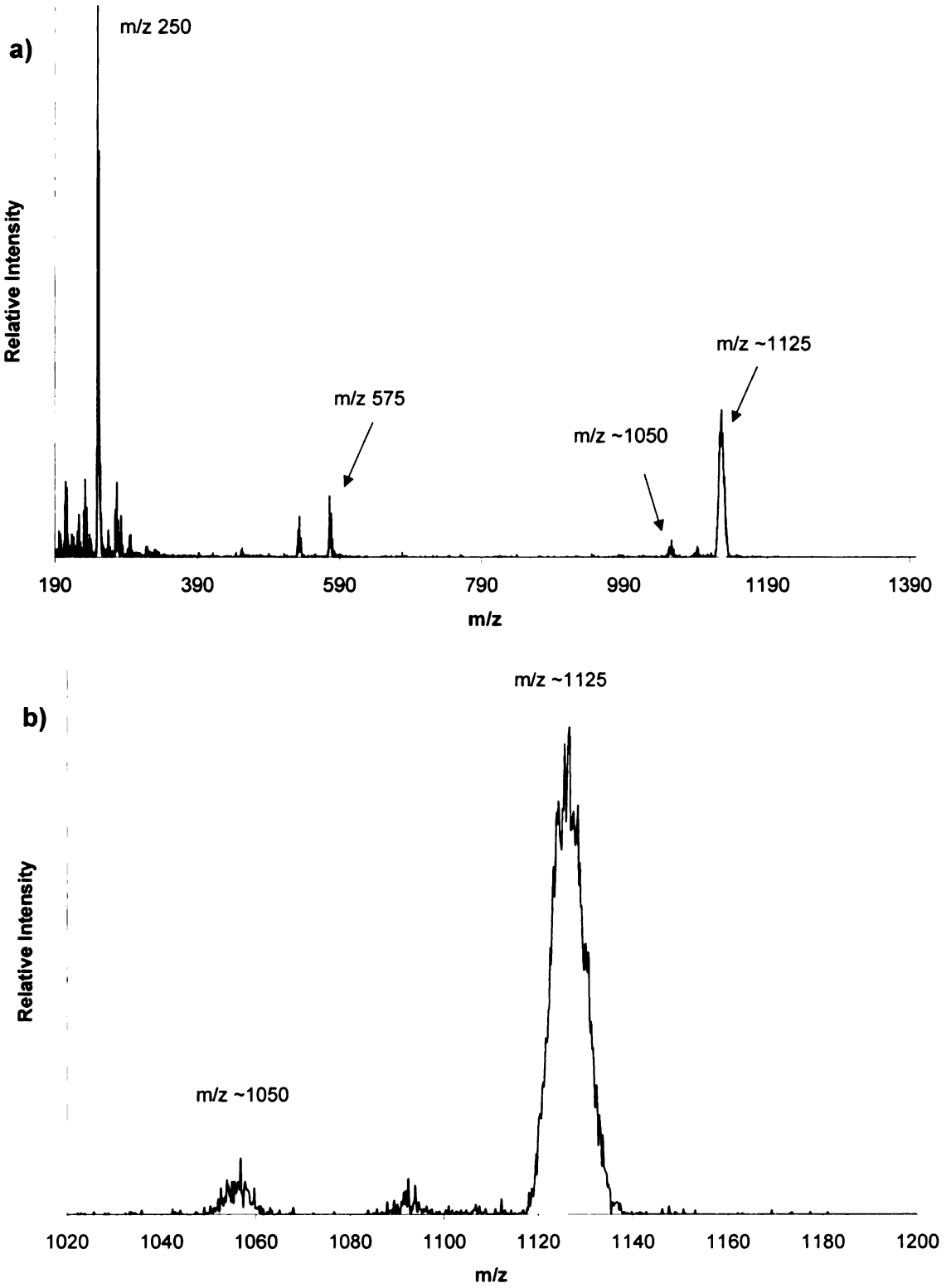

Figure 8.9: Negative-ion LD mass spectrum of chartreuse region of cotton fabric (Laser power = 2480) a) m/z 190-1390 and b) m/z 1020-1200

Even at high laser intensity, the positive-ion mass spectrum (Fig. 8.10) of the salmon (peach-colored) region of the fabric did not contain distinct peaks suggesting the presence of a neutral or cationic dye.

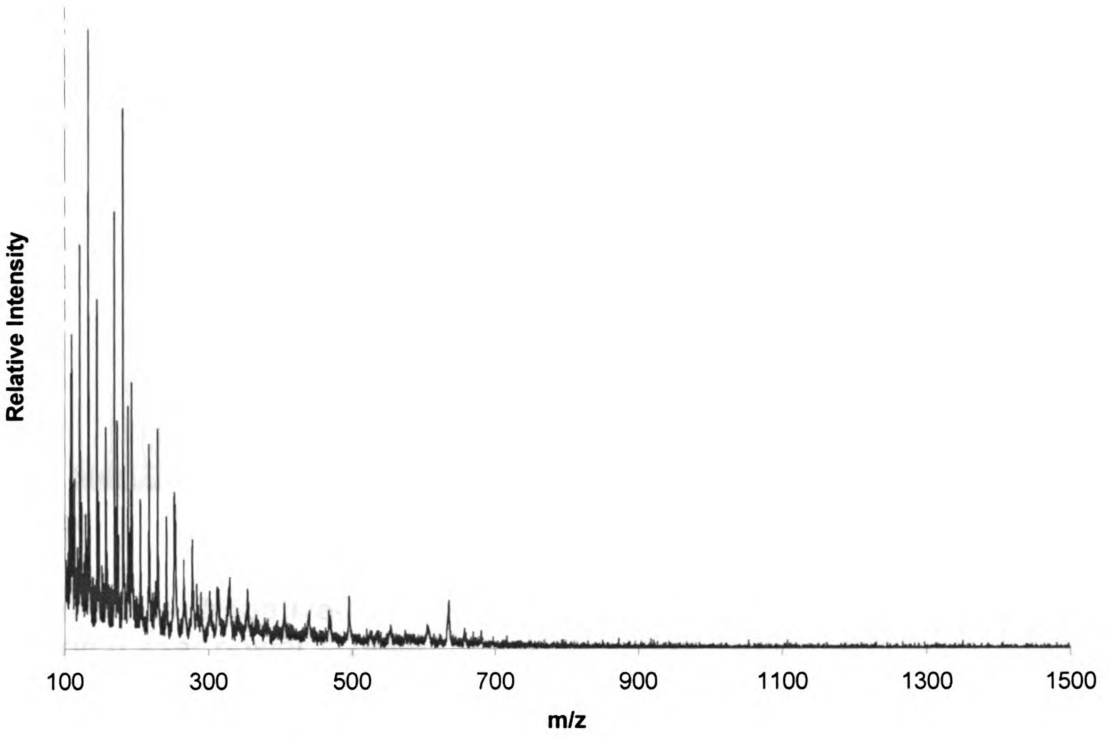

Figure 8.10: Positive-ion LD mass spectrum of salmon region of cotton fabric (Laser power = 2780)

The negative-ion mass spectrum (Figure 8.11) of the same region contained higher mass peaks (at approximately m/z 600 and m/z 630). These likely represent anionic dyes. As an example of such a dye, Acid Red 151 is shown in Figure 8.12.

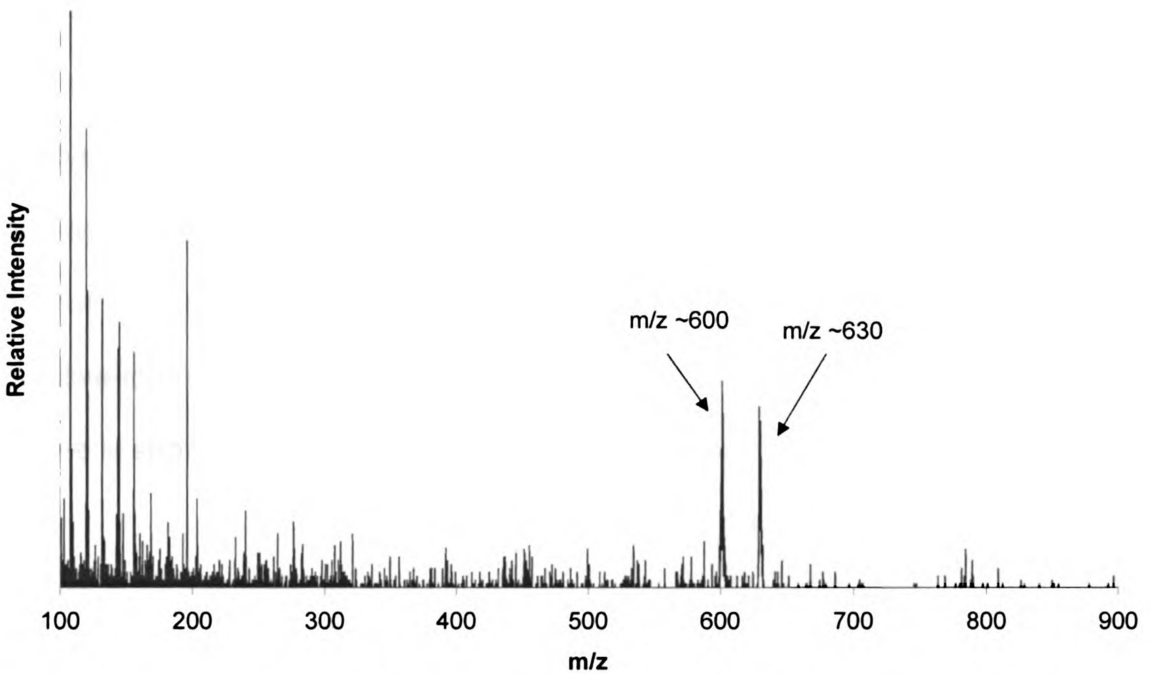

Figure 8.11: Negative-ion LD mass spectrum of salmon region of cotton fabric (Laser power = 2480)

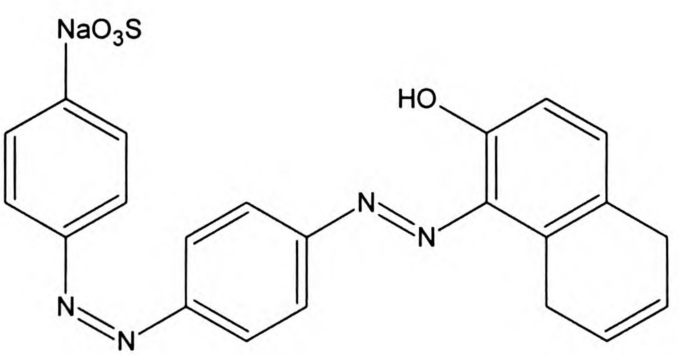

Figure 8.12: Structure of Acid Red 151

Analyzing a single fiber is relevant and desirable to minimize sample intrusion of valuable historical fabrics or because a single fiber may be all the evidence a forensic analyst has to work with. Because of the small spot size of the laser, it was possible to obtain interpretable mass spectra from a single fiber. With the analysis of single fibers, one is not able to average spectra as freely as one can average spectra obtained over a large area of fabric, so the resolution of peaks is poorer in mass spectra obtained through laser irradiation of single fibers. A positive-ion mass spectrum of a yellow fiber from the same sample described above is shown in Figure 8.13.

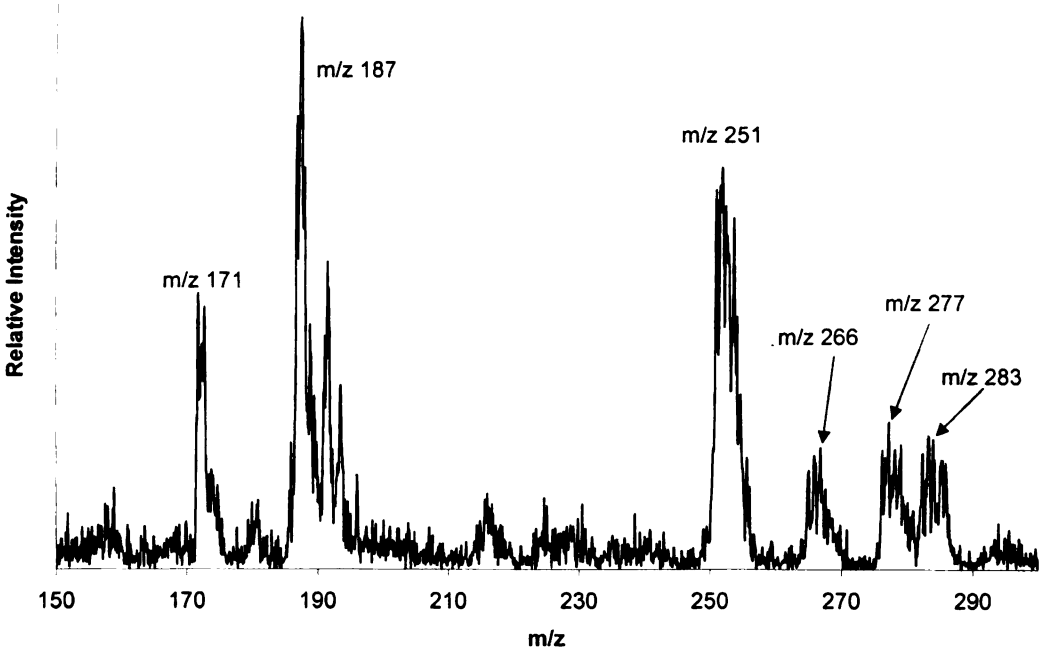

Figure 8.13: Positive ion LD mass spectrum of single yellow fiber (from cotton fabric) (Laser power = 2511)

Interpretation of the mass spectra presented in this section was facilitated by the finite number of dyes, inks, and pigments available on the market. As demonstrated in the analysis of the yellow region of fabric, when a colorant has been established as lightfast, colorfast, and useful in one application (i.e., printing inks) proven it may find versatile use in other related areas (i.e., fabric dying).

Reactive Dyes (Procion class)

A second class of dyes, known as reactive dyes, relies on covalent bonds to attach the dye molecules to the fiber[12]. These dyes are desirable for their colorfastness. Example of one type of reactive dyes (the Procion MX dyes) are shown in Figure 8.14.

These dye molecules contain three main components: (1) an extended aromatic region (the actual dye), (2) sulfonic acid groups which help solubilize the dye in aqueous dye baths, and (3) one or more reactive sites (-Cl) at which the molecule may covalently attach to functional groups on the fiber. Samples of fabric that were commercially dyed with the three dyes in Figure 8.14 were analyzed using LD/MS. Neither the positive-ion nor negative-ion mass spectra of each of the fabrics contained peaks representing the dyes. It is believed that because these dye molecules are covalently bound to the cotton fabric, they cannot be desorbed and ionized.

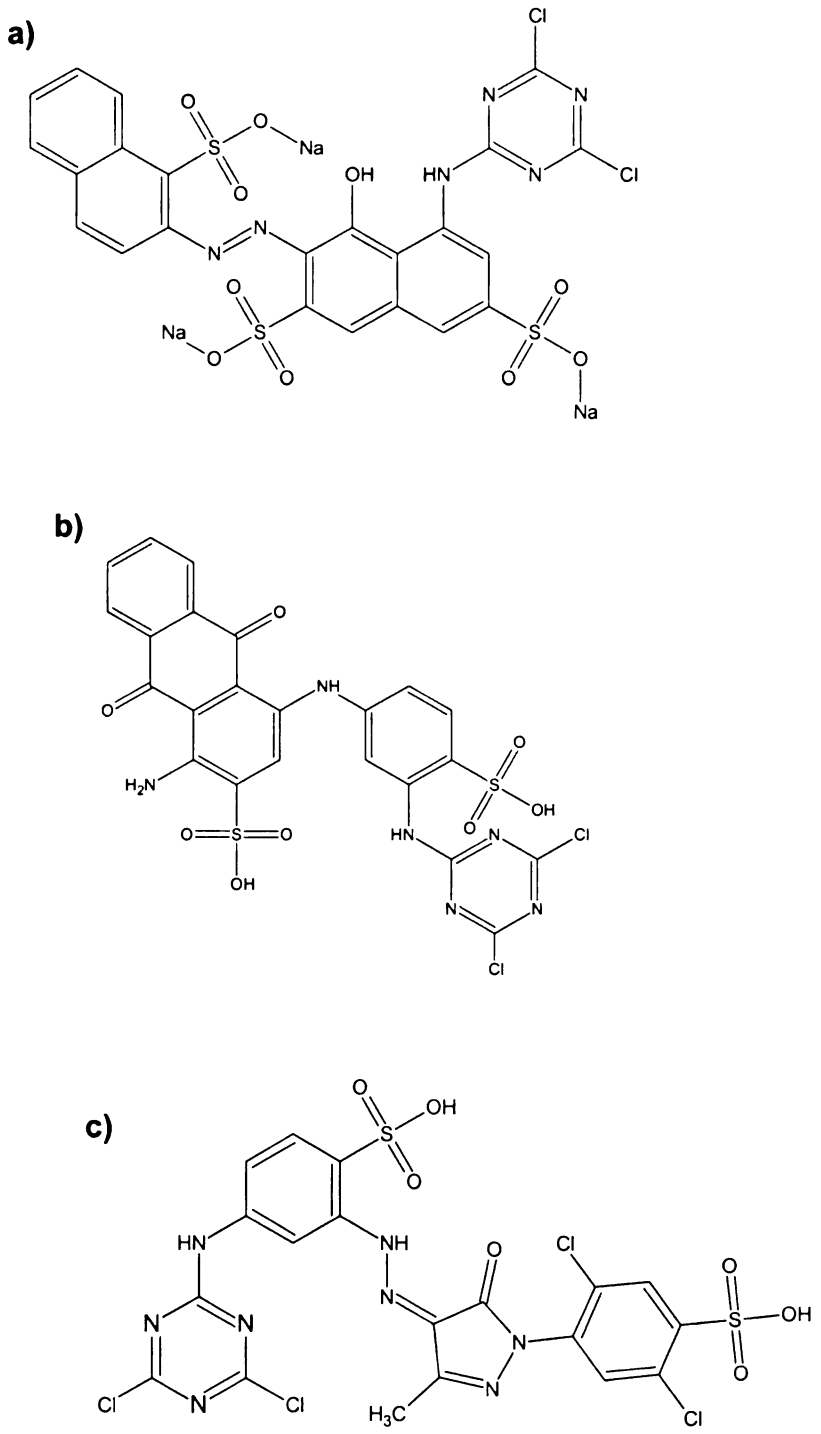

Figure 8.14: Structure of Procion MX dyes: a) "Cool Red MX-8B," b) "Blue MX-R," and c) "Yellow MX-6G"

Summary

As described above, LD/MS has limited application in the analysis of fabric dyes using direct laser irradiation of fabric samples. Some common direct dyes were detected. These dyes are not covalently bound to fabric and hence are similar to the "dye-on-paper-substrate" systems discussed in other parts of this thesis. Another class of dyes that covalently bond to the fabric during the dying process (reactive dyes) were not detected through laser irradiation of dyed fabric. The technique of LD/MS would be appropriate for the analysis of some, but not all, fabric dyes. Additionally, it was demonstrated that informative mass spectra could be obtained through laser irradiation of a single fiber.

References

(1) R. Saferstein, Forensic Science Handbook: Vol III, Regents/Prentice Hall: New Jersey, 1993.

(2) M. C. Grieve, R. M. Griffin, R. Malone, *Science & Justice,* **38** (1998) 27-37.

(3) J. V. Miller, E. G. Bartick, *Applied Spectroscopy,* **55** (2001) 1729-1732.

(4) K. G. Wiggins, R. Cook, Y. J. Turner, *Journal of Forensic Sciences* **33** (1988) 998-1007.

(5) D. F. Rendle, K. G. Wiggins, *Review of Progress in Coloration and Related Topics* **25** (1995) 29-34.

(6) K. G. Wiggins, S. R. Crabtree, B. M. March, *Journal of Forensic Sciences* **41** (1996) 1042-1045.

(7) D. K. Laing, L. Boughey, A. W. Hartshorne, *Journal of the Forensic Science Society* **30** (1990) 299-307.

(8) S. Suzuki, Y. Suzuki, H. Ohta, R. Sugita, Y. Marumo, *Science & Justice* **41** (2001) 107-111.

(9) B. Brackman, Clues in the Calico: A Guide to Identifying and Dating Antique Quilts Howell Publishing, 1983.

(10) Beth Donaldson, MSU Fabric curator, personal communication

(11) J. Rivlin, The Dyeing of Textile Fibers: Theory and Practice Philadelphia College of Textiles and Science. PA, 1992.

(12) D. R. Waring, G. Hallas. The Chemistry and Application of Dyes, Plenum Press, New York, 1990.

Chapter 9: Glass

Introduction and motivation

Glass fragments are commonly encountered as trace evidence. Comparison of two glass samples (one of known origin and the other of unknown origin) is common practice in forensic laboratories. Analysts often compare the refractive indices of each of the glass samples to determine if they could have had a common origin. Much work[1-4] has shown that elemental analysis of the glass is a powerful tool in comparing glass samples. Scientists are interested in the elemental composition of the glass (as the ratios of elements such as sodium, magnesium, aluminum, iron, etc.). Some of the techniques currently used in elemental analysis of glass can require extensive sample preparation[5,6]. Because LD/MS can produce well-resolved mass spectra in low (elemental) mass ranges, we wanted to study whether LD/MS could be a helpful tool in glass analysis.

Analysis of automobile windshield glass

Glass from a variety of automobile windshields was collected. The float glass side of a chunk of glass (the side of the glass that is cast onto metal during manufacturing) was determined by UV-fluorescence. The float glass side of the glass was then analyzed using a scanning electron microscope (SEM-EDS). The data output from the SEM is percent composition of various elements (i.e., Na, Al, Fe, etc.). These percent compositions were then transferred into an excel file and the ratios of elements to one another were compared. A sample of the data output is shown in Figure 9.1.

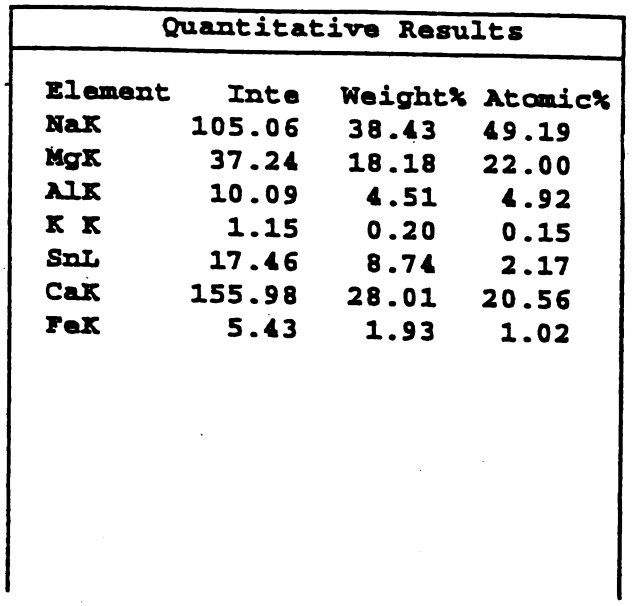

Quantitative Results

Element	Inte	Weight%	Atomic%
NaK	105.06	38.43	49.19
MgK	37.24	18.18	22.00
AlK	10.09	4.51	4.92
K K	1.15	0.20	0.15
SnL	17.46	8.74	2.17
CaK	155.98	28.01	20.56
FeK	5.43	1.93	1.02

Figure 9.1: Sample of SEM data output from analysis of windshield glass from 1993 Hyundai Sonata (K and L which follow the elemental symbol denote the x-ray emitted during analysis)

Initially, for consistency, I attempted analyzing the glass chunks as prepared for SEM. This meant analyzing the float glass side of the glass, while the opposite (non-float-glass) side was pressed to the base of the sample plate with double stick tape. A sample positive-ion mass spectrum obtained using this minimal sample preparation is shown in Figure 9.2. This method, though desirable for SEM, was not optimal for LD/MS. In these initial LD/MS spectra, the peaks were very broad and unintelligible. This strategy was also inconvenient because the top of the glass was out of the depth of field of the CCD camera used to show the laser's location when irradiating the sample plate, and the glass sample was hard to see.

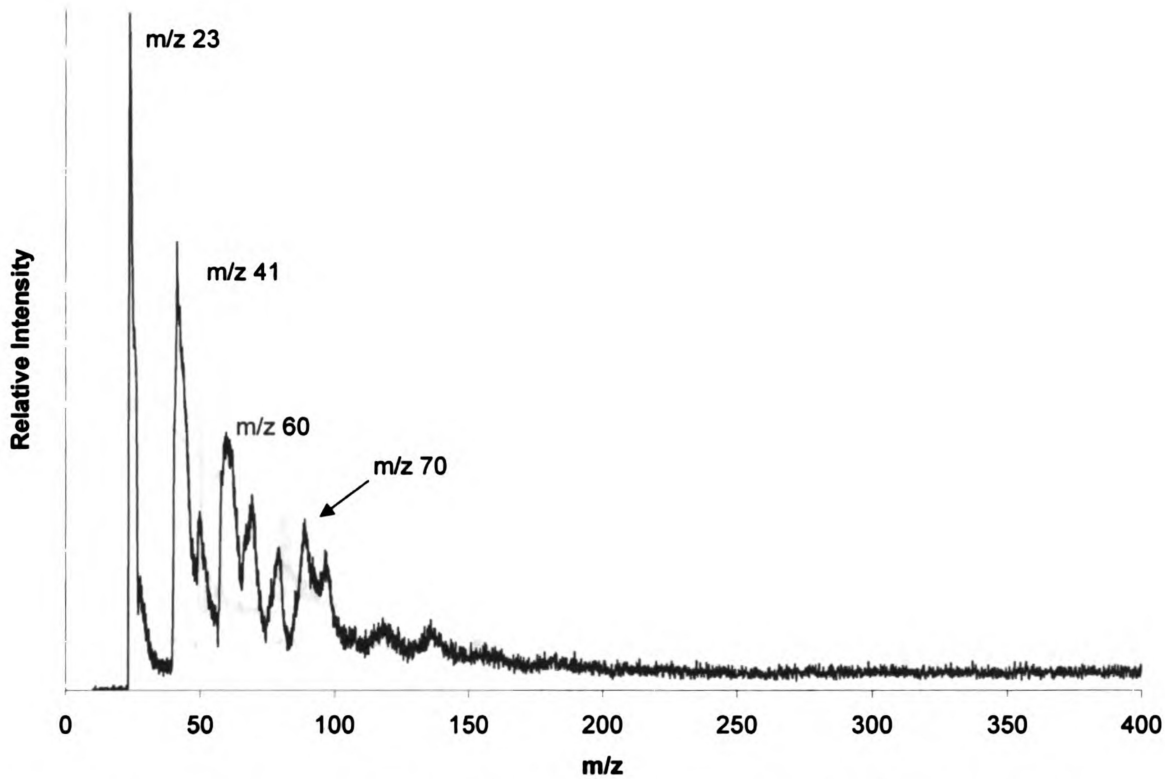

Figure 9.2: Positive-ion LD mass spectrum of unprepared float glass side of windshield glass from 1993 Hyundai Sonata

Grinding a small amount of glass and pressing the powder onto a piece of double stick tape on a sample plate proved a more effective method. Spectra from samples prepared in this manner were much better resolved and interpretable, as seen in the positive-ion mass spectrum below (Figure 9.3) of the same glass sample. The peak at m/z 23, m/z 27, and m/z 39 represent sodium ions, aluminum ions, and potassium ions respectively. The peak at m/z 56 likely represents iron ions.

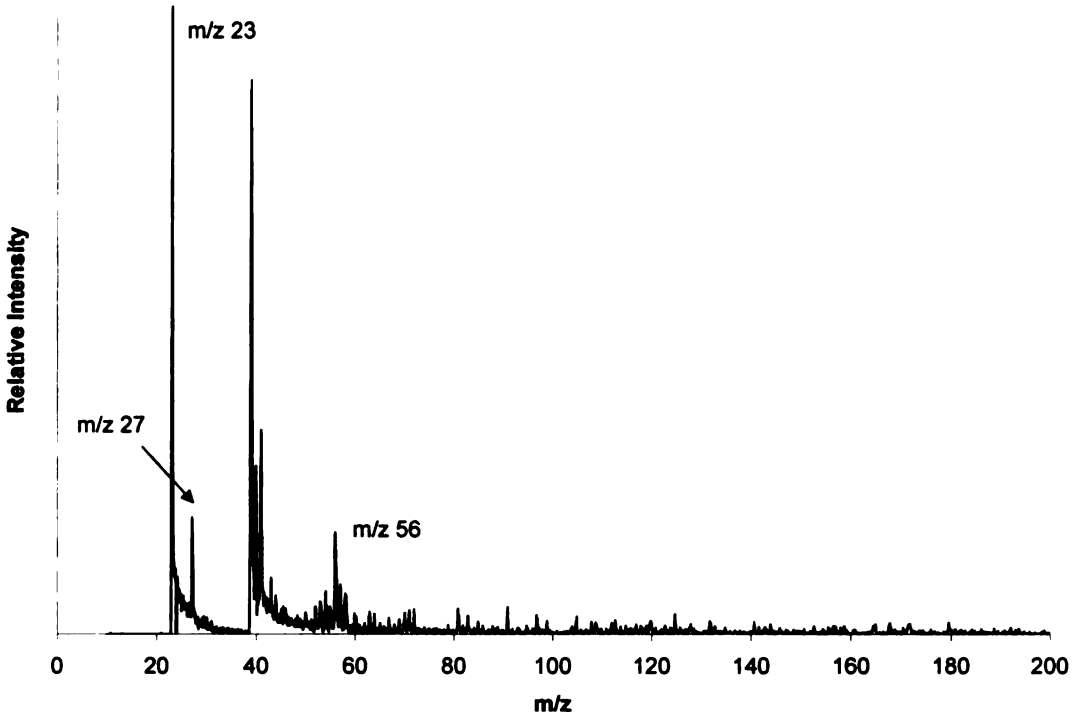

Figure 9.3: Positive-ion LD mass spectrum of crushed sample of windshield glass from 1993 Hyundai Sonata

LD/MS Results vs. SEM-EDX Results

LD/MS spectra of glass were very location-dependent; depending on the region of the crushed glass analyzed, the intensity of peaks could vary significantly (even using the same instrument parameters). This variation could relate to surface morphology; the size and shape of the glass fragments may affect how ions are desorbed from the surface. With SEM, one consistently analyzes the float-glass side of the glass, so the technique is inherently more consistent.

With LD/MS, the intensity of the irradiating laser can affect spectra. If component A is present in 100-fold excess to component B, instrumental conditions can be chosen yielding (1) no peaks representing component B, (2) a peak for component B that is 1% the height of the peak representing component A, or (3) a peak for component B that is 15% the height of the peak representing component A! Also, LD/MS is not selective enough for forensic auto-glass comparisons. For example, initially one assumes that a peak appearing at m/z 56 represents iron ions, however, other ions could have the same mass. The mass analyser does not distinguish between iron ions appearing at m/z 56 and organic ions appearing at m/z 56.

For some elements, resolution is better using SEM; one can distinguish between certain compounds with similar mass. For other elements, resolution is better using LD/MS; these elements emit X-rays that are very similar in energy, but have significantly different masses. In LD/MS the sample can be "exhausted" of ions by the third consecutive laser shot. This demonstrates just how surface sensitive the technique is.

After the not-so-useful results of the standard elemental comparison, we instead looked to identify elements used as colorants for glass. For example, some elements used to tint glass brown include iron, titanium, and carbon. Elements that color glass blue and purple include iron, copper, vanadium, cobalt, and

titanium. Identifying the elements used to color glass can yield information about the history of the glass.[7,8]

Analysis of colored glass

Samples of colored glass were prepared in the same way as auto windshield glass samples were; a small amount of glass was ground and pressed onto a piece of double stick tape on a sample plate.

Blue glass conclusions

Three samples of commercially available blue glass were analyzed (from an "Arizona iced tea" bottle, from a "Skyy Blue" bottle, and from a "Badger Mountain" champagne bottle. Positive-ion and negative-ion spectra were taken of crushed samples of each of these samples. A representative positive-ion mass spectrum (of the Arizona iced tea bottle) is shown in Figure 9.4. The peaks at m/z 23 and m/z 39 represent Na^+ and K^+, respectively. The peak cluster around m/z 48 represents Ti^+, and the peak cluster around m/z 64 is TiO^+. The presence of titanium is not surprising, as titanium is used to tint glass bluish-purple. The theoretical isotope distribution of each of these ions are shown in Figure 9.5.

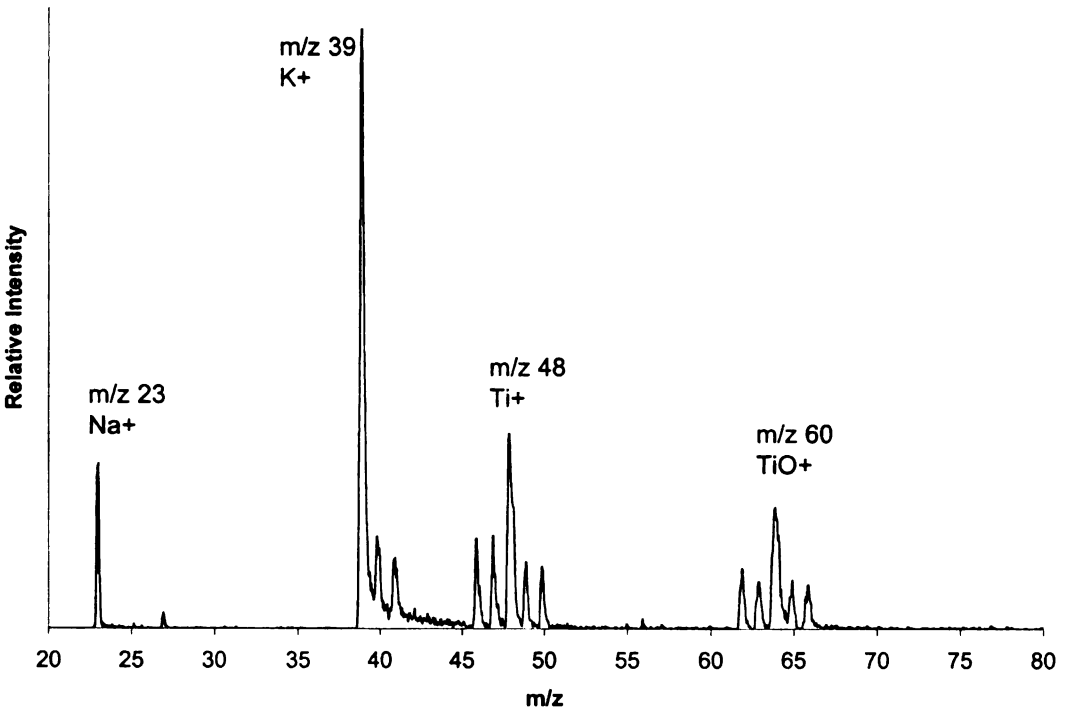

Figure 9.4: Positive-ion LD mass spectrum of Arizona Iced Tea bottle

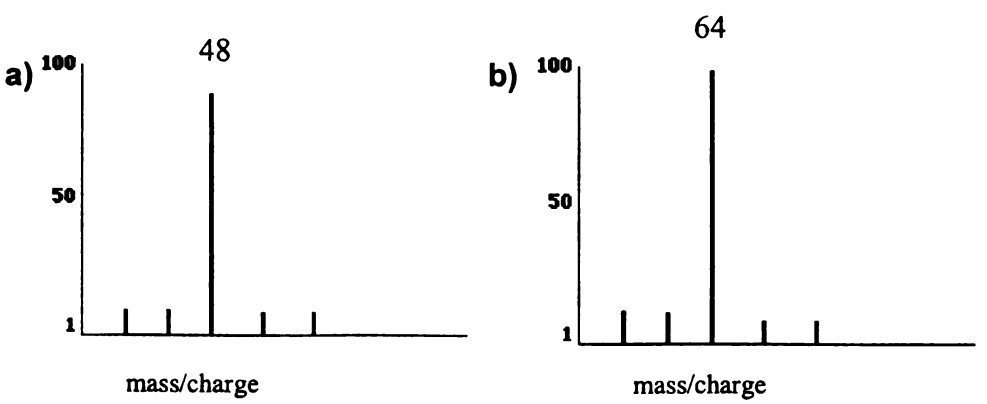

Figure 9.5: Theoretical isotope distribution of a) Ti^+ and b) TiO^+

Evidence of other colorants such as iron, copper, vanadium or cobalt was observed in neither the positive-ion nor negative-ion spectra. Positive ion mass spectra of each three blue glass samples contained peaks representing Ti^+ and TiO^+.

Peaks representing titanium were not observed on the negative-ion mass spectrum (Figure 9.6) of the crushed blue glass; however peaks representing chlorine ions (at m/z 35 and m/z 37) and bromine ions (at m/z 79 and 81) were observed.

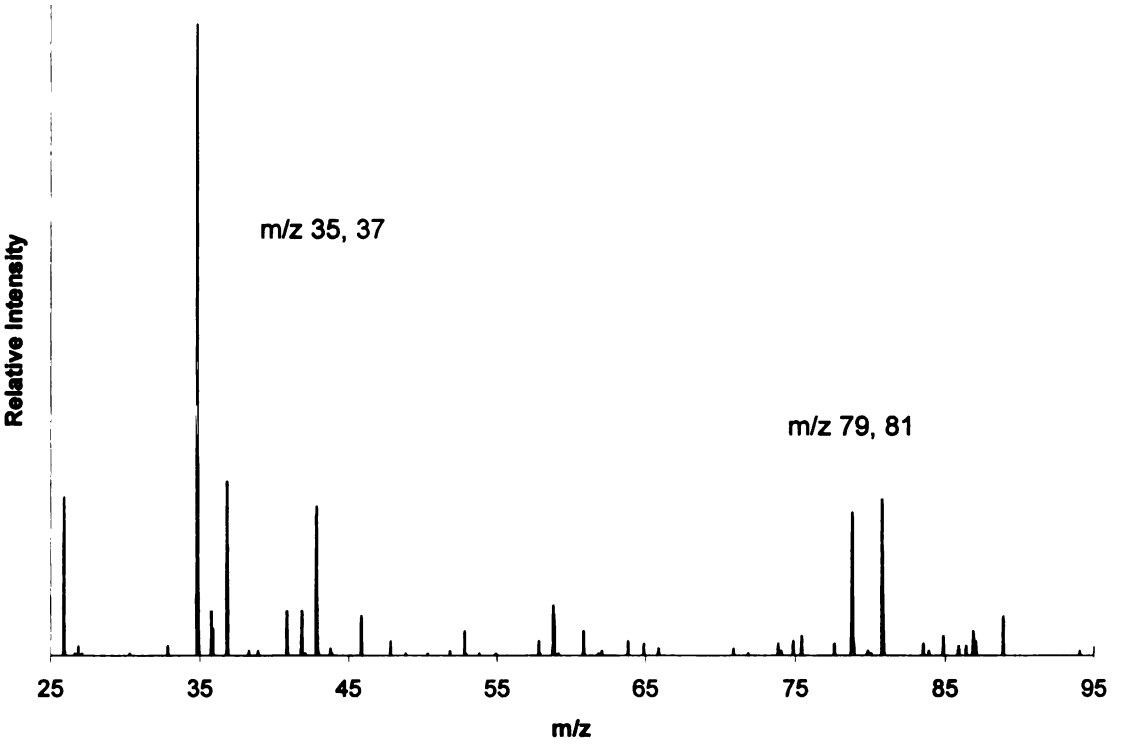

Figure 9.6: Negative-ion LD mass spectrum of Arizona Iced Tea bottle

Brown glass conclusions:

On the positive-ion mass spectrum of crushed brown glass, peaks at m/z 23 and m/z 39 represent Na^+ and K^+, respectively. The peak at m/z 52 represents Cr^+ and the peak at m/z 56 represents Fe^+. The theoretical isotope distribution of each of these ions are shown in Figure 9.7. These elements (as well as carbon and sulfur) are common colorants used to tint glass brown.[8]

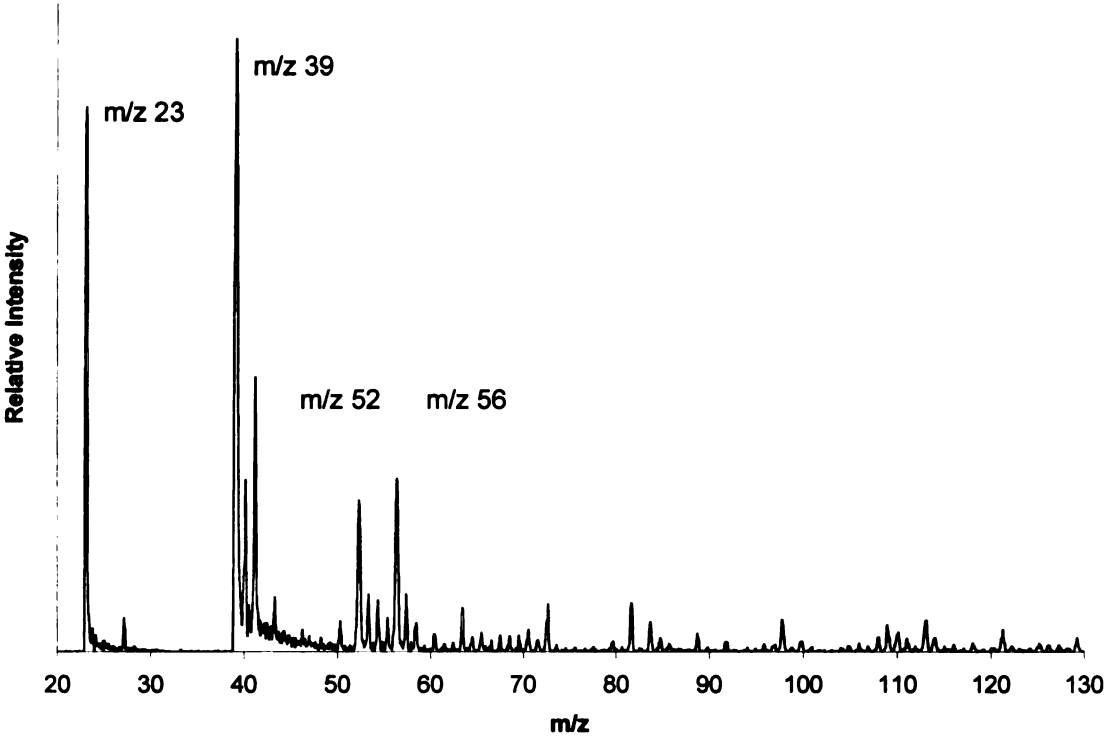

Figure 9.7: Positive-ion LD mass spectrum of brown glass

On the negative-ion mass spectrum (Figure 9.8) of the same sample, some peaks represent the silica nature of the bulk of the glass. Peaks at m/z 60, m/z 88, and m/z 104 likely represent SiO_2, Si_2O_2, and Si_2O_3 respectively. However,

no peaks representing elemental additives to the glass were observed in the negative-ion mass spectrum.

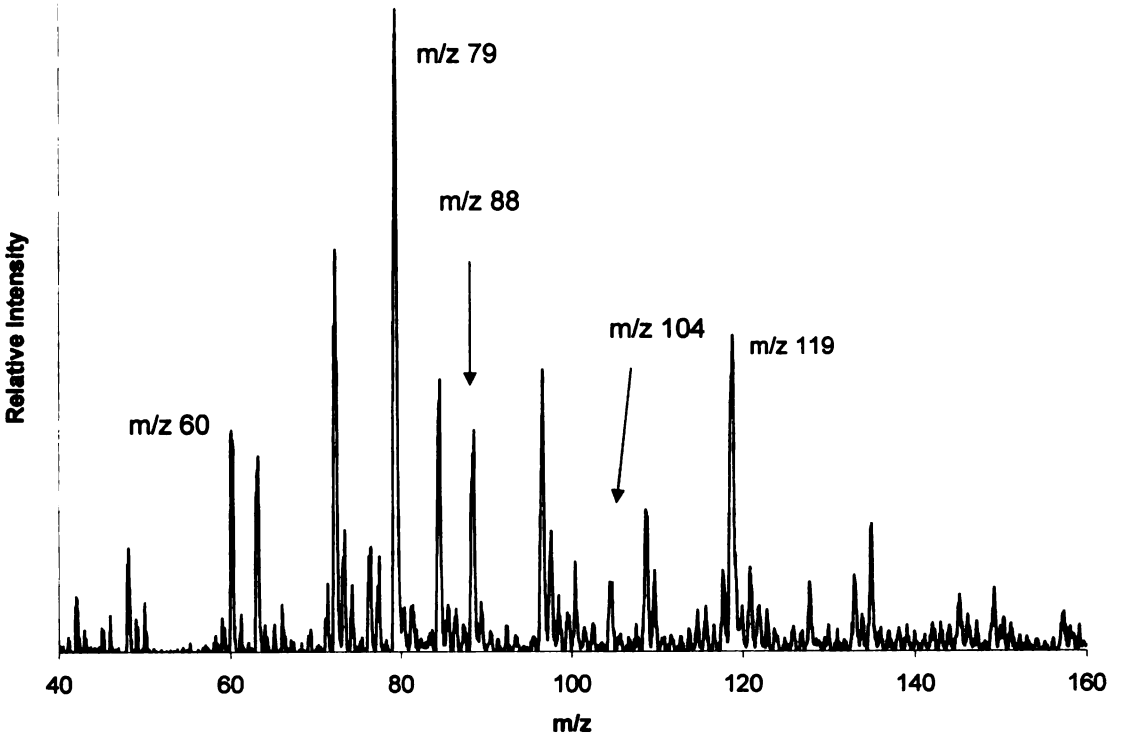

Figure 9.8: Negative-ion LD mass spectrum of brown glass

References

(1) D. C. Duckworth, S. J. Morton, C. K. Bayne, R. D. Koons, S. Montero, J. R. Almirall, *Journal of Analytical Atomic Spectrometry,* **17** (2002) 662-668.

(2) R. D. Koons, J. Buscaglia, *Journal of Forensic Sciences,* **44** (1999) 496-503.

(3) S. Becker, L. Gunaratnam, T. Hicks, W. Stoecklein, G. Warman, *Z Zagadnien Nauk Sadowych,* **47** (2001) 80-92.

(4) D. A. Hickman, *Forensic Science International* **33** (1986) 23-46.

(5) T. Parouchais, I. M. Warner, L. T. Palmer, H. Kobus, *Journal of Forensic Sciences* **41** (1996) 351-360.

(6) J. B. Headridge, I. M. Riddington, *Analyst* **109** (1984) 113-18.

(7) A. M. Pollard, C. Heron, Archeological Chemistry, The Royal Society of Chemistry, England, 1996.

(8) J. B. Lambert, Traces of the Past: Unraveling the Secrets of Archeology Through Chemistry, Perseus Books, Massachusetts, 1997.

Chapter 10: Conclusions

Effectiveness of LD/MS

As just seen in the previous chapters, LD/MS can be a helpful tool in the analysis of some samples. We have demonstrated several "case studies" in which useful chemical information about the sample was obtained using LD/MS. Spectra were obtained from direct laser irradiation of photographs, postage stamps, paper painted with watercolor pigments, paper currency, fabric, and other samples. Some of the compounds studied have been analyzed using other techniques, such as microscopy (electron and light), infrared spectroscopy, Raman spectroscopy, or even other mass spectrometric techniques (such as GC/MS and ICP-MS). However, much of the data produced by LD/MS in this thesis is unique to the technique and could not be obtained using other instrumentation. Clear spectra were not obtained with every sample, because there are uncontrolled variables in the LD/MS experiment that are not well understood.

Limitations of LD/MS

The theoretical (and demonstrated) limit of detection for laser TOF mass spectrometry is very low (spectra are routinely obtained using picomoles of analyte in MALDI). However, with "real-life," "forensic" samples, one does not have control over near as many experimental variables as one has during analysis of samples prepared for MALDI. For example, salt concentration, pH, and the presence of contaminants can affect the quality of mass spectrum produced. As noted in the description of desorption/ionization on silicon (DIOS),

surface morphology can affect how ions are desorbed off a substrate. Spectra can occasionally be deceptive. In the analysis of crushed glass, for example, one can obtain a clear spectrum containing peaks representing sodium, potassium, and aluminum ions. One may believe the results are complete, but after instrument parameter adjustment, peaks representing iron ions may also be observed. While it helps to know what to look for during analysis, this is not always possible with the analysis of complete unknowns, such as one may encounter in a forensic laboratory.

Analysis of organics and inorganics

Using LD/MS one can obtain well-resolved spectra of dye molecules of a variety of structures (ranging in mass from m/z 200 to over m/z 1100). Neutral dyes are detected in positive and negative-ion modes and can be detected as the molecular ion, the deprotonated ion, the protonated ion, and salt adducts of the molecular ion ($(M+Na)^+$ and $(M+K)^+$). This is consistent with other reports of LD/MS. Cationic dyes were detected exclusively in positive-ion mode and anionic dyes were detected exclusively in negative-ion mode. Identification of dyes was often straight-forward, though not always (in the case of some compounds containing only carbon, hydrogen, oxygen, and nitrogen). Identification of compounds related to the dye molecule of interest helps confirm peak assignment (i.e., in addition to peaks representing the molecular ion, the spectra may also contain peaks representing deethylation or dechlorination of the dye molecule). These related compounds, either degradation products or

manufacturing impurities, help individualize a sample even further, and also could be of forensic use. Quantatition was not seriously attempted with the samples discussed in this research because quantation, even in the more established technique of MALDI, is difficult due to many instrument and sample variables.

Some inorganic compounds (such as silver halides and photograph toners) were also detected using LD/MS. This is consistent with previous research. Metal cluster ions (for chemical reactivity interest, rather than forensic interest) have been studied since the early days of LD/MS. Curiously, some inorganics were not detected. For example, in the analysis of blue glass, one might expect a host of peaks representing various silicon oxides (Si_xO_y), reflecting the bulk composition of glass. However, in the positive-ion mass spectra of this sample, peaks representing the titanium present in the glass were dominant and in the negative-ion mass spectra of the blue glass, peaks representing chlorine and bromine were dominant! While we believe that the organic dye molecules discussed in this thesis gain the energy required for desorption and ionization by directly absorbing the wavelength (337 nm) of the irradiating laser, a different pathway seems to exist for desorption and ionization of inorganics. The mechanism for desorption of inorganic ions likely relies more on the morphology of the sample. This resonates with the early observations by Tanaka that fine platinum power matrix helped desorb and ionize organic molecules and with the surface

morphology dependence observed in the study of desorption/ionization on silicon (DIOS).

Have the goals of this research been met?

The purpose of this thesis was not to establish the mechanisms by which some analytes desorb/ionize or to exhaustively analyze every colored object that might be encountered in a forensic laboratory. Rather, previous research in our lab demonstrated that LD/MS could detect dyes in writing inks and we were curious to evaluate whether LD/MS has value in the analysis of other dyes and pigments. We obtained positive-ion and negative-ion LD mass spectra of a variety of samples of forensic interest. Most of these spectra provided relevant chemical information about the surface composition of the sample. Some compounds are not detected in LD/MS; this facilitates mass spectral interpretation, as not every component of a mixture produces a peak on the mass spectrum. We encountered challenges with "actual unknowns" because we never could know for sure whether we had detected all of the pigments present. Additional work can be (and is being) done: (1) to analyze additional dyes and pigments to elucidate the mechanisms of desorption and ionization, (2) to continue to establish LD/MS as a useful tool in the characterization of dyes and pigments, and (3) to continue to apply the technique of LD/MS to specific forensic analytical questions.